European Funds
for Social Development

Republic
of Poland

Co-funded by the
European Union

NAWA
POLISH NATIONAL AGENCY
FOR ACADEMIC EXCHANGE

MICROCOURSES IN BUILDING MATERIALS ENGINEERING: SUSTAINABLE MATERIALS AND TECHNOLOGIES

edited by
Izabela Hager

European Funds for Social Development
Republic of Poland
Co-funded by the European Union
NAWA POLISH NATIONAL AGENCY FOR ACADEMIC EXCHANGE

Cracow University of Technology (PK) is implementing a project
NAWA SPINAKER IMPK Intensive International Educational Programmes

"IMPK – Sustainable Building Materials and Technologies"
Project No. BPI/SPI/2024/1/00026

Project duration: 2025-06-01 to 2026-07-31
Funding amount: PLN 299,810.00

This initiative is funded under the **European Funds for Social Development 2021–2027 (FERS)** programme implemented by NAWA – Polish National Agency for Academic Exchange.

Project title: "Support for the Creation and Implementation of International Education Programmes"

Project No. FERS.01.05-IP.08-0436/23

Total project value: PLN 119,892,080.00

European Funds contribution: PLN 98,934,944.42

Beneficiary: NAWA – Polish National Agency for Academic Exchange

#EUFunds #EuropeanFunds #FERS #NAWA

MICROCOURSES IN BUILDING MATERIALS ENGINEERING: SUSTAINABLE MATERIALS AND TECHNOLOGIES

edited by
Izabela Hager

Cracow 2026

CHAIRMAN OF THE CRACOW UNIVERSITY OF TECHNOLOGY PRESS EDITORIAL BOARD
Tomasz Kapecki

SCIENTIFIC EDITOR
Izabela Hager

REVIEWERS
Marta Choinska Colombel
Marcin Górski

ENGLISH PROOFREADING
Zuzanna Małecka

PUBLISHING EDITOR
Agnieszka Filosek

TYPESETTING
Adam Bania

LAYOUT DESIGN
Małgorzata Murat-Drożyńska

COVER DESIGN
Mateusz Indyka

e-ISBN 978-83-68481-21-1

Wydawnictwo PK, ul. Skarżyńskiego 1, 31-866 Kraków; tel. 12 628 37 25, fax: 12 628 37 60
e-mail: wydawnictwo@pk.edu.pl ☐ www.wydawnictwo.pk.edu.pl
Correspondence address: ul. Warszawska 24, 31-155 Kraków

Free copy

CONTENTS

PREFACE

The academic textbook *Microcourses in Building Materials Engineering: Sustainable Materials and Technologies* is the result of an innovative educational initiative carried out within the **SPINAKER Programme of the Polish National Agency for Academic Exchange (NAWA**. "IMPK – Sustainable Building Materials and Technologies"the project BPI/SPI/2024/1/00026). The publication was developed through the collaboration of two units of the Cracow University of Technology: the Faculty of Civil Engineering, Chair of Building Materials Engineering, and the Faculty of Materials Engineering and Physics, Chair of Materials Engineering.

This interdisciplinary cooperation brought together expertise in civil engineering, and materials science to prepare a modern educational resource that addresses current scientific and technological challenges in the field of construction materials. The textbook reflects a shared conviction that the future of engineering education must combine academic rigor, practical relevance, and a strong commitment to sustainable development.

The project is particularly significant because it marks **the first implementation at Cracow University of Technology of microcourses in English and micro-credentials** as innovative educational tools. These new forms of learning respond to the changing expectations of students and professionals by offering concise, modular, and flexible educational units focused on specific competencies. In a world where knowledge evolves faster than concrete sets (and occasionally faster than administrative procedures), microcourses provide a practical and efficient way to acquire advanced expertise.

The SPINAKER NAWA project enabled the development of English-language teaching materials designed for an international audience. The modular structure of the textbook allows individual chapters to function both as independent learning units and as components of a broader course in Building Materials Engineering. This approach supports diverse teaching formats, including intensive courses, blended learning, continuing education, and specialized training for industry professionals.

A central theme of the publication is **sustainable development**, which is integrated throughout the textbook rather than treated as an isolated topic. The environmental impact of construction materials, durability, circular economy principles, low-carbon technologies, and innovative solutions are discussed as essential aspects of modern engineering practice. This perspective reflects the urgent

need to transform the construction sector in response to climate change, resource depletion, and evolving societal expectations.

The textbook presents selected advanced topics that illustrate both established knowledge and emerging research directions in Building Materials Engineering. The following chapters are included:

- High Performance Concrete (HPC) and Ultra-High Performance Concrete (UHPC)
- Fibre Reinforced Concrete
- Self-Compacting Concrete
- Geopolymers and Alkali-Activated Materials
- 3D Printing of Cement-Based Materials
- Fire Behaviour of Building Materials
- Ageing Processes of Materials
- Non-Destructive Testing
- Virtual and Augmented Reality in Engineering Education

Each chapter has been prepared by specialists actively engaged in research and teaching. The contributions combine theoretical foundations with practical applications, experimental methods, and examples of current technological developments. Together, they provide a coherent overview of materials and technologies that are shaping the future of sustainable construction.

The publication is intended primarily for graduate students in civil engineering and related disciplines, but it may also serve doctoral candidates, researchers, and practicing engineers seeking to broaden their knowledge of advanced construction materials. Thanks to its modular organization, the textbook can be used selectively, allowing readers to focus on topics most relevant to their educational or professional needs.

This book demonstrates that engineering education can be both scientifically demanding and pedagogically flexible. By introducing microcourses and micro-credentials for the first time at Cracow University of Technology, the SPINAKER NAWA project has opened new possibilities for internationalization, lifelong learning, and competency-based education.

I hope that this publication will inspire students and professionals to explore innovative materials and technologies, and to contribute to the development of a more sustainable built environment.

Ph.D. D.Sc. Eng. Izabela Hager
Cracow University of Technology Professor
Head of Chair of Building Materials Engineering
SPINAKER NAWA Coordinator

Cracow 2026

1

DESIGN OF HIGH-PERFORMANCE AND ULTRA-HIGH-PERFORMANCE CONCRETE

Tomasz Tracz

High-Performance Concrete (HPC) and Ultra-High-Performance Concrete (UHPC) represent a milestone in concrete technology, originating from the modification of ordinary concrete to eliminate its drawbacks, such as high porosity or low durability [1, 2]. HPC is most commonly defined as a composite with a characteristic compressive strength exceeding 60 MPa, in which mechanical properties and durability have been enhanced through the careful selection of component proportions. In turn, UHPC refers to next-generation materials with extremely high performance, characterised by compressive strength exceeding 150 MPa and potentially reaching up to 350 MPa under laboratory conditions. This group of next-generation concretes is also characterised by exceptional durability, low permeability, and enhanced frost resistance [3, 4]. The table below presents a comparison of the fundamental properties of Ordinary Concrete (OC), High-Performance Concrete (HPC), and Ultra-High-Performance Concrete (UHPC).

Table 1.1. Comparison of the properties of Ordinary Concrete (OC), High-Performance Concrete (HPC), and Ultra-High-Performance Concrete (UHPC) [1–4]

Property	**Ordinary Concrete (OC)**	**High-Performance Concrete (HPC)**	**Ultra-High-Performance Concrete (UHPC)**
Compressive Strength	< 60 MPa	60–150 MPa	> 150 MPa
Water/Cement (w/c) Ratio	> 0.40	0.25–0.35	< 0.20
Durability	Moderate	High	Exceptional
Permeability	High	Low	Extremely Low/ Negligible
Freeze-Thaw Resistance	Standard	High	Excellent

The use of HPC and UHPC enables the design of lighter, slimmer engineering structures while maintaining the same load-bearing capacity, which in ordinary concrete would require significantly larger cross-sections. Furthermore, these concretes frequently exhibit high resistance to aggressive environmental agents due to the limited accessibility of their porous structure.

The basic composition of these concretes includes high-quality cements, selected high-strength aggregates, modern superplasticisers, and active mineral additives, particularly silica fume. The foundation of the design process is the pursuit of a significant reduction in the water-binder ratio, which for HPC falls below 0.35, and

in the case of UHPC, reaches values close to 0.20. By maximising particle packing, a very dense microstructure almost entirely devoid of capillary pores is achieved, resulting in exceptional tightness and low water absorption in the composite.

A key component of UHPC is dispersed reinforcement, most commonly in the form of steel or polymer fibres, which provides the material with ductility and prevents sudden, brittle failure. These concretes are characterised by excellent durability, frost resistance, and high abrasion and chemical attack resistance, making them far more resistant to environmental influences than ordinary concrete. They find wide application in high-rise construction (e.g. slender columns), bridge engineering, marine structures, and the production of lightweight precast elements with complex shapes. The use of HPC and UHPC allows for a significant reduction in the self-weight of structural elements and extends the service life of buildings, which – despite higher production costs – provides measurable economic and ecological benefits.

1.1. COMPONENTS OF HPC AND UHPC – QUALITATIVE DESIGN

The role of components in High-Performance Concrete (HPC) and Ultra-High-Performance Concrete (UHPC) is fundamental; it is the unique properties of individual constituents, combined with their meticulous qualitative and quantitative selection, that enable the properties of the composite to be tailored.

The application of numerous components with diverse interaction profiles, their compatibility, and variations in their interaction mechanisms lead to complexities in evaluating the kinetics of the setting and hardening processes [5]. Consequently, the assessment of the impact of individual constituents on the properties of fresh mixes and hardened concrete is conducted through experimental testing. Neville [6] asserts that an empirical approach to the design of high-performance concretes is inevitable. The properties of these next-generation concretes primarily depend on the characteristics of three elements: the matrix (hardened paste), the filler (aggregate), and the bonds between them (i.e. the interfacial transition zone (ITZ) and adhesion at the interface) [7, 8].

1.1.1. BINDERS

In the production of High-Performance Concrete (HPC) and Ultra-High-Performance Concrete (UHPC), the meticulous selection of high-quality cements with stable properties is pivotal [4, 9]. Portland cements of classes 42.5 R and 52.5 R are most commonly employed, providing the composites with high

strength potential. The dominant choice for UHPC matrices is pure Portland cement (CEM I), often in a low-alkali (NA) variant, which minimises the risk of alkali-silica reaction [1, 4, 9]. Binders with high sulphate resistance (SR or HS) and a low heat of hydration are preferred, as they help mitigate the formation of thermal and shrinkage cracks [10, 11]. In structures exposed to severe chemical aggression or requiring specific limitations on the heat of hydration, blast-furnace slag cements (CEM III/A) or blended Portland cements, such as CEM II/B-S, are utilised [4, 10].

A critical technical parameter is a low tricalcium aluminate content ($C_3A < 10\%$), which significantly improves the cement's compatibility with modern superplasticisers [7, 11]. The efficiency of these admixtures is vital for achieving adequate workability of the mix at extremely low water-binder ratios, which in UHPC often reach approximately 0.20 [4, 7, 11]. It is noteworthy that at such low water content, up to 30% of the cement grains remain unhydrated, thus creating a binder reserve that enables the "self-healing" of microcracks within the structure [4]. The cement content in these composites is substantially higher than in ordinary concrete, ranging from 450 kg/m^3 in HPC to 700–1000 kg/m^3 in ultra-high-performance concrete.

1.1.2. MINERAL ADDITIVES

The most effective and widely used mineral additive is silica fume (microsilica), which is nearly pure, amorphous silica (SiO_2) with characteristically spherical grains. It is characterised by an extremely high degree of fineness (grains approximately 100 times smaller than cement grains) and a vast specific surface area, allowing it to interact with the paste both physically and chemically [7]. The silica particles are spherical, with an average diameter of about 0.2 μm, and approximately 90% of the particles are smaller than 1 μm (Fig. 1.1). Silica fume features an immense specific

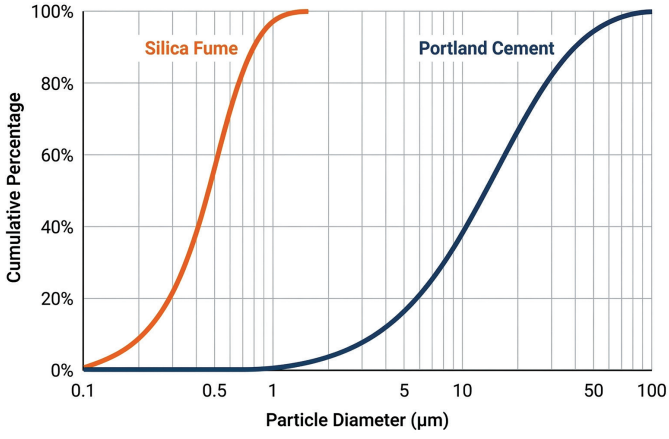

Fig. 1.1. Particle size distributions of silica fume and CEM I Portland cement

surface area, ranging from 150,000 to 222,000 cm^2/g. For comparison, the specific surface area of CEM I 52.5 cement is approximately 4,850 cm^2/g [7].

The physical interaction effect involves the tight filling of voids (interstitial spaces) between cement grains, thereby significantly increasing particle packing density [7, 11]. Fig. 1.2 illustrates the physical interaction effect, showing how these ultrafine silica fume particles lodge in the spaces between cement grains to seal the matrix.

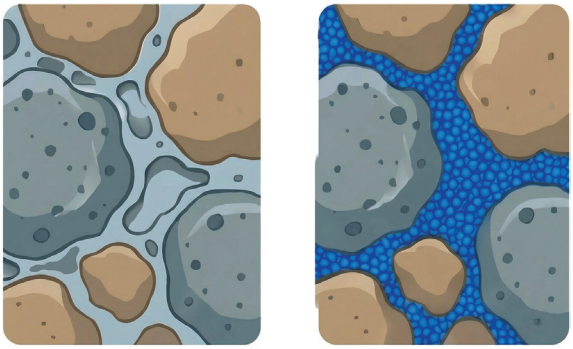

Fig. 1.2. Physical interaction effect of silica fume particles – increase in packing density

The chemical interaction effect of silica fume on cement hydration products, known as pozzolanic activity, involves the reaction of amorphous silica (SiO_2) with calcium hydroxide ($Ca(OH)_2$), also known as portlandite. Portlandite is formed as a by-product of cement hydration and is a relatively weak, porous, and water-soluble constituent. As a result of the pozzolanic reaction, portlandite is transformed into additional calcium silicate hydrate (C-S-H) phase, which is the primary factor determining the paste's strength [7, 11]. The C-S-H phase is considerably more durable and insoluble, thereby significantly reinforcing the cement matrix. This process is critical for densifying the Interfacial Transition Zone (ITZ) between the paste and the aggregate, where silica fume reduces the portlandite content and replaces it with a stronger C-S-H gel.

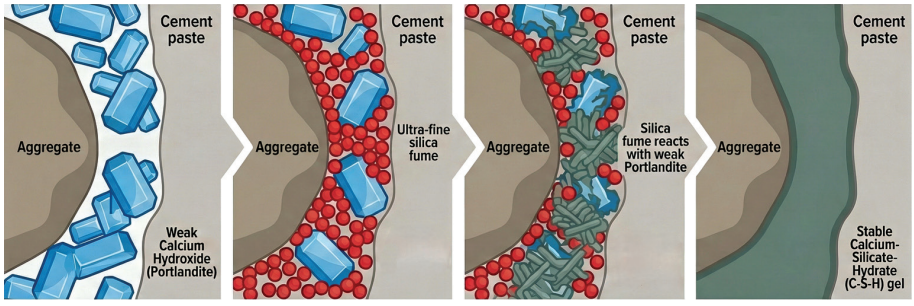

Fig. 1.3. Chemical interaction effect of silica fume in the interfacial transition zone (ITZ) between the paste and the aggregate

In UHPC, the chemical effect is often enhanced through thermal treatment (e.g. at 90°C), which accelerates silica binding and the formation of high-density phases [3, 4]. Consequently, the composite microstructure becomes almost entirely devoid of capillary pores and exceptionally dense [4]. Additionally, by adsorbing water onto its immense specific surface area, silica fume reduces excessive water concentration around aggregate grains, thereby preventing local structural weaknesses [7]. The ultimate result of pozzolanic activity is not only an increase in compressive strength but also a significant enhancement of the concrete's durability and resistance to chemical attack [2]. The synergy between the micro-filler (physical) effect and the pozzolanic (chemical) activity enables HPC and UHPC to achieve parameters unattainable in ordinary concrete.

Another important additive is fly ash, which, due to its spherical particles, improves mix workability (the so-called "ball-bearing effect"), lowers the heat of hydration, and allows for a reduction in cement content. The use of high-quality fly ash contributes to long-term strength gain and improved composite density. Ground Granulated Blast-Furnace Slag (GGBS) is used to further reduce superplasticiser demand and increase the concrete's resistance to chemical aggression, particularly sulphate attack [4, 11, 12].

In UHPC technology, metakaolin is also frequently used, as it exhibits very high pozzolanic activity, promoting early strength gain and pore refinement. Inert microfillers, such as quartz flour, also play a vital role by filling the granulometric gap between sand and cement, which is crucial for optimizing packing density in reactive powder concretes (RPC). Modern solutions also employ nanosilica, whose even finer particles enable near-total elimination of capillary pores, resulting in a structure with properties similar to those of ceramics [1, 4, 11].

The primary objective of using this broad range of additives is to achieve maximum matrix density, resulting in exceptional durability, high strength, and resistance to the ingress of harmful environmental agents.

1.1.3. CHEMICAL ADMIXTURES

In High-Performance Concrete (HPC) and Ultra-High-Performance Concrete (UHPC), high-efficiency chemical admixtures play a crucial role and are primarily used to achieve adequate workability at extremely low water-binder ratios (often below 0.30, and even as low as approximately 0.20). The use of highly active admixtures is essential, as such a significant reduction in water content renders the mix unworkable, impossible to place, and challenging to compact properly. The mechanism of these substances is based on electrostatic and steric effects that prevent the aggregation of matrix particles. Consequently, they induce the de-aggregation of cement grain clusters and fine microfillers, releasing the water trapped within these agglomerates and allowing optimal utilisation of the binder [7–9].

The most common and widely used admixtures in this group of composites are superplasticisers, powerful water-reducing agents that significantly reduce water demand. In modern HPC and UHPC, new-generation polymer superplasticisers based on polycarboxylate ethers (PCE) are predominantly used. These compounds, characterised by a comb-like polymer structure, exhibit significantly higher liquefying efficiency than traditional plasticisers based on lignosulphonates, melamine, or naphthalene. In addition, shrinkage-reducing admixtures (SRA) may optionally be used to control early drying shrinkage and autogenous shrinkage (which is particularly hazardous in UHPC), and occasionally air-entraining admixtures are applied to enhance frost resistance [1, 2, 11].

A critical and complex issue during the design stage of HPC and UHPC is the compatibility (functional consistency) between specific cements and admixtures – for example, the interaction between silica fume and the introduced admixtures [5]. As the mix becomes a sophisticated multi-component system, highly active superplasticisers may interact with various binders in diverse, and sometimes unpredictable ways [4, 8]. A lack of compatibility between the cement and the superplasticiser leads to serious technological issues, such as excessive viscosity, which severely hinders the placement and de-aeration of the concrete. This incompatibility may also result in a drastic retardation of the hydration and setting processes (which is particularly detrimental in precasting) or the incorporation of excessive entrapped air into the structure, ultimately causing a significant drop in strength [11]. The optimal dosage and efficiency of superplasticisers must always be meticulously verified through experimental trial batches using the specific raw materials [7].

Several specific physicochemical characteristics of the cement itself influence the effectiveness of these admixtures. Its mineralogical composition is vital, particularly a low tricalcium aluminate (C_3A) content [4, 8]. It is strongly recommended that the C_3A content in the binder be less than 10%, which significantly facilitates interaction with admixture molecules, reduces viscosity, and ensures longer rheological stability of the fresh mix. Furthermore, other binder characteristics – such as alkali content, water demand resulting from the fineness of the grind, and the type of set regulator used in the cement (e.g. calcium sulphate) – can significantly impact admixture performance [4, 11]. In some cases, it is even recommended to use multi-component admixtures, which, due to their varied polymer structures, can seamlessly de-aggregate both coarse cement grains and fine silica fume particles. Careful selection of superplasticisers ultimately enables the production of pumpable, workable, and sometimes self-compacting HPC and UHPC mixes.

1.1.4. AGGREGATE

In High-Performance Concrete (HPC) and Ultra-High-Performance Concrete (UHPC), aggregate selection is crucial. In these modern composites, the interfacial transition zone between the paste and the aggregate is highly densified, potentially making the aggregate the "weakest link" of the composite [1]. For this reason, crushed aggregates derived from dense rocks with very high mechanical strength and low porosity – such as basalt, granite, diabase, dolomite, or syenite – are most commonly used. It is generally required that the compressive strength of the parent rock used to produce the aggregate be at least 150 MPa [1].

In the case of fine-grained UHPC, coarse aggregate is entirely omitted in favour of fine quartz sand, with a maximum grain size usually limited to 1.0 or 2.0 mm. Conversely, in HPC and modern coarse-grained UHPC, coarse aggregate is used; however, its maximum grain size (d_{max}) is strictly limited compared to that of ordinary concrete. For concretes with strengths up to approximately 100 MPa, this dimension is typically restricted to 16 mm, whereas for concretes with strengths exceeding 150 MPa, it is reduced to 8–12 mm, and in some mixes even to 2–5 mm. The primary reason for using smaller grains is that large grains induce stress concentrations at the interface with the matrix, leading to the formation of microcracks under external loads. Additionally, a smaller grain size of the crushed rock material implies fewer natural defects (fissures) within the aggregate itself and facilitates better interaction with the dense paste [4, 10, 11]. The figure below illustrates the heterogeneity of stress distribution in a composite containing large aggregate grains.

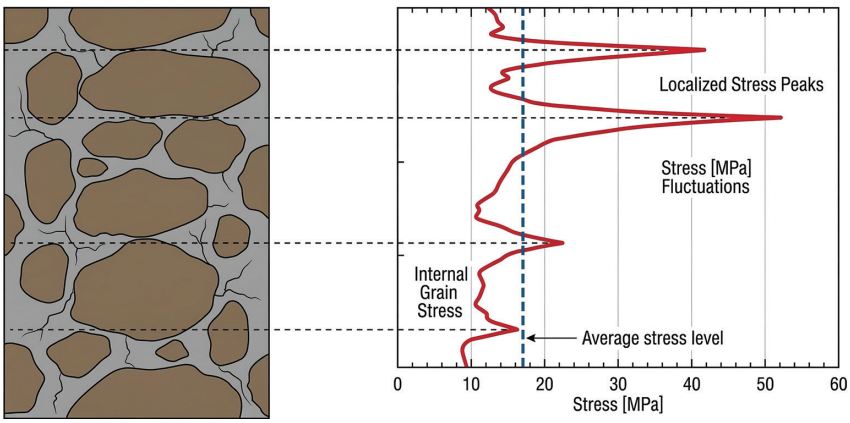

Fig. 1.4. The effect of high stress concentrations occurring at the interface between large aggregate grains and cement paste

It is of utmost importance that the aggregate features a precisely selected, continuous grading curve (granulometric composition). A carefully composed mixture of various fractions guarantees optimal, high-density particle packing and

minimises the voids (interstitial volume) within the granular skeleton. Low void content is desirable because it reduces the volume of cement paste required to fill gaps and coat grains, thereby mitigating concrete shrinkage [2, 7].

In addition to aggregate grading, particle shape is also critical. The use of elongated and flat particles must be strictly avoided, as they exhibit a low capacity to transfer high internal loads within the concrete structure and increase the total specific surface area of the aggregate. The external surface of the grains should be rough and textured. The high surface roughness of mechanically crushed aggregates enhances adhesion and facilitates the formation of strong bonds between the matrix (continuous phase) and the dispersed granular inclusions (aggregate) [1, 7, 8].

1.1.5. FIBRES

In Ultra-High-Performance Concrete (UHPC), dispersed fibres are frequently used to mitigate the inherent brittleness of the material. The addition of fibres imparts ductility to the composite and beneficially modifies its post-cracking behaviour.

Short and slender steel fibres with very high tensile strength (e.g. 9–17 mm in length and up to 0.20 mm in diameter) are most commonly used. These are typically dosed at 1.0%–2.5% by volume (equivalent to approximately 78–196 kg/m^3). Their presence within the UHPC composite structure enables effective crack bridging, significantly increasing the concrete's tensile strength and enhancing its fracture energy.

The second type of commonly used fibres is synthetic fibres, primarily polypropylene (PP), typically added in smaller quantities (e.g. 0.3%–0.66% by volume). These are employed to enhance the fire resistance of UHPC. The extremely dense structure of the concrete prevents the escape of water vapour during a fire, leading to explosive spalling. PP fibres melt at approximately 160°C, creating microchannels through which internal water pressure can be released.

1.2. QUANTITATIVE DESIGN OF HPC AND UHPC MIXTURES

The quantitative design of High-Performance Concrete (HPC) and Ultra-High-Performance Concrete (UHPC) is a significantly more complex process than that of ordinary concrete and requires the integration of analytical methods with experimental testing. Traditional methods based on simple volumetric balance, such as the classical "three-equation method", prove entirely insufficient in this case, as they yield excessive discrepancies between the predicted and actual composite strength. This is because well-known relationships, such as Bolomey's strength equation, lose validity at very low water-binder (w/b) ratios, which in these concretes

typically drop below 0.35 and can reach as low as 0.20 in UHPC. Among classical mathematical tools, the only one that remains fully applicable is the absolute volume equation (density equation), which assumes that the sum of the volumes of all constituents must equal the unit volume of the compacted mix.

Instead of Bolomey's formula, modern empirical relationships are used for the preliminary estimation of HPC compressive strength, such as de Larrard's equation. This equation correlates strength with the water-cement (w/c) ratio, the silica fume content relative to the cement mass, and parameters accounting for the type of aggregate and cement strength [7, 9, 11, 13].

De Larrard's equation is used to estimate the 28-day compressive strength (f_{c28}) of concrete cured under standard conditions.

$$f_{c28} = \frac{k_G \times k_c}{\left[\frac{1+3.1(W/C)}{1.4-0.4\exp(-11SF/C)}\right]^2}$$

where:

k_G – a coefficient accounting for the influence of the type of aggregate used. For most aggregates intended for HPC, their value ranges from 4.8 to 5.2;
k_C – actual strength of the cement used, expressed in MPa;
W/C – water-cement ratio;
SF/C – proportion of silica fume content relative to the cement mass (kg/kg).

In cases where the addition of silica fume is not planned for the designed high-performance concrete composition (value SF/C = 0), the equation is simplified and takes the following form:

$$f_{c28} = \frac{k_G \times k_c}{\left[1+3.1W/C\right]^2}$$

The graph of this simplified relationship is a flat parabola that, in its profile, closely resembles the classical linear Bolomey relationship, with the distinction that it is calibrated for the low W/C ranges characteristic of HPC (Fig. 1.5) [7].

In the practical concrete mix design process, de Larrard's equation is utilised in the initial calculation phase. After assuming the target strength and deciding on the qualitative selection of components (cement, aggregate, and silica fume), de Larrard's equation allows for the estimation of the target W/C ratio and the required proportion of silica fume. However, it must be noted that the parameters derived from this equation are merely a starting point; due to the complex nature and sensitivity of multi-component HPC systems, final proportions must be strictly verified and adjusted through laboratory trial batches.

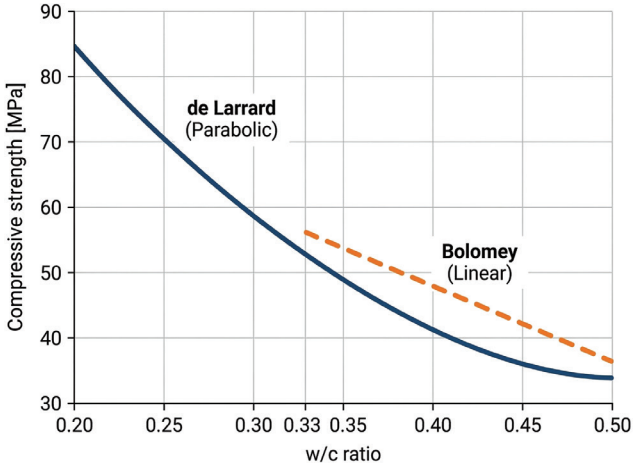

Fig. 1.5. Comparison of the relationships between w/c and compressive strength developed by Bolomey and de Larrard (assumed: $k_G = 4.9$ and actual cement strength, $k_C = 45$ MPa)

A key stage in the analytical design of UHPC is maximising the packing density of ultra-fine particles, thereby minimizing porosity and the water required to fill voids [4, 11]. To optimise the granular skeleton, mathematical models based on continuous particle-size distributions are successfully employed, such as the classical Andreasen model and its modification proposed by Funk and Dinger [11]. Currently, this process is supported by advanced algorithms that divide the grading curve into dozens of fractions to simulate the filling of interstitial spaces between larger grains by smaller ones. Furthermore, UHPC calculations often shift away from the traditional mass-based w/c ratio toward a volumetric water-to-fine-particle ratio, which better reflects the physical packing effects of submicron grains [4, 11].

However, it must be strongly emphasised that analytical design alone is insufficient, as HPC and UHPC mixes are exceptionally complex multi-component systems, often consisting of five or six constituents [8, 9]. The properties of these composites are extremely sensitive to parameters that are difficult to model mathematically, such as the local physicochemical variability of the raw materials. For this reason, the type and precise dosage of special components – particularly superplasticisers – must be established through rigorous laboratory experimentation in each instance. Trial laboratory batches are essential to verify the so-called compatibility between the chosen cement type, silica fume, and the specific liquefying admixture. A lack of such compatibility results in serious technological issues: rapid loss of workability, excessive viscosity that prevents compaction, the entrapment of excessive air (which lowers strength), or a drastic retardation of setting time [9, 11]. Practical experiments also verify the actual water demand of the theoretically composed, ultra-dense system of fine particles. Additionally, the proportions of steel fibres are selected through testing to evaluate their impact on the mix's flowability and homogenisation. The entire design process concludes with

several verification trial batches (at a laboratory scale) to assess the final consistency, the air content of the fresh mix, and the actual properties of the hardened composite. If the results for the hardened and fresh concrete deviate from the assumptions, quantitative corrections are introduced, and the entire procedure is repeated. In summary, an effective HPC/UHPC mix design is a strictly iterative process in which analytical estimates and numerical optimization models serve only as a starting point for the necessary, decisive laboratory verifications and calibrations.

1.3. TECHNOLOGICAL PROCESSES APPLIED TO HPC AND UHPC

In High-Performance Concrete (HPC), the critical technological stage is exceptionally meticulous and intensive wet curing. Due to the use of a very low water-binder ratio, often below 0.30, the dense internal structure rapidly lacks the free water necessary for the full progression of cement hydration. This leads to an intense phenomenon known as self-desiccation, during which water is rapidly drawn from the capillary pores by the still-unhydrated binder grains [7, 10]. This results in immediate and severe autogenous shrinkage (spontaneous) within the first 24 hours alone [3, 9].

The absence of external wet curing at this early stage would lead to the formation of numerous microcracks, drastically reducing the composite's tightness, durability, and mechanical parameters [1, 9]. Consequently, curing consisting of abundant water spraying must commence as soon as possible after placement, typically no later than 10 to 12 hours after casting the element. Fig. 1.6 below illustrates the approximate progression of shrinkage strains, justifying the initiation of intensive wet curing during the very early hardening period [3].

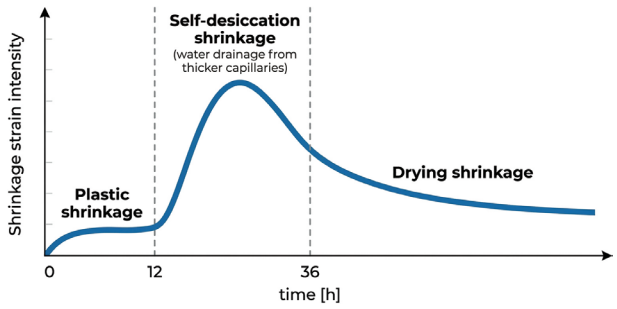

Fig. 1.6. Progression of shrinkage strains during the hardening process of HPC [3]

It is worth emphasizing that traditional film-forming curing compounds (membranes) intended to prevent evaporation are entirely insufficient for HPC. These coatings only protect against moisture loss to the outside (inhibiting drying

shrinkage) but do not compensate for the water deficit induced by destructive internal self-desiccation [3, 11]. The primary goal of proper water curing is, therefore, the continuous physical supply of water from the external environment into the structure, which halts the development of early shrinkage stresses and enables seamless hydration [7, 11]. Crucially, high-performance concrete cured early and abundantly with water may even exhibit slight swelling during the first few days rather than shrink; this is a highly desirable phenomenon that ensures a dense, entirely crack-free matrix [3].

Regarding Ultra-High-Performance Concrete (UHPC), hydrothermal treatment is a widely used technological process that significantly accelerates strength gain, increases ultimate strength, and reduces shrinkage and creep [4]. This process involves subjecting hardened concrete to elevated temperatures under high humidity, which, due to its requirements, is most commonly performed in precasting plants. The standard procedure involves leaving the elements in their moulds for the first 24 hours at approximately 20°C, followed by steam curing at 80–90°C for 48 hours.

During heat treatment, the concrete must be tightly covered (e.g. with foil) to prevent drying; upon completion of the heating cycle, slow cooling of the elements is vital to avoid thermal stresses and microcracking [4]. In specialised applications, process parameters can be even higher, and treatment at 250°C allows for compressive strengths of up to 360 MPa. The primary chemical objective of steam curing is to accelerate and intensify the pozzolanic reaction, during which silica fume reacts with calcium hydroxide (portlandite) to form additional amounts of hard C-S-H gel. As a result, with standard treatment at 90°C, compressive strength typically increases by 20–30 MPa compared to identical specimens cured in water [4]. The result is densification of the microstructure, reducing the material's capillary porosity to approximately 2%. Equally important from an engineering standpoint, after properly conducted heat treatment, further hydration processes in UHPC become negligible, and thus further shrinkage no longer occurs. The result is a finished composite with exceptional dimensional stability, negligible creep, and unparalleled durability [4].

1.4. SUMMARY

High-Performance Concrete (HPC) and Ultra-High-Performance Concrete (UHPC) are innovative composites distinguished by high and ultra-high compressive strength, as well as unprecedented durability and tightness. The binder composition of these concretes relies on a high content of high-grade cements and active mineral additives, such as silica fume. This silica fume physically densifies interstitial spaces between grains and, through its pozzolanic activity, chemically reinforces the cement matrix. To ensure the workability of a mix with such low water

content, the use of modern superplasticisers is essential. These composites employ high-strength crushed aggregates with strictly limited grain sizes; in fine-grained UHPC, coarse aggregate is often entirely replaced by quartz sand. Additionally, to mitigate the inherent brittleness of UHPC, dispersed steel fibre reinforcement is commonly incorporated into the mix.

The design of component proportions is a complex process in which preliminary estimates are based on advanced particle packing models and empirical equations, such as de Larrard's strength equation. However, since multi-component mixes are extremely sensitive to raw material variability, analytical calculations alone are insufficient. Therefore, the final composition must always be determined iteratively through laboratory trial batches, which verify, among other factors, the critical compatibility between selected cement, silica fume, superplasticiser, and other specialised constituents.

REFERENCES

[1] Aïtcin, P. C.: *The Art and Science of Durable High-Performance Concrete*. In Proceedings of the Conference Proceedings "Beton na progu nowego milenium" [Concrete at the Threshold of the New Millennium], Wisła: Stowarzyszenie Producentów Cementu i Wapna, Polski Cement, 2002, pp. 1–30.

[2] Jasiczak, J.; Wdowska, A.; Rudnicki, T.: *High-Performance Concrete*; Kraków: Stowarzyszenie Producentów Cementu, 2008.

[3] Śliwiński, J.; et al.: *New Generation Cement Concretes – Ideas, Design, Technology and Applications*; Śliwiński Jacek, Ed.; materials for students Lifelong Learning Programmes Erasmus, 2010.

[4] Grzybowska, A.: *Wybrane problemy projektowania betonów o niskim stosunku wodno-spoiwowym* [Selected Problems in the Design of Concrete with a Low Water-Binder Ratio]; Wydawnictwa Uczelniane Uniwersytetu Technologiczno-Przyrodniczego w Bydgoszczy, 2015.

[5] Heidelberg Materials: *High-Performance Concrete (Wysokiej Wytrzymałości)*.

[6] Sobczak-Piąstka, J.; Podhorecki, A.: *Niektóre aspekty projektowania betonu wysokowytrzymałego o niskim skurczu* [Certain Aspects of Designing High-Strength Concrete with Low Shrinkage]. Materiały Budowlane, 2014, 7, pp. 36–38.

[7] Fehling, E.; Schmidt, M.; Walraven, J.C.; Leutbecher, T.; Fröhlich, S.: *Ultra-High-Performance Concrete UHPC: Fundamentals, Design, Examples*; Ernst & Sohn, 2014; ISBN 978-3-433-03087-5.

[8] Usherov-Marshak, A.; Ciak, M.J.: *Principles of Modern Concrete Science*. In Proceedings of the Conference Proceedings "Dni betonu – tradycja i nowoczesność" [Concrete Days – Tradition and Modernity], Wisła: Stowarzyszenie Producentów Cementu i Wapna, Polski Cement, 2018, pp. 185–186.

[9] Neville, A.M.: *Properties of Concrete*; London: Pearson Education Limited, 2011; ISBN 978-0-273-75580-7.

[10] Śliwiński J.: *Principles of High-Performance Concrete Mixture Proportioning*. Cement-Wapno-Beton 2003, 6, pp. 317–325.

[11] Górak, P.; Cichy, M.; Jelonkiewicz, P.: *High-Performance Concrete as a Construction Material in Bridge Objects*. In Proceedings of the Conference Proceedings "Dni betonu – tradycja i nowoczesność" [Concrete Days – Tradition and Modernity], Wisła: Stowarzyszenie Producentów Cementu i Wapna, Polski Cement, 2021, pp. 443–459.

[12] Schmidt, M.; Fehling, E.; Geisenhanslüke, C.: *Ultra-High- Performance Concrete (UHPC)*, Proceedings of the International Symposium on Ultra High-Performance Concrete, Kassel, Germany, September 13–15, 2004; Kassel University Press, ISBN 3-89958-086-9.

[13] Olek, J.: *High-Performance Concrete – Review of US Practices*. In Proceedings of the Conference Proceedings "Dni betonu – tradycja i nowoczesność" [Concrete Days – Tradition and Modernity], Wisła: Stowarzyszenie Producentów Cementu i Wapna, Polski Cement, 2002, pp. 1–21.

2

MINERAL FIBRE-REINFORCED MATERIALS PROPERTIES, APPLICATION, AND DESIGN

Tomasz Zdeb

2.1. INTRODUCTION

Numerous examples confirming the use of dispersed reinforcement to strengthen brittle, mineral materials since the times of ancient Rome (300 BCE–476 CE) can be found in literature. Straw was used to reinforce sun-dried bricks, while horsehair was used to strengthen mortar and plaster. In the United States, the Pueblo house is an example of one of the oldest structures (circa 1540) built using sun-dried clay brick technology reinforced with straw fibres. When Portland cement concrete began to gain popularity in the 19th century, attempts were made to improve it by adding fibres. The first patent for fibre-reinforced concrete (FRC) was filed in California by Bernard in 1874, who proposed using iron scrap in the concrete mix. A few decades later, asbestos fibres began to be used commercially. Construction products made from this material were widely used worldwide, especially in the 1960s. Currently, due to negative health impacts, a total ban on asbestos has been in force in the EU since 2005. In the case of Poland, the production of cement composite products with asbestos fibres has been banned since 1997, and the "National Asbestos Removal Program" was launched in 2009, scheduled for completion in 2032.

The first attempts to use glass fibres in concrete were made in the late 1950s. It was determined that ordinary glass fibres are unstable due to reactions with alkalis in the cement paste. Research into alkali-resistant glass led to the development of glass containing zirconium oxide, often designated as AR (Alkali Resistant). Today, this solution is widely used in commercial products. Initial attempts to use synthetic fibres such as PE (polyethylene) or PP (polypropylene) in concrete were not as spectacular as in the case of glass or steel fibres. However, advancements in the principles of fibre reinforcement and new manufacturing methods have led researchers to conclude that both synthetic and natural fibres can effectively not only strengthen concrete but also increase its durability.

Extensive research and industrial development of Fibre Reinforced Concrete (FRC) are taking place worldwide. Industrial interest and potential business opportunities are confirmed by continuous new achievements in the field of fibre-reinforced building materials. These developments are described in numerous scientific articles and state-of-the-art reports published by industry associations such as RILEM or ACI. The growing interest in reinforcing concrete with dispersed reinforcement can be traced by analysing the chart below, generated in 2026 from the ScienceDirect database, showing the number of publications related to the keyword FRC.

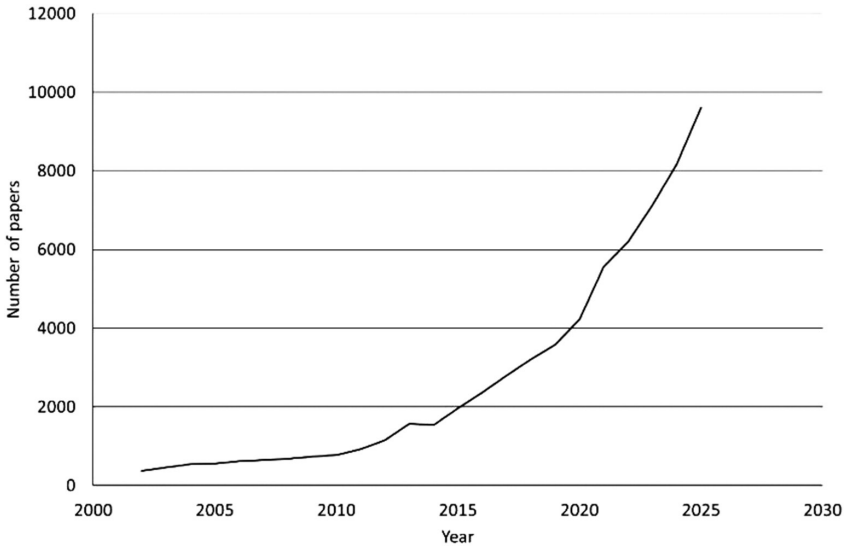

Fig. 2.1. Number of publications for the keyword "fibre reinforced concrete" based on ScienceDirect database (2026)

The use of Fibre Reinforced Concrete (FRC) offers a range of significant structural benefits, the most important of which is the transformation of concrete's behaviour from a brittle to a ductile material. This allows for energy absorption and the preservation of structural load-bearing capacity even after cracking occurs. The fibres create a three-dimensional reinforcement system that effectively controls the initiation and propagation of cracks resulting from plastic shrinkage during the early hardening phase and drying shrinkage in the long term.

Through the crack-bridging mechanism, the composite gains high residual strength, enabling stress distribution even in the post-cracking state. An additional advantage is the significant improvement in parameters such as impact strength, fatigue strength, and abrasion resistance, which contribute to increased durability of real structures. Polypropylene microfibres play a special role as a form of passive fire protection, preventing explosive spalling of concrete by creating escape channels for water vapour.

Despite its numerous advantages, this technology also has certain drawbacks and limitations. A key challenge is the reduction in workability of the mix, which often requires adjusting the composition with superplasticisers. Incorrect dosing or an improper an improper fibre aspect ratio leads to the risk of "balling" – the formation of fibre conglomerates that prevent the achievement of a homogeneous composite. In the case of steel fibres, a significant disadvantage is their susceptibility to surface corrosion, which can lead to unsightly rust stains on facades. Furthermore, steel dispersed reinforcement accelerates the wear of mixing and pumping machinery due to its abrasive properties [1–4].

2.2. FACTORS AFFECTING THE EFFICIENCY OF DISPERSED REINFORCEMENT IN CONCRETE

The effectiveness of fibres in concrete depends on a range of factors related to both their properties and the method of their incorporation into the mix. Proper fibre dispersion is of key importance, which is influenced by correct packaging, dosing, quantity, and control of mixing intensity. Appropriate selection of these factors ensures homogeneity and eliminates the risk of clumping.

Equally important is the anchorage of the fibres within the cement matrix – high bond strength and the ability to transfer loads determine the overall reinforcement efficiency. The choice of fibre material, such as steel, polypropylene, glass, or cellulose, affects their durability and mechanical properties. Furthermore, the geometry and shape of the fibres cannot be overlooked, as parameters such as length, diameter, and aspect ratio also determine the effectiveness of the reinforcement.

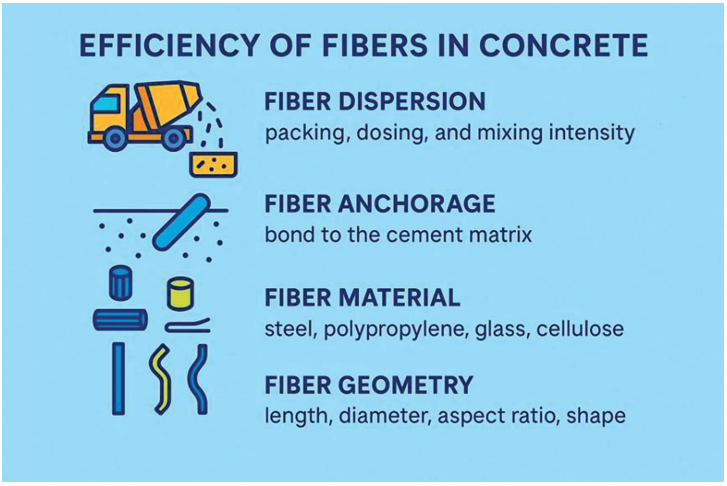

Fig. 2.2. Factors affecting the efficiency of dispersed reinforcement in cement composites

2.2.1. TYPES OF FIBRE MATERIALS

Steel fibres (Steel Fibre Reinforced Concrete – SFRC) represent the largest and most widely used group of dispersed reinforcement used in engineering practice. They are primarily manufactured from cold-drawn wire, cut sheet metal, or metal alloys, with tensile strengths ranging broadly from 400 to as much as 2500 MPa. A key feature of these fibres is their geometry; they can be straight, corrugated, or hooked-end, designed to enhance mechanical anchorage in the concrete matrix and prevent premature pull-out. The primary function of steel fibres is to transform

concrete behaviour from brittle to ductile, allowing the material to carry significant loads even after cracking. Due to their high modulus of elasticity (approx. 210 GPa), these fibres work excellently with the cement matrix, improving impact strength and fatigue resistance, making them an ideal solution for industrial floors, tunnel linings and foundation slabs.

Glass fibres are distinguished by high physical parameters and are approximately 75% lighter than traditional steel reinforcement. In concrete technology (Glass Fibre Reinforced Concrete – GFRC), only glass with enhanced resistance to alkaline environments is used, most commonly with the addition of zirconium oxide (AR-type glass). These fibres are characterised by very high tensile strength (1500–4000 MPa) and are hydrophobic and chemically inert. Their decisive advantage is the lack of susceptibility to corrosion, which eliminates the need for thick concrete covers and allows for the creation of thin-walled, aesthetic facade elements with minimal thickness. During production, glass fibres can be introduced into the matrix as chopped, continuous, or in the form of mats; their presence not only improves the mechanical properties of composites but also effectively reduces plastic shrinkage cracking.

Synthetic and polymer fibres (Polymer Fibre Reinforced Concrete – PFRC) are divided into microfibres and structural macrofibres. Microfibres, most commonly polypropylene (PP) with a diameter below 0.30 mm, primarily serve to control shrinkage cracks during the early hardening phase and act as passive fire protection. In contrast, synthetic macrofibres, with larger diameters and specifically textured (embossed) surfaces, function as structural reinforcement, increasing the post-cracking load-bearing capacity of the concrete and are capable of replacing traditional reinforcing meshes. Polymeric materials are entirely corrosion-resistant (to acids and alkalis), making them ideal for the construction of tanks, pipes, and structures in aggressive chemical environments.

Natural fibres (Natural Fibre Reinforced Concrete – NFRC) are the oldest type of dispersed reinforcement, utilised since antiquity in the form of straw or animal hair. Today, this group includes plant fibres such as coconut, bamboo, jute, flax, or sisal, as well as cellulose fibres obtained through industrial processes. They are environmentally friendly, renewable, and inexpensive, which makes them attractive for low-cost construction in developing countries. Although they possess good mechanical properties, their main disadvantage is susceptibility to biodeterioration and degradation in the highly alkaline environment of concrete. Research shows that their durability can be improved by chemical coating or by replacing part of the cement with silica fume, which reduces the alkalinity of the matrix.

Carbon and basalt fibres are modern materials with the highest strength parameters. Carbon fibres used in (Carbon Fibre Reinforced Concrete – CFRC) contain at least 92% carbon and are characterised by extremely high tensile strength, up to 4000 MPa and a very high modulus of elasticity. Their unique feature is

electrical conductivity, which allows for the creation of self-deicing concretes or those acting as stress sensors within the structure. Basalt fibres (BFRC), obtained from melted basalt, are entirely natural and resistant to corrosion, acids, and alkalis. They are lightweight (about three times lighter than steel) and characterised by high hardness, resulting in increased abrasion resistance and resistance to dynamic loads. Both fibre groups are resistant to extreme temperatures and material fatigue; however, due to relatively high production costs, their use is currently limited to specialised engineering structures, repairs, retrofitting, and elements with the highest durability requirements [1–4].

The table below provides a comparison of the most commonly used fibres in FRC-type composites, along with their most significant physical and mechanical properties.

Table 2.1. Physical and mechanical properties of common fibres in FRC composites

Fibre Material	E-Modulus [GPa]	Tensile Strength [MPa]	Strain to Rupture [%]	Density [g/cm^3]
Steel (normal)	210	500–2000	3–4	7.84
Polypropylene (PP)	1.5–4.2	240–550	20	0.91
Polyvinyl alcohol (PVA)	20–42	1100–1600	6	1.31
Basalt	50–90	700–2100	0.5–1.6	1.7–3.2
Glass fibres	80	2500	5	2.7
Carbon fibres	300	4000–4500	1.5	1.7
Natural Sisal	9–22	600–700	2-3	1.3–1.5
Cellulose fibres	10	300–500	–	1.2

2.2.2. INFLUENCE OF FIBRE SHAPE AND GEOMETRY ON ITS ANCHORAGE

Fibre anchorage in concrete is a critical factor determining the effectiveness of dispersed reinforcement in cement composites. Geometric parameters and fibre shape influence the force transfer mechanism, pull-out resistance, and the ability to bridge cracks in the tension zone. Fibre geometry, and specifically the ratio of length l_f to diameter d_f, known as the aspect ratio, plays a vital role in the anchorage process. Fibres with a high aspect ratio (long and thin) provide superior force transfer in hardened concrete, as their greater length allows for deeper anchorage within the cement matrix. Experimental data indicate that the optimal aspect ratio range lies between 40 and 80, ensuring a proper balance between reinforcement efficiency and ease of mixing.

$$\text{Aspect Ratio} = \frac{l_f}{d_f} \tag{2.1}$$

However, an excessively high aspect ratio can cause issues in the fresh mix – fibres tend to entangle, leading to non-uniform distribution. Conversely, short and thick fibres (low aspect ratio) disperse well in the mix, but their ability to bridge cracks in hardened concrete is limited.

The fibre shape determines the anchorage mechanism and pull-out resistance. Straight fibres have a limited capacity for force transfer because their anchorage relies primarily on surface adhesion. To increase efficiency, deformed fibres are used, depending on the material type. Such modifications increase resistance during fibre pull-out from the concrete, which enhances crack-bridging capacity and improves the tensile strength of the composite.

Regarding the most common materials used for manufacturing fibres – namely steel and polymers – European standards have been established. These not only define shape types but also the range of other properties that manufacturers must declare: EN 14889-1 Fibres for concrete – Part 1: Steel fibres – Definitions, specifications, and conformity [5] and EN 14889-2 Fibres for concrete – Part 2: Polymer fibres – Definitions, specifications, and conformity [6].

For steel fibres, five groups are distinguished based on their origin:

Group I – cold-drawn wire;

Group II – cut sheet;

Group III – melt extracted;

Group IV – shaved cold-drawn wire;

Group V – milled from blocks.

For synthetic fibres, three classes are distinguished:

Class Ia – microfibres (d < 0.3 mm, monofilamented);

Class Ib – microfibres (d < 0.3 mm, fibrillated);

Class II – macrofibres (d > 0.3 mm, monofilamented).

The most common fibre shapes are presented in the table below. In both cases (steel and synthetic), manufacturers are required to declare other essential properties such as density, tensile strength, modulus of elasticity, effect on the consistency of the concrete mix, and the effect on the residual strength of the reference concrete. Additionally, for synthetic fibres, information regarding the melting point and flash point must be provided.

However, it should be emphasised that excessive bond strength between the fibre and the matrix can lead to fibre rupture, which occurs when its tensile strength is exceeded. This phenomenon is critical in the context of composite design, as it indicates the necessity of a balance between adhesion force and the tensile strength of the fibre. This balance is used to determine the so-called critical fibre length L_c (see the fig. 2.3 and equations (2.2)–(2.6) below).

Table 2.2. Commonly used configurations and geometries of steel and synthetic fibres in FRC [7]

SYNTHETIC FIBRES			
MICRO-FIBRES		MACRO-FIBRES	
Mono-filamented		Embossed	
Fibrillated		Undulated	
STEEL MACRO-FIBRES			
Group I – Cold-drawn wire		Group II – Cut sheet	
Hooked	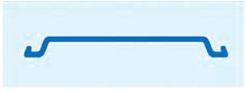	Hooked	
Flat end		Flat end	
Undulated		Undulated	
Twisted		Straight	
Group III – Melt extract		Group V – Milled from blocks	
			

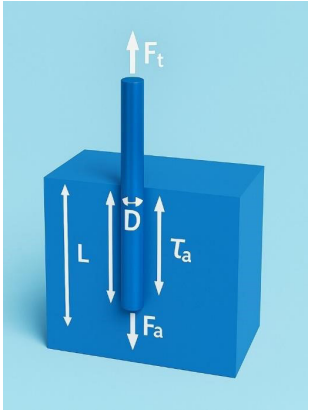

Fig. 2.3. The distribution of forces and stresses in the fibre-reinforced composites

$$F_t = F_a \tag{2.2}$$

In the case of cylindrical fibre:

$$f_t \cdot \pi \cdot \frac{D^2}{4} = \tau_a \cdot \pi \cdot D \cdot L \tag{2.3}$$

$$L = \frac{f_t \cdot D}{4 \cdot \tau_a} \tag{2.4}$$

Critical length of cylindrical fibre:

$$L_c = 2 \cdot L = \frac{f_t \cdot D}{2 \cdot \tau_a} \tag{2.5}$$

Critical length of any fibre shape:

$$L_c = \frac{2 \cdot A \cdot f_t}{\tau_a \cdot P_f} \tag{2.6}$$

where:
F_t – fibre rupture force,
F_a – adhesion force between fibre and matrix,
D – fibre diameter,
L – fibre anchorage length,
L_c – fibre critical length,
A – fibre cross-sectional area,
P_f – fibre perimeter,
f_t – fibre tensile strength,
τ_a – tangential stress (adhesion).

The above relationships indicate that the critical fibre length depends on its diameter. With a very limited diameter D, the fibre can be significantly shortened due to the reduction in the force required to cause fibre rupture. Conversely, large-diameter fibres require a much greater force – and thus a longer anchorage length – to be broken. This raises the question of what fibre length should be used, assuming a constant volume fraction of dispersed reinforcement in the concrete V_f.

An explanation can be found in the figure below, which illustrates the roles of short and long fibres. Short ones are responsible for bridging emerging micro-cracks, but they play no significant role when larger cracks propagate. On the other hand, long fibres bridge numerous micro-cracks to a negligible extent due to their lower count (lower number of fibres for the same volume), but they play a fundamental role in the case of large crack widths [7, 8].

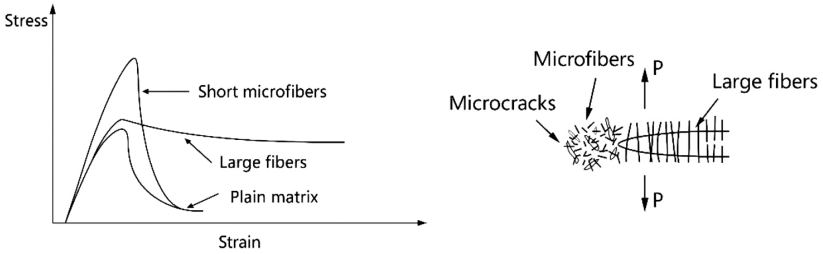

Fig. 2.4. The role of short and long fibres in FRC [9]

2.2.3. FIBRE DOSAGE

The dosage level of various types of fibres added to the concrete mix is defined as the volume fraction V_f and typically does not exceed a few percent. Specific dosages depend on the material type and the desired properties.

- Steel fibres in structural applications are most commonly used in the range of 20–40 kg/m^3. Research indicates that a significant impact on compressive strength appears at a content of approximately 1.5% by volume. The upper safe limit for typical concretes is considered to be 2.0%, although in Ultra-High-Performance Concrete (UHPC), these dosages can reach 5–9%.
- Polypropylene microfibres are mainly used to reduce plastic shrinkage in dosages of 0.6–0.9 kg/m^3. For fire protection (preventing explosive spalling), a dosage of approximately 2 kg/m^3 is recommended.
- Polypropylene macrofibres used as structural reinforcement are typically dosed in amounts of 3–6 kg/m^3 (0.5–1.0% vol.).
- Glass fibres (GFRC) used in the spray-up process are applied at a minimum of 4% by weight, while in the premix process, manufacturers state the possibility of mixing up to 5% of fibres without the clumping effect.

Fibres that are too long or thin (aspect ratio above 100) show a strong tendency toward the previously mentioned "balling" phenomenon – the formation of entangled lumps that prevent uniform reinforcement distribution. A key rule is never to add fibres as the first ingredient into an empty mixer. Sources indicate several effective methods of fibre incorporation, including dosing onto the aggregate during conveyor transport to the mixer, which promotes preliminary dispersion. The second, more common method is dosing into the ready-mixed concrete. In truck mixers, fibres should be added slowly while the drum is at full speed. It is recommended to mix for a minimum of 5 minutes after all components have been added.

It should also be noted that the addition of fibres increases the specific surface area of the ingredients that must be coated by the cement paste, resulting in a decrease in workability but an increase in the cohesion of the mix. This effect should not be corrected by adding water, but rather by using plasticisers and superplasticisers. At high fibre dosages, the entrapped air in the mix should also be monitored, as fibres hinder the free escape of air bubbles during compaction [1–4, 7, 10].

2.3. MITIGATING THE DRAWBACKS OF ORDINARY CONCRETE THROUGH THE USE OF DISPERSED REINFORCEMENT

2.3.1. SHRINKAGE REDUCTION

Fibres limit concrete shrinkage primarily by controlling the initiation and propagation of cracks, both in the early stage (plastic shrinkage) and in the long term due to drying shrinkage. The primary mechanism of dispersed reinforcement is crack bridging, where fibres crossing a formed gap take over the tensile stresses that the cement matrix is unable to sustain. Fibres restrict crack propagation by transferring the forces occurring in the crack tip region.

The incorporation of fibres changes the nature of shrinkage cracks. Instead of a few wide and dangerous cleavages, a system of densely distributed micro-cracks is formed. In the fresh concrete mix, fibres additionally act as an internal suspension system that mechanically supports the aggregate grains, effectively limiting their sedimentation and the phenomenon of bleeding (water accumulation on the surface).

Furthermore, fibres increase the early-age tensile strength of the concrete, allowing it to more effectively resist stresses caused by the rapid evaporation of moisture from the surface [1, 7].

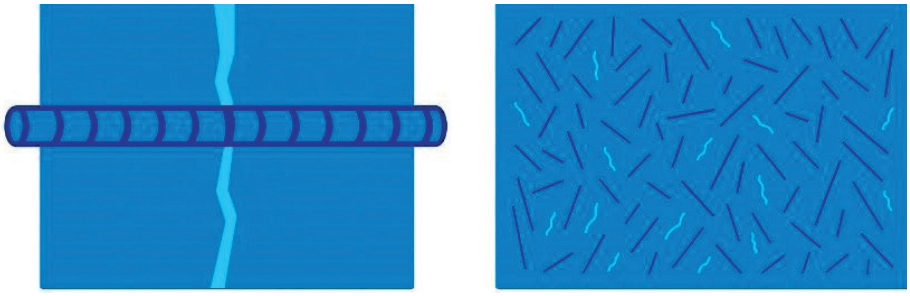

Fig. 2.5. Crack patterns induced by tensile stress distribution in standard and fibre-reinforced composites under binder shrinkage

2.3.2. IMPROVEMENT OF MECHANICAL PROPERTIES

The primary objective of adding steel fibres to concrete is the improvement of its mechanical properties. Plain concrete is known for its low tensile strength, where the ratio of tensile strength f_t to compressive strength f_c is estimated at 1/10. Unfortunately, as concrete strength increases, this proportion becomes even less

favourable; in the case of High-Performance Concrete (HPC) with a strength of approximately 140 MPa, the f_t/f_c ratio is about 1/15. Furthermore, for Ultra-High-Performance Concrete (UHPC), such as Reactive Powder Concrete (RPC), whose strength exceeds 200 MPa, this ratio oscillates around 1/20. This relationship was described by Raphael using the following equation [11]:

$$f_t = 0.3 \cdot f_c^{\frac{2}{3}} \tag{2.7}$$

The indicative influence of structural steel fibres on the mechanical and technological properties of concrete is summarized in Table 2.3. Their effectiveness depends, among other factors, on the properties and volume fraction V_f of the fibres, their geometry, and their adhesion to the cement composite matrix. An analysis of numerous research results indicates that tensile strength, determined through both flexural and axial tension tests, improves significantly in the presence of fibres. This also applies to resistance against dynamic mechanical loading and fatigue strength.

Conversely, compressive strength, modulus of elasticity, and Poisson's ratio do not change significantly with the addition of dispersed reinforcement. It has been shown that compressive strength may increase only by up to approximately 15% at a fibre content V_f = 2%. However, it is important to note that since the presence of fibres generally impairs the workability of the concrete mix during the manufacturing stage, it may lead to an increase in entrapped air content, which in turn may reduce the mechanical properties of the composite [7, 10].

Table 2.3. Indicative influence of dispersed reinforcement on the properties of FRC

Feature	Effect of dispersed reinforcement
Tensile strength at bending	↑
Axial tensile strength	↑
Residual strength	↑
Fatigue strength	↑
Compressive strength	↗/→
Bulk density	↗/↘
Modulus of elasticity	→/↘
Workability of concrete mixture	↓
Entrapped air	↗
Electrical resistivity	↘

In the case of increasing tensile stresses in an element made of plain concrete, the appearance of a crack leads to its rapid propagation, resulting in brittle failure. Conversely, the presence of fibres can prevent this phenomenon by inducing a so-called pseudo-plastic failure mode. This effect is associated with several interaction mechanisms between the dispersed reinforcement and the concrete matrix, as presented in the figure below.

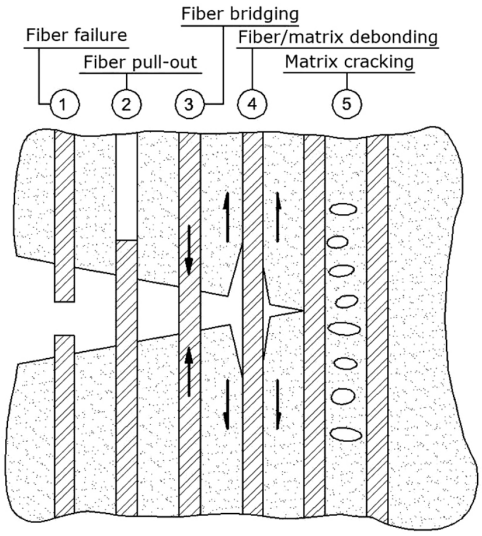

Fig. 2.6. Interaction mechanisms between dispersed reinforcement and the cement matrix [12]

Taking into account all the fibre-matrix interaction mechanisms illustrated above, as well as other dispersed reinforcement parameters – namely their length, diameter, shape, and finally volume fraction – the resulting failure mode of an FRC structural element can exhibit diverse characteristics. This can be illustrated by a three-point bending test, where a load is applied to the centre of a concrete beam's span. In all cases, a linear load-deflection relationship is initially observed up to the LOP (Limit of Proportionality) point, where the uncracked matrix works in conjunction with the dispersed reinforcement. The higher modulus of elasticity of the fibres enables the distribution of tensile stresses before cracking.

Depending on the adopted reinforcement parameters, two fundamentally different behaviours of the tested element can be expected in the post-cracking region: strain-hardening, where the limit of proportionality is lower than the Modulus of Rupture LOP < MOR, or conversely, strain-softening, where LOP > MOR. For obvious reasons, the former is the safest failure mode for a reinforced structural element [7].

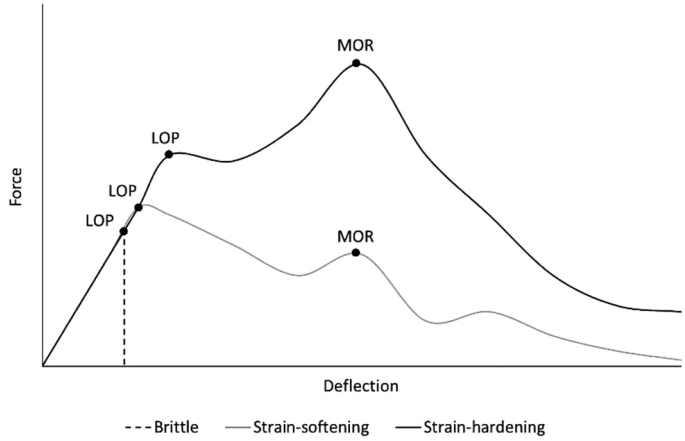

Fig. 2.7. Qualitative evaluation of fibre reinforcement effectiveness, LOP > MOR strain-softening material, MOR > LOP – strain-hardening material

2.3.3. IMPROVEMENT OF DURABILITY UNDER FIRE CONDITIONS

The phenomenon of explosive spalling occurs most frequently in high-strength (HPC) and ultra-high-performance (UHPC) dense concretes, where the compact pore structure blocks the escape of moisture during a fire. Under conditions of rapid temperature increase, the water trapped inside the material turns into superheated steam, generating enormous internal pressure. Once this pressure exceeds the tensile strength of the composite, it leads to violent failure, typically manifested by the detachment of concrete fragments of various sizes.

Polypropylene (PP) fibres eliminate this hazard through several interacting mechanisms. The first involves the melting of PP fibres at a relatively low temperature of approximately 160–170°C. When the internal temperature of the element reaches this level, the melted fibres leave behind a network of tiny, empty micro-channels in the concrete matrix. These channels act as an evacuation system, allowing the superheated steam to safely evaporate to the outside. Consequently, internal pressure is reduced to a safe level, preventing the concrete structure from bursting.

The literature also describes a phenomenon involving the initiation of micro-cracks caused by the higher thermal expansion of PP fibres compared to the cement paste. These micro-cracks connect with the channels left by the melted fibres, creating an even more efficient system for steam release and pressure reduction. The use of PP fibres is considered a form of passive fire protection, as the reinforcement is an integral part of the concrete and requires no external activation in the event of a fire. To effectively counteract spalling, a dosage of monofilament polypropylene microfibres at approximately 2 kg/m^3 is recommended. Research indicates that in

this process, shorter fibres (e.g. 12 mm) often exhibit greater efficiency than longer ones (e.g. 20 mm). This technology is widely used in underground construction, such as tunnel linings, to ensure structural integrity at extreme temperatures [1, 2, 4].

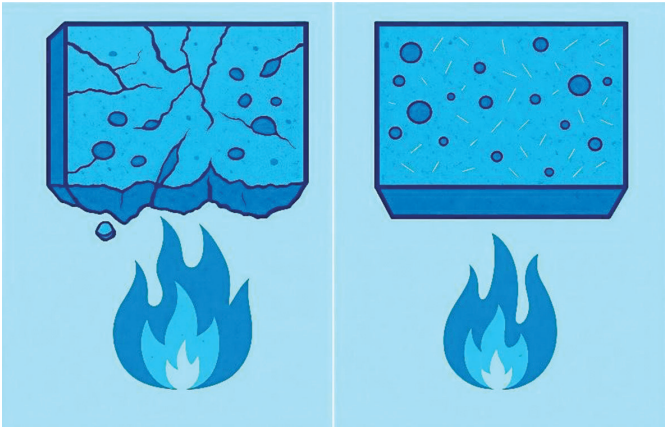

Fig. 2.8. Comparison of spalling mechanisms in plain concrete and PP fibre-reinforced concrete

2.4. METHODS FOR EVALUATING THE EFFICIENCY OF DISPERSED REINFORCEMENT – FRC TESTING

Testing of the mechanical properties of FRC primarily focuses on determining the interaction between the fibres and the concrete matrix, both before and after the onset of cracking. In most cases, these tests are conducted using three-point or four-point bending configurations, either with or without a pre-initiated crack (notch). Due to the necessity of recording post-critical stresses (following the cracking of the matrix), a common feature of all FRC composite bending tests is a constant rate of deformation increment (in the case of bending – deflection) as a function of time. This differs from the testing of brittle materials such as plain concrete, ceramics, or natural stone, where the test speed is typically defined by the rate of stress increase over time, usually in units of MPa/s.

Testing in accordance with EN 14651 standard [13] involves recording the relationship between the force F acting on the specimen and the CMOD (Crack Mouth Opening Displacement) parameter during a three-point bending test of a notched specimen. Based on the F-CMOD relationship, parameters such as the Limit of Proportionality (LOP) and residual strength values are determined for specific crack openings specified in the standard, namely at 0.5, 1.5, 2.5, and 3.5 mm. An alternative method involves measuring the beam deflection δ at mid-span and analysing the F–δ graph. There is a linear relationship between the CMOD and δ values, described by the following formula:

$$\delta = 0.85 \cdot \mathrm{CMOD} + 0.04 \tag{2.8}$$

The specimen should have a square cross-section with a side length of 150 mm and a total length ranging from 550 to 700 mm. A notch with a depth of 25 mm must be made at the beam's mid-span. During the test, the support span (distance between support axes) should be 500 mm. The support geometry and the measurement method are shown in the schematic below.

In a similar JCI-S-002 method [14], the beam dimensions depend on the fibre length. For fibres shorter than 40 mm, it is permitted to use a square cross-section with a side length of at least 100 mm. Strength parameters are calculated using the following formula:

$$f_{Rj} = \frac{3F_j l}{2bh_{sp}^2} \tag{2.9}$$

where:

f_{Rj} [MPa] – residual flexural tensile strength at CMOD = 0.5, 1.5, 2.5, 3.5 mm,
F_j [N] – load corresponding to CMOD = 0.5, 1.5, 2.5, 3.5 mm,
l [mm] – span length,
b [mm] – width of the specimen,
h_{sp} [mm] – distance between the tip of the notch and the top of the specimen.

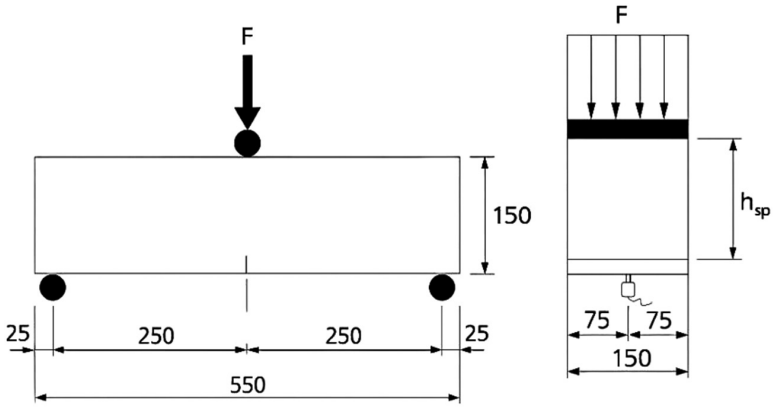

Fig. 2.9. Scheme of the three-point bending test according to the standard EN 14651 [13]

Example FRC test results are presented in the chart below. The graph shows a sample load-CMOD relationship with highlighted characteristic points, which are used to determine the Limit of Proportionality (LOP) stress that causes cracking of the concrete matrix, as well as the force values at crack openings specified by the standard. These parameters serve to calculate the residual strength values f_{Rj}.

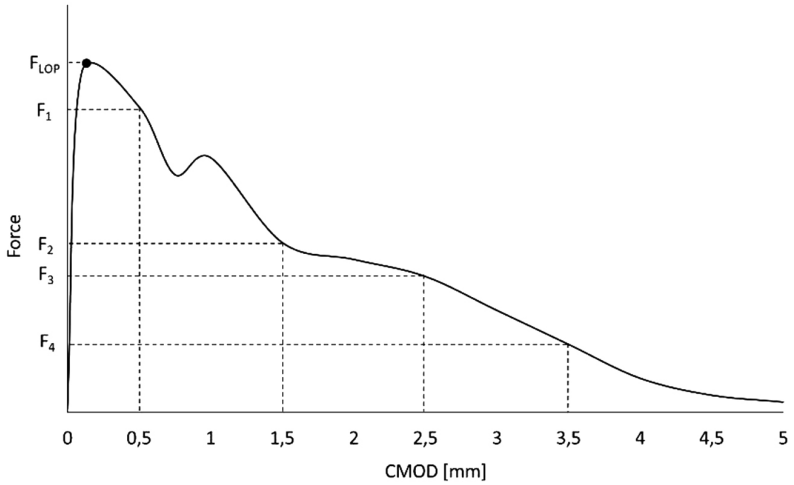

Fig. 2.10. Representative results of the FRC beam bending test according to EN 14651

Conceptually, the analysis of the flexural strength of shotcrete according to EN 14488-3 Testing of shotcrete – Part 3: Flexural strength (at first peak, maximum and residual) of fibre-reinforced beam samples (Method B) [15] is quite similar to the method described above.

Test specimens are produced using the spraying method in a mould measuring 100 x 600 x 600 mm. The square slab specimen is notched on the underside to a depth of 10 mm at the centre of its width. During the three-point bending test shown in the figure below, the F-CMOD relationship is measured, similarly to the EN 14651 method. Based on this relationship, force values are determined at crack openings of CMOD = 0.5, 1.5, 2.5, and 3.5 mm. The residual strength is calculated using the same formula as in the EN 14651 standard [13].

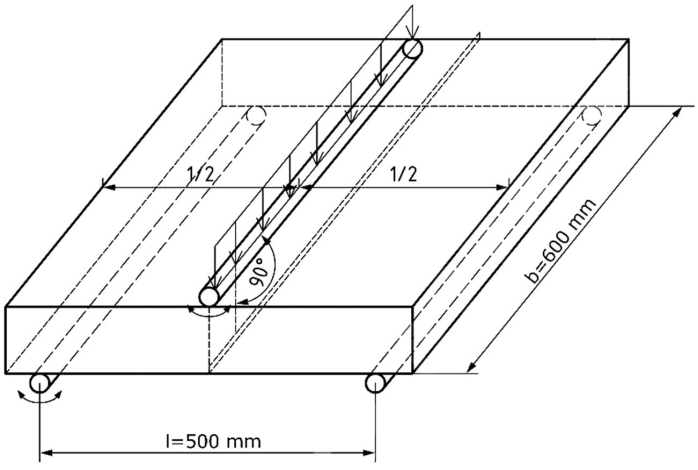

Fig. 2.11. Three-point bending test configuration for slab specimens according to EN 14488-3 [15]

A completely different approach to determining the efficiency of dispersed reinforcement in concrete elements is presented in EN 14488-5 Testing sprayed concrete – Part 5: Determination of energy absorption capacity of fibre reinforced slab specimens [16]. The test involves determining the energy absorbed during the bending of a square slab with dimensions of 600 x 600 x 100 mm.

Table 2.4 . Ductility classes according to EN 14487-1 [17]

Ductility class	Energy absorption [J]
A	500
B	700
C	1000

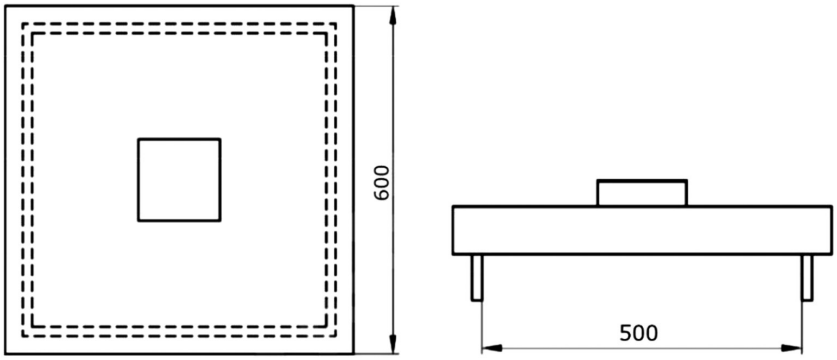

Fig. 2.12. Scheme of the FRC slab bending test according to EN 14488-5 [16]

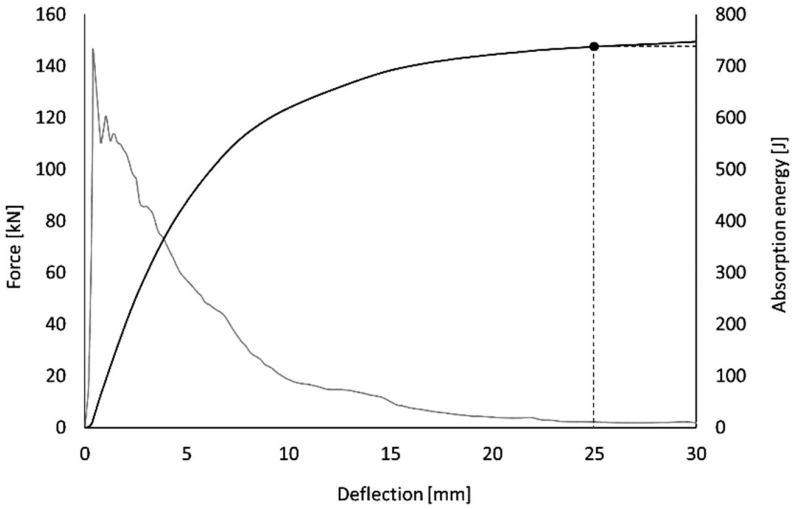

Fig. 2.13. Representative results of the FRC slab bending test according to EN 14488-5

The specimen is placed on a rigid square support frame. A point load is applied to the upper surface of the slab via a 100 x 100 mm square steel block. Electronic transducers are used to measure the specimen's deflection as the load increases, which is controlled by the deflection rate of the slab at 1 mm/min. The test concludes when the deflection exceeds 30 mm. The concrete's energy absorption capacity in joules is determined by integrating the load-deflection curve F–δ in the range from 0 to 25 mm. The final value of the energy consumed to produce a deflection of 25 mm is evaluated against the criteria of EN 14487-1 Sprayed concrete – Part 1: Definitions, specifications, and conformity [17].

2.5. APPLICATIONS OF FRC

The most widespread application of fibre-reinforced concrete is in industrial floors and slabs-on-grade. In these structures, dispersed reinforcement allows for the effective redistribution of internal forces after cracking. Steel and synthetic fibres are also commonly used in the construction of road, bridge, and airfield pavements, where enhanced fatigue resistance and dynamic load capacity are crucial. The use of fibres in these structures enables the reduction of traditional steel meshes, significantly accelerating project execution and lowering total costs.

FRC composites also play a vital role in underground construction, particularly in tunnel linings and the reinforcement of mine workings. It is frequently utilised in shotcrete (sprayed concrete) technology, where it eliminates the need for labour-intensive installation of reinforcing meshes on uneven surfaces. This material is also applied in hydraulic structures such as tanks and dams, as well as in seismic-resistant structures due to its ability to absorb significant amounts of energy during tremors. Furthermore, it is used in the construction of nuclear power plants and bunkers, where the highest degree of safety and impact resistance is required.

In the precasting sector, fibres allow for the manufacturing of thin-walled elements, shells, and building roof structures that would be impossible to produce using traditional reinforcing bars. An example of an advanced application is facade panels made of Reactive Powder Concrete (RPC) reinforced with steel fibres. FRC is also used for the production of precast pipes, piles, columns, and tunnel segments (tubbing) [1–4, 7, 10].

REFERENCES

[1] Hassan H.Z., Saeed N.M., Fiber reinforced concrete: a state of the art, Discov. Mater. 4 (2024). https://doi.org/10.1007/s43939-024-00171-w.

[2] Paul S.C., van Zijl G.P.A.G., Šavija B., Effect of fibers on durability of concrete: A practical review, Materials 13 (2020) 1–26. https://doi.org/10.3390/ma13204562.

[3] Daniel J.I., Gopalaratnam V.S., et al., State-of-the-Art Report on Fiber Reinforced Concrete, 2001.
[4] Sayyad A.S., Sayyad R.A., A review of research on fiber reinforced concrete, 2023.
[5] EN 14889-1:2007, Fibres for concrete – Part 1: Steel fibres – Definitions, specifications, and conformity.
[6] EN 14889-2:2007, Fibres for concrete – Part 2: Polymer fibres – Definitions, specifications, and conformity.
[7] Taylor D., Rieger C., Atkinson T., SikaFiber® Reinforced Concrete Handbook, 2025.
[8] Mujalli M.A., Dirar S., Mushtaha E., Hussien A., Maksoud A., Evaluation of the Tensile Characteristics and Bond Behaviour of Steel Fibre-Reinforced Concrete: An Overview, Fibers 10 (2022). https://doi.org/10.3390/fib10120104.
[9] Betterman L.R., Ouyang C., Shah S.P., Fiber-Matrix Interaction in Microfiber-Reinforced Mortar, 1995.
[10] Glinicki M.A., Beton ze zbrojeniem strukturalnym, Szczyrk 2010.
[11] Neville A.M., Właściwości betonu, 4th ed., Polski Cement, 2000.
[12] Zollo R.F., Fiber-reinforced Concrete: An Overview after 30 Years of Development, 1997.
[13] EN 14651+A1:2007, Test method for metallic fibre concrete – Measuring the flexural tensile strength (limit of proportionality (LOP), residual).
[14] JCI-S-002-2025, Method of test for load-displacement curve of fiber reinforced concrete by use of notched beam.
[15] EN 14488-3:2024-25, Testing sprayed concrete – Part 3: Flexural strengths (first peak, ultimate and residual) of fibre reinforced beam specimens.
[16] EN 14488-5:2008, Testing sprayed concrete – Part 5: Determination of energy absorption capacity of fibre reinforced slab specimens.
[17] EN 14487-1:2023-24, Sprayed concrete – Part 1: Definitions, specifications, and conformity.

3

SELF-COMPACTING CONCRETE – PROPERTIES, APPLICATIONS, AND COMPOSITION DESIGN

Maciej Urban

3.1. INTRODUCTION

Self-compacting concrete (SCC) is a type of concrete that consolidates under its own weight (i.e. without external force) in any formwork shape – even complex ones – without losing stability or homogeneity.

The properties of SCC in its fresh state (before the cement reaches its initial setting time) are so unique that the EN 206 standard treats it as a separate domain. Therefore, specific criteria for assessing SCC properties have been established, along with dedicated testing methods for its fresh properties (EN 12350, Parts 8–12). These methods are discussed in the first part of this chapter.

Due to its unique properties, particularly the ease of achieving high-quality production in demanding situations such as highly reinforced structural elements, architectural concrete, and high-speed placement, the potential applications of SCC are very broad. For this reason, both a brief description of its properties and selected applications are included in this chapter.

The differences between SCC and conventional concrete, in terms of transport and placing technology, are so significant that they may be considered almost contradictory systems. This issue is discussed in the next part of the study.

Achieving the unique properties of SCC and satisfying the criteria of self-compactability requires substantial changes in mixture design strategies compared with traditional concrete. Consequently, both design efficiency (a quick and repeatable procedure that yields satisfactory results) and economic efficiency (minimising the cost of SCC) are central challenges in SCC technology. Although SCC has been available on the market for more than twenty years, its mixture-design procedures remain under discussion, and no consensus exists regarding either the overall design strategy or the detailed solutions used in practice. Therefore, this study presents a brief overview of the main approaches to SCC mixture design and describes in detail the method developed by the author.

In terms of hardened properties, SCC is generally similar to traditional concrete, and therefore there is no need to establish separate design rules for this material in standards such as **EN 206**. Any differences that do occur usually result from variations in mixture composition. For this reason, a short summary of hardened properties is presented at the end of the chapter following the description of SCC mixture design.

All tests and procedures described below conform to the European standardization system.

3.2. BASIC PROPERTIES OF FRESH SCC

Almost all differences between conventional concrete and SCC concern the fresh state. In the case of general-purpose conventional concrete, it is typically sufficient to define and verify only one basic property in the fluid state, namely the consistency range, and the concrete may then be accepted for use. In the case of SCC, however, the acceptance criteria are far more complex, as four independent requirements must be satisfied simultaneously.

3.2.1. SELF-DEAERATION (SELF-COMPACTION) / FLUIDITY

Self-deaeration is the ability of a concrete mix to remove entrapped air bubbles from its entire volume without the use of external forces, *i.e. solely under the action of gravity and buoyancy.* This requirement is relatively easy to satisfy because it is directly related to the fluidity of the concrete mixture. In practice, this means that SCC must be sufficiently fluid to flow easily and enable efficient deaeration.

This property is measured according to EN 12350–8 regulations. The standard Abrams cone ($d_b = 200$ mm, $d_t = 100$ mm, $H = 300$ mm) is placed on a flat, rectangular slab with a minimum side length of 900 mm (see Fig. 3.1a). The cone must be held down – either manually by the operator or using a dedicated steel ring – to counteract the buoyancy force exerted by the concrete during pouring. The concrete is poured into the mould without any compaction, and the top surface is smoothed if necessary. The cone is then lifted vertically (after a rest period of approximately 10–15 s), and the final spread diameter (in mm) of the concrete flow is measured (see Fig. 3.1b). The corresponding fluidity classes are presented in Table 3.1.

a)  b) 

Fig. 3.1. SCC slump-flow/fluidity testing: a) the equipment, b) slump example

Table 3.1. Slump flow consistency limits according to EN 206

Class	Slump-flow in mm
SF1	550 to 650
SF2	660 to 750
SF3	760 to 850

3.2.2. VISCOSITY

Viscosity may be defined as the measure of the "stickiness" between two neighbouring layers of fluid, or as the resistance of a fluid to deformation under external forces. In practice, it is a crucial criterion for SCC because it is responsible for stabilising highly fluid concrete mixes against sedimentation. To observe this phenomenon, compare Figs. 3.1b and 3.2. These figures present the results of Abrams cone tests performed on stable SCC (first case) and excessively fluid conventional concrete (second case). When conventional concrete reaches a sufficiently high fluidity level, segregation follows a characteristic pattern: coarse aggregate stops immediately in the centre, fine aggregate flows for some distance and then stops, and the cement paste flows almost without limit, as its fluidity is similar to that of water. To prevent segregation, the most effective solution is to convert the cement paste into a viscous binding phase capable of holding the coarser particles together, so that they move collectively with the surrounding fluid during flow, as shown in the first case (Fig. 3.1b). Thus, obtaining a sufficiently **high viscosity is the primary criterion for SCC stability during flow,** particularly during pumping and placement in formwork. Two standard viscosity assessment methods are presented below.

Fig. 3.2. Unstable concrete mix (i.e. severe segregation occurrence)

The first method is based on the Abrams cone flow test according to EN 12350-8. On the test slab a 500 mm diameter ring is traced (see Fig. 3.1a). The purpose of the test is to measure the time required for the concrete flow to reach the 500 mm diameter, starting from the moment when the cone is lifted. This time is referred to as t_{500}. Naturally, the longer the time, the higher the viscosity level. The range of viscosity classes according to this method is shown in Table 3.2.

Table 3.2. Viscosity classes measured on slump-flow testing according to EN 206

Class	t_{500} [s]
VS1	< 2.0
VS2	≥ 2.0

The second method, according to EN 12350-9 is based on measuring the emptying time of concrete flowing from an inverted V-shaped vessel known as the V-funnel (see Fig. 3.3), denoted t_V. During the test, the vessel is filled with concrete; next, the gate is opened, and the time required for the vessel to empty completely is measured in seconds. The viscosity classes according to EN 206 are listed in Table 3.3.

Fig. 3.3. V-funnel equipment according to EN 12350–9

Table 3.3. Viscosity classes measured in V-funnel according to EN 206

Class	V-funnel flow time [s]
VF1	< 9.0
VF2	9.0 to 25.0

Unfortunately, the results obtained using these two methods cannot be compared directly. The first method is simpler and easier to perform on-site, however, it is significantly less accurate because the measured time intervals are shorter and it is more difficult to determine precisely when to stop the measurement, as the concrete flow is typically not perfectly symmetrical.

3.2.3. STATIC SEGREGATION RESISTANCE

The third criterion of self-compactability is to ensure that **the coarsest aggregate fraction remains uniformly distributed within the formwork, without visible settlement after the concrete hardens**, as illustrated in Fig. 3.4. The test is performed according to EN 12350-11. A sample (approximately 5 dm^3) of SCC is left in a bucket for 5 minutes to observe any signs of segregation. Then, 5 kg of the mixture is poured from a height of 500 mm onto a 5 mm sieve. After 120 seconds, the percentage mass of mortar collected at the bottom of the container is measured. The corresponding resistance classes are listed in Table 3.4.

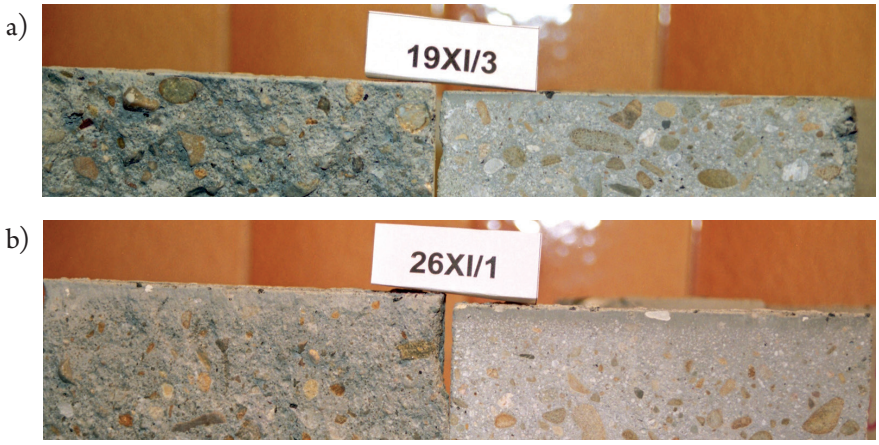

Fig. 3.4. Cross-sections of hardened SCC: a) no segregation, b) severe segregation

Table 3.4. Sieve segregation test classes according to EN 206

Class	Segregated portion (%)
SR1	≤ 20
SR2	≤ 15

3.2.4. PASSING ABILITY

Passing ability is the ability of fresh concrete to flow through obstacles such as reinforcement bars or narrow spaces without blockage, i.e. without coarse aggregate particles becoming trapped. It is tested according to EN 12350-10 (L-box test) or EN 12350-12 (J-ring test).

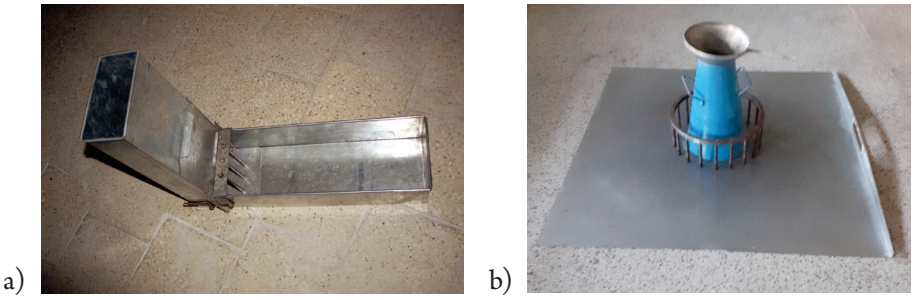

Fig. 3.5. Passing ability tests: a) L-box, b) J-ring

The L-box test (Fig. 3.5a) is performed in an L-shaped container, whose top, vertical part is filled with 12 dm^3 of SCC. This part is equipped with a gate that closes the opening located at the joint between the vertical top part and the horizontal

bottom part of the container. An obstacle consisting of smooth vertical rebars is placed 7 cm from the joint. There are 2 or 3 rebars equally spaced in the obstacle. The passing ability class assessed depends on the type of obstacle used. During the test, the gate is opened and the concrete flows through the obstacle into the horizontal part of the container. The limit value for passing ability is established at 80%, expressed as the ratio between the final heights of the concrete measured at the ends of the container after the flow stops. Typical results range from 80% to 94%, as SCC is not perfectly self-levelling. The passing ability classes are shown in Table 3.5.

Table 3.5. Passing ability test classes measured in L-box according to EN 206

Class	L-box ratio
PL1	≥ 0.8 with 2 rebars
PL2	≥ 0.80 with 3 rebars

The second method, also known as the Japanese ring, consists of a standard Abrams cone used together with a steel ring (300 mm in diameter) containing a specified number of smooth rebars evenly distributed around the ring. The EN 12350-12 standard assumes the use of rings containing either 12 or 16 rebars (see Fig. 3.5b). The test procedure is straightforward. It is performed in the same way as the fluidity test, but with the ring placed concentrically with the cone on the plate (see Fig. 3.5b). After the concrete flow stops, the height of the concrete layer is measured at the centre (or at the top) of the spread "cake" and at four uniformly distributed points located just outside the ring. The average value of these measurements is then taken into consideration. The difference between these two values must not exceed 10 mm, therefore, the accuracy of this method is relatively low. The passing ability classes according to this test are listed in Table 3.6.

Table 3.6. Passing ability test classes measured with J-ring according to EN 206

Class	J-ring step [mm]
PJ1	≤ 10 with 12 rebars
PJ2	≤ 10 with 16 rebars

The J-ring method is easier to perform on-site compared with the L-box method. However, its accuracy is significantly lower.

In some regions, local standards may require different numbers and diameters of the rebars used in the J-ring. The same applies to the assessment of the results. Consequently, there is no absolute worldwide comparison of the results obtained using this method.

3.2.5. THE COMPARISON OF PROPERTIES BETWEEN SCC AND TRADITIONAL CONCRETE

Conventional concrete is tested in the fresh state using one of four methods to determine its consistency or fluidity level. This is typically sufficient to assess its workability. In the case of SCC, however, there are four criteria to be fulfilled, as mentioned above.

The first criterion of self-deaeration is achieved by ensuring sufficiently high fluidity. High fluidity may render the concrete mixture unstable and prone to segregation. To prevent this, the second criterion – sufficiently high viscosity – must be achieved, as discussed above. The third requirement is adequate passing ability, which is obtained through appropriate aggregate grading supported by a sufficient paste content. The details of this process are discussed later in the section on mixture design. The final requirement is adequate resistance to segregation. When the second and third conditions are satisfied, this property is typically ensured without any additional effort.

3.3. APPLICATIONS OF SCC

Nowadays, SCC is widely used worldwide, and its importance and application continue to grow. In fact, SCC may be used as the conventional concrete replacement in all cases where the concrete is cured or hardened in formwork without a significant slope on the top surface. In practice, however, the most common applications of SCC are more limited and are described below.

- Complex formwork geometries (including architectural concrete). SCC is capable of filling formwork with very complex geometries, even shapes resembling sculptural forms.
- Complicated and dense reinforcement. SCC is often used as an "emergency solution" in situations where reinforcement congestion is sufficiently high to cause serious problems when conventional compaction methods are used.
- Situations in which both rapid formwork filling and manpower reduction are crucial from economic and technological points of view.

The reasons for these limitations in the use of SCC during structure erection are discussed in the next section.

Examples of applications include:

- Newton-le-Willows Station, St Helens (UK). In this project, all three key advantages of SCC were used in the construction of the tunnel walls: highly congested reinforcement, waterproof tunnel walls, erected rapidly under active rail traffic, and architectural surface finish (see linked pdf: Link 1).

- Renovation of the viaduct in Myślenice (Poland). A new cover of the existing girt was formed by filling the space between the existing structure, cleaned from the corroded concrete, and the formwork. This eliminated the need for shotcrete and provided an architectural surface finish (see linked materials: Link 2; photograph: Link 3).
- Burj Khalifa (UAE). SCC was used in the foundation base slab. Such structures are typically 2–3.5 m thick and present significant challenges during compaction. The use of SCC significantly accelerates construction, as larger sections can be concreted in a shorter period of time, thereby resulting in considerable savings in both time and cost (see video: Link 4).
- Precast concrete pre-tensioned beams (EU). The formwork may be filled with SCC four to five times faster than with conventional concrete. Automated pumping systems are used instead of manual labour. An architectural-quality surface finish is an additional benefit (see video: Link 5).
- Precast manhole base elements (EU). The use of SCC significantly increases the durability of these elements because they can be cast in a single layer, even when highly complex channel geometries are required. The main disadvantage of traditional technology is the need to cast the channels separately as additional inserts into the precast external structure. This results in rapid deterioration due to sewage-water penetration at the interface between the two concrete layers (see video: Link 6; element details: Link 7).

SCC is currently used most frequently in precast concrete production, where experienced personnel and controlled working conditions allow for both high production quality and increased productivity.

3.4. STRUCTURE ERECTION PROCESS USING SCC

3.4.1. INTRODUCTION

In general, SCC is a demanding solution, especially when handled by inexperienced personnel. The main difficulty in its use lies in its significantly different behaviour when compared with conventional concrete. If handled improperly, it may fail to perform as intended. For this reason, SCC is currently used on-site mainly in situations where the application of conventional concrete is highly problematic. In the precast industry, the use of SCC is far more common, as craftsmanship is typically much better and new technology implementation is significantly easier.

3.4.2. TRANSPORT

SCC is prone to segregation; therefore, any vibration during transport must either be avoided or properly controlled. For this reason, transport should be carried out using tilting-drum mixer trucks only, with the drum rotating continuously at an appropriate speed throughout the process. The rotational speed should be selected while considering both the viscosity and the fluidity of the mixture.

3.4.3. ON-SITE TESTING

Each batch or truck must be checked for basic properties (at least fluidity and viscosity) just before dispatching to avoid problems during placement. Unfortunately, SCC cannot be re-tempered with superplasticiser on-site because this type of concrete is highly sensitive to any imperfections in its composition. Therefore, if the measured parameters fall outside the target range, the batch cannot be used. For this reason, inexperienced or low-quality producers are often reluctant to supply SCC. Additionally, as with all other types of concrete, the consistency of SCC decreases over time (i.e. fluidity decreases and viscosity increases). As a result, there is a limited time window within which SCC must be placed. Therefore, careful scheduling of production, transport, and delivery is crucial for the success of on-site operations (for example, by avoiding delays caused by traffic during transport). These requirements are undoubtedly much more demanding than those associated with conventional concrete.

3.4.4. PUMPING

The pumping process of SCC differs significantly from that of conventional concrete. The main difference results from the high viscosity of SCC. High viscosity leads to increased flow resistance, especially at higher flow velocities. For this reason, the pumping process should be organised as described below. At the very beginning, the high viscosity of SCC results in very high energy demand during the filling of the pipeline with concrete, and there is a considerable risk of pump blockage. Wetting the pump or the pipeline with water is strictly forbidden, as SCC is extremely sensitive to any change in water content. Using water for this purpose almost always leads to severe segregation during pumping. To avoid this problem, pre-wetting with either cement paste or thick mortar (i.e. mortar with a low sand content) of an appropriate composition is recommended. SCC can be pumped only after the pipeline has been filled with the pre-wetting material, which must then be removed (pumped out) from the pipeline before filling the formwork begins.

The pumping process must then be conducted continuously (i.e. without breaks). Any interruption longer than approximately 30–60 seconds may lead to pump blockage due to the thixotropy of SCC. Thixotropy is a reversible phenomenon associated with high viscosity: at rest, the mixture rapidly "solidifies", meaning that its viscosity increases significantly. When the material is agitated, the viscosity decreases again within a few seconds. The higher the viscosity, the shorter the time available to move the boom pump outlet to the next position when necessary. Therefore, pumping SCC requires a constant and regular delivery of batches to ensure uninterrupted formwork filling. Maintaining a suitable buffer, i.e. one or two transport vehicles waiting for dispatch, is recommended. In addition, production, transport, and waiting times should be synchronised so that the fresh concrete has a consistent age at dispatch, as mentioned earlier. During pumping, the energy consumption is proportional to the viscosity of the mixture and is the lowest at low pumping speeds. To sum up, moderate pumping speeds are generally preferable because they provide lower power consumption, improved pumping efficiency, and a reduced risk of pump blockage. Despite its high viscosity, the pumping process for SCC is usually faster than for conventional concrete due to its high fluidity. A typical pumping rate is approximately 1 m^3/min.

3.4.5. PLACING/CASTING

The next step is the distribution of concrete within the formwork. Traditionally, concrete is poured from the pipeline outlet at an appropriate height and compacted using a poker vibrator. In the case of SCC, the use of vibrators is prohibited due to the high risk of segregation. Furthermore, the pipeline outlet should be immersed below the surface of the previously placed concrete. The purpose of this is to prevent both secondary aeration and segregation of the placed concrete.

In the case of conventional concrete, the pipeline outlet is moved along the formwork together with the poker vibrator. Since the use of vibrators is replaced by the free flow of concrete in the case of SCC, the opposite approach must be applied. The outlet should remain in a fixed position while the concrete flows freely. This is essential for the effective self-deaeration of the concrete. However, the risk of segregation increases significantly with increasing free-flow distance. Typically, a free-flow distance of 5–10 m is considered safe, with the upper limit depending on the viscosity of the SCC. When longer formworks are filled, two different approaches can be used, as described below.

If the element is flat (e.g. slabs), SCC is placed from a single position until the maximum allowable flow distance is reached. SCC is not perfectly self-levelling. The typical slope ranges between 1:60 and 1:20 (corresponding to 90% and 65% in the L-box test), which allows a considerable volume of concrete to be placed from

a single location. After reaching the safe flow-distance limit, the boom is moved quickly to the next placement point, located approximately 1.5 times the safe flow distance from the previous point, and concreting continues. When these rules are followed, a single pump is usually sufficient to fill the formwork.

If the element is high, long, and narrow (e.g. thin walls), multiple pumps or pipelines may need to operate simultaneously. In such cases, the pumping speed in all pipelines must be maintained at the same level to prevent excessive free-flow distances.

3.4.6. FORMWORK, CONCRETE PRESSURE AND DEAERATION

Another important limitation when concreting with SCC concerns the formwork itself, particularly panel tightness and the load-bearing capacity of the supporting structure. Due to the high fluidity of SCC, the tightness of the formwork panels is crucial; however, no additional sealing systems or special fittings are required, provided that the panels are properly aligned and fitted. Regarding the load-bearing capacity of the formwork, several limitations must be considered. The main disadvantage of SCC is the high initial pressure exerted on the formwork, which is significantly higher than in the case of conventional concrete. This pressure is typically 110–115% of the hydrostatic pressure, due to the additional influence of dynamic pressure generated during pumping. In contrast, the horizontal pressure in SCC decreases rapidly due to thixotropy. Mixtures with high thixotropy may show a reduction of up to 50% of the initial formwork pressure within one hour, which represents one of the fastest pressure drops observed in concrete technology. This property allows the use of standard formwork, provided that the vertical rate of formwork filling is limited. Safe limits are typically assumed not to exceed 5 m/h of continuous filling for mixtures with high thixotropy. Higher filling rates are technically possible, but in such cases, the formwork must be reinforced using specially designed external supports. Moreover, rapid filling may adversely affect the self-deaeration process, as air bubbles tend to move laterally rather than vertically under thixotropic conditions. As thixotropy leads to a rapid reduction in horizontal pressure (while vertical pressure remains largely unchanged), air bubbles tend to migrate along the horizontal pressure gradient. When they reach the formwork panel, they accumulate and become trapped, often beneath coarse aggregate grains. This effect is particularly pronounced in areas where aggregate grains are partially locked beneath reinforcement bars. The result is clear: the formation of surface defects (air voids), often accompanied by local exposure of reinforcement.

3.4.7. CONCRETING FROM THE BOTTOM

The use of additional structural support is required in the case of a specific SCC formwork-filling technique known as bottom-up pumping. In this method, the pipeline outlet is connected to a one-way valve installed in the formwork wall as close to the bottom as possible. The system has two advantages. Firstly, there is no need to supply concrete from the top of the formwork. Instead, it is sufficient to leave a few-millimetre-wide opening enabling the concrete to deaerate. This makes it possible to construct new structural elements directly beneath existing ones (for example, casting a wall beneath a ceiling while maintaining a tight joint with the ceiling). Secondly, the flow of concrete is one-directional (upwards), which also directs the flow of the de-aeration process. As a result, the side surfaces of the element are of high quality, since no air-bubble coagulation is observed. As the vertical filling rate in this method is typically high, the use of external supports for the formwork structure is necessary.

3.4.8. SURFACE SMOOTHING/SURFACE FINISH

The surface of conventional concrete must be smoothed as quickly as possible after compaction, until the surface is workable. In the case of SCC, this method is ineffective, as SCC deaerates for a rather long time (proportional to its viscosity). Typically, the surface should be left for 20–40 minutes to deaerate. After that, it may be gently smoothed, preferably using a rubber blade mounted on a telescopic handle. The purpose here is to push any protruding coarse aggregate grains beneath the surface, and to remove all surface foam. Stepping onto the freshly placed concrete should be avoided, as this may lead to secondary aeration caused by the reversal of thixotropy.

3.5. SCC COMPOSITION DESIGN

3.5.1. INTRODUCTION

Although SCC technology has been developed over the past 30 years, the problem of mixture design remains far from being fully resolved. Numerous methods and approaches have been described in the literature [9–16], and the total number of published solutions likely exceeds 100. Given this large number of approaches, selecting an appropriate method is difficult, particularly because some of these proposals are based on contradictory assumptions. For this reason, the present chapter is divided into several parts. First, a brief overview of the main materials used in SCC production is provided. Next, the existing design methods are classified.

This is followed by an introduction to the assumptions that appear most promising for achieving reliable results, particularly in terms of minimising the number of trials required to obtain the final mixture composition. Finally, the method developed at Cracow University of Technology (CUT) is presented.

3.5.2. MATERIALS

The materials used in SCC production do not differ from those used in conventional concrete, except for certain additional restrictions related to their performance in SCC mixtures.

3.5.2.1. CEMENT

All types of commercially available cements are acceptable. However, it should be noted that the cement content in SCC may be higher than in conventional concrete of comparable strength. Due to the high fluidity required for SCC mixtures, the use of cement with a high specific surface area may result in an increased demand for superplasticiser.

3.5.2.2. ADDITIONS

Additions to concrete are crucial for obtaining high viscosity with moderate use of both admixtures and cement. For this reason, they are almost always added to SCC as a separate material. All additions permitted for use in concrete may be applied, provided that the following rules are observed.

- Excessive addition content may negatively affect the properties of hardened concrete. Therefore, the external addition of materials already present in the cement as additions is not recommended.
- The main purpose of applying additions is viscosity enhancement. It is obtained by densifying the microstructure of the fresh paste and reducing the amount of water required to fill the spaces between paste grains. Therefore, the specific surface area of the addition should differ significantly from that of the cement. This choice is also beneficial for hardened concrete properties, since a denser microstructure results in both higher strength and improved durability.
- Additions may also be used to reduce the cement content, acting as a partial and more economical cement replacement. In such cases, materials with lower density and a specific surface area similar to that of cement are preferred.
- Typically, additions are lighter than cement, which means they tend to sediment first. The smaller the density difference between the cement clinker and the

addition, the more stable the cement paste becomes. As a result, greater fluidity of SCC may be achieved. This rule also applies to additions already incorporated in cement.

- The rounded grain additions slightly increase the fluidity of the paste, except in the case of moderate to high contents of silica fume, whose extremely high specific surface area tends to reduce it.

3.5.2.3. ADMIXTURES

All commercially available admixtures may be used in SCC in a conventional way, i.e. with the same restrictions and recommendations. However, two types of admixtures are essential for SCC: superplasticisers (SPs) and viscosity-modifying admixtures (VMAs).

SPs are crucial to obtain high fluidity of SCC. For this type of concrete, a dedicated group of SPs is preferable, namely those combining steric hindrance and electrostatic repulsion effects. Such SPs are characterised by a long-lasting fluidity-retention effect (often up to 2 hours), which means that redosing them on-site is forbidden. Their fluidising effect is strong enough that lower dosages are often sufficient compared with traditional superplasticisers used in conventional concrete. They are typically dosed as a percentage of the total mass of dry paste components (i.e. the binder mass). Moreover, they often exhibit three side effects. The first is slight additional aeration of fresh concrete (typically about 1–1.5% additional air), caused by the affinity of air for the steric-hindrance side chains of the polymer. This side effect enhances fluidity but simultaneously reduces viscosity. Additionally, compressive strength may be slightly reduced, while frost resistance may improve. However, this effect is not always desirable. To counteract it, some commercially available SPs contain a secondary deaerating component, which makes their simultaneous use with air-entraining admixtures questionable. The second side effect is a slight increase in paste viscosity caused by the length of the polymer main chain (backbone). This effect becomes significant only at high SP dosages. High SP content may also lead to the third side effect, namely a slight retardation of cement setting.

An additional issue related to the use of SPs in SCC is that the efficiency of the admixture (both the achieved fluidity level and the fluidity-retention time) is significantly dependent on ambient temperature. It should also be noted that, as fluidity decreases over time, the viscosity of the mixture typically increases.

The second essential admixture, the viscosity-modifying admixture (VMA), is used to achieve and stabilise the required viscosity level. Its use is typically limited to cases where mineral additions alone are insufficient to stabilise the mixture. VMA is generally not the first choice for increasing viscosity because of two drawbacks. Firstly, VMA reduces fluidity (proportionally to dosage and time), which requires

compensation through an increased SP dosage. Secondly, eliminating mineral additions from the SCC composition may lead to higher cement content and potentially lower durability of the hardened concrete.

3.5.2.4. AGGREGATE

Generally, there is only one widely accepted restriction concerning aggregates used in SCC. It is the limitation of the maximum aggregate size to D_{max} = 20 mm (which, in EU practice, usually corresponds to D_{max} = 16 mm). The use of larger aggregate grains may lead to aggregate blocking at obstacles, which prevents the passing ability criterion from being fulfilled.

It is possible to use both rounded and crushed aggregate. However, the use of crushed aggregate typically results in a significantly higher paste demand.

Additionally, the sand content in SCC is significantly higher than in conventional concrete. The reasons for this are discussed later.

3.5.3. EXISTING METHODS TYPES

The basic approach to SCC mixture design may be described as a "step-by-step" method [13], although the individual steps may vary. In terms of their internal organisation, two main approaches can be distinguished [14]: *sequential methods*, where each subsequent step uses the optimised result of the previous step; and *parallel methods*, where two or more constituent groups are optimised independently in parallel. In the latter case, the optimised constituents are typically combined into a final mixture in the last step. Sequential methods usually begin either with well-performing conventional concrete, which is then significantly modified to obtain SCC, or they follow the material grain-size hierarchy (most commonly: cement paste → binder → mortar → concrete). In contrast, parallel methods typically optimise aggregate and binder systems independently, after which the optimised components are combined to obtain SCC. Although some alternative approaches exist, they are not particularly relevant for the purposes of this short course.

Theoretically, the parallel method should be more efficient, as it involves fewer optimisation steps, and individual optimisation blocks can be modified without significantly affecting the others, except for the final combination step.

Another important distinction between SCC design methods concerns the main theoretical assumption of the design process. Four main approaches can be identified here [14, 15]:

- minimum coating-radius assumption (fluidity is achieved by coating coarse grains with an appropriate layer of finer material),

- minimum level of void overfilling assumption (fluidity is achieved by using sufficient fine material content to separate coarse grains by overfilling all free spaces between them),
- to establish and use a proper formula that defines the primary proportions between constituents considered in a given design step (e.g. aggregate proportions, aggregate volume, addition-to-cement ratio, minimum paste content etc.),
- to establish and use nomograms showing approximate proportions between the main constituents, such as water content, paste content, aggregate volume etc.

In fact, these approaches are largely analogous to those used in conventional concrete design.

The final important distinction concerns the main criterion of aggregate composition design. There are several possible methods that are commonly applied.

The first and most widely used approach is minimising the void volume between aggregate grains. Three main variants can be distinguished here:

- Minimum voids in the compacted state. This is the oldest method, taken directly from conventional concrete design without any modification.
- Minimum voids in the intermediate state between the compacted and the loose state, developed to account for the higher paste content required in SCC; typically based on models derived from the compacted aggregate state.
- Minimum voids in a loose state. Sometimes this approach is used as a simple design assumption, while in other cases it results from analysis of the potential SCC self-compaction process.

Other approaches include:

- Estimation of the maximum coarse aggregate content, ensuring the required level of passing ability. This value may be either estimated or calculated, depending on the design method.
- Optimisation of aggregate grading, based on a selected grading model or function, either adapted from conventional concrete design or specifically developed for SCC.
- Optimisation of aggregate grading based on compaction theories (for example CPM, DMDA, or 3PM).

In the case of binder paste optimisation, numerous different approaches exist, making systematic classification difficult. For this reason, this issue is not discussed in detail here. Nevertheless, one important limitation should be highlighted. In most existing methods, there is no procedure for estimating the final dosage of superplasticiser (SP). As a result, the final stage of mixture optimisation often becomes time-consuming and cumbersome. An attempt to address this problem, at least partially, is presented in the next section.

3.5.4. THE PROPOSED METHOD

3.5.4.1. ASSUMPTIONS

The method developed at CUT is based on several assumptions.

1. The parallel design approach is applied. The binder and the aggregate compositions are chosen independently at first, and then they are mixed together to obtain SCC.
2. The equipment used for testing must be standard, i.e. easily obtainable in any typical concrete laboratory.
3. The binder block is internally organised sequentially, but the primary goal is to test the given material set (cement + addition + SP) comprehensively, using a comparatively short procedure. The resulting nomograms allow the selection of proportions for the required composition without the need to repeat the whole procedure.
4. The superplasticiser dosage must be assessed at as early a stage of design as possible to avoid excessive testing at the last stage.
5. The aggregate composition assessment should be simple and efficient, while ensuring the highest possible passing ability.

3.5.4.2. THE IDEA OF SCC COMPACTION PROCESS AND AGGREGATE GRADING SELECTION

In conventional concrete, the aggregate grading is typically designed in the compacted state. This assumption is beneficial from both economic and engineering points of view, as the aggregate is usually cheaper, stronger, and less porous than the typical cement paste. Moreover, when using a proper compaction method, obtaining this state in the structure is not a difficult task. In the case of SCC, the use of any external force to compact aggregate in the formwork is forbidden, as it always results in severe segregation. This means that the aggregate grading for SCC should be designed in a different way. Any granular material, when forced either to move or to flow, self-organises into a loose state. Therefore, any kind of concrete poured into a vessel without external compaction contains a significant number of voids filled with paste and air bubbles. In conventional concrete, a vibrator is used to remove air and to densify the aggregate structure. In SCC, this is not possible, so the aggregate skeleton should be as dense as possible during flow in order to minimise air entrapment. When this condition is fulfilled, the grain structure remains dense enough to remain stable (i.e. dislocation-free) after the flow stops. The result is segregation prevention while maintaining the possibility to remove all large air bubbles due to the action of buoyancy forces. This implies that, in SCC, the **aggregate skeleton/grading should be optimised in the loose state,** with the voids slightly overfilled by the

binder. Consequently, a significantly higher paste or binder content is expected in SCC compared with conventional ready-mixed concrete.

3.5.4.3. THE IDEA OF BINDER COMPOSITION SELECTION

The gradual fluidisation of conventional concrete always leads to severe segregation and sedimentation, as shown in Fig. 3.2. This occurs when the stability limit of the cement paste or binder is exceeded. The cement paste becomes too fluid and flows out of the coarser grain skeleton. The aim of the composition selection is to obtain a stable mix, as illustrated in Fig. 3.1b. The simplest way to achieve such an effect is **to convert the paste or binder into a kind of viscous "glue"** joining all coarse grains together so firmly that they flow along the main current without any disruption until the motion stops naturally. The key factor contributing to the conversion of the fluid paste into such a "glue" is viscosity. Since water is the least viscous component in SCC, reducing the water content is essential for increasing viscosity. To achieve this, the most effective and economical approach is to minimise the void volume between the binder grains, i.e. to design the binder "micro-skeleton" using materials with significantly different specific surface areas, similarly to aggregate optimisation. Therefore, **the addition used in SCC has to be either significantly finer or coarser than the cement**. Since direct measurement of specific surface area is not always feasible in standard laboratory conditions, an indirect testing method is proposed.

3.5.4.4. THE METHOD OF BINDER TESTING AND OPTIMISATION

In practice, viscosity in the construction industry is measured using conical vessels such as the Marsh Cone or V-funnel. They enable comparative assessment of fluid viscosity; however, they do not evaluate fluid stability. To address this limitation, an additional test for SCC, known as the Visual Stability Index (ASTM C1611), has been developed in the USA. On the basis of the visual segregation level (concerning mixtures behaving in a manner similar to that shown in Fig. 3.2), SCC mixtures are classified as follows: no segregation, traces of segregation, visible segregation, significant segregation, and severe segregation.
This concept was adapted for cement-paste testing using the Haegermann cone, according to EN 1015-3. As cement paste exhibits different sedimentation behaviour than concrete, specific segregation-assessment criteria were developed. The first indication of cement-paste instability is the migration of lighter components to the paste surface, resulting in visible colour traces (see Fig. 3.6a). As fluidity increases further, a peripheral rim of fluid material appears (see Fig. 3.6b).

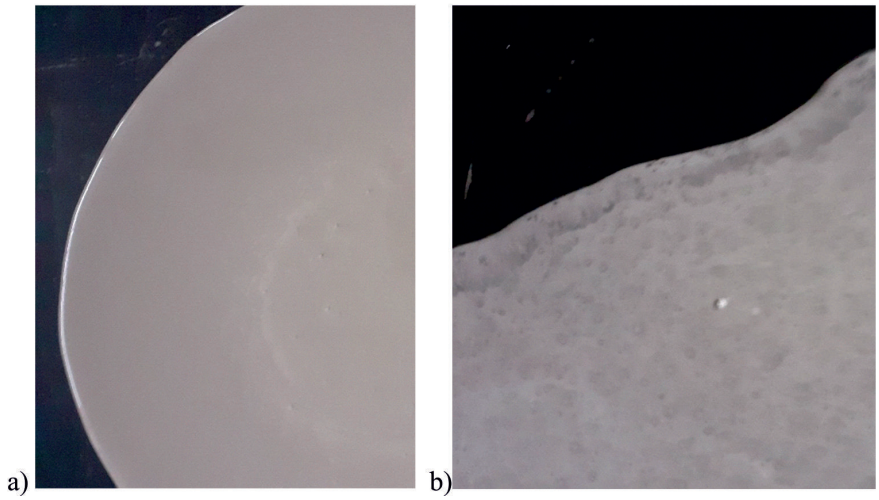

Fig. 3.6. Sedimentation of cement paste observed on the surface of the Haegermann cone slump flow: a) white trace of limestone powder, b) dark trace of fly ash on the rim

The optimisation procedure:

1. Determine the fluidity curve of the cement paste or binder using the Haegermann cone. An example is shown in Fig. 3.7. Each curve corresponds to a test with fixed parameters (w/c and addition-to-cement ratio), while the SP dosage varies. Water is gradually added, and a consistent mixing procedure is maintained. The aim is to identify the range from the onset of sedimentation to the point where the peripheral rim reaches at least 20 mm in width.
2. Establish a safe fluidity limit for the cement paste. The cement paste may exceed the stability limit in a reasonable way, as part of its fluidity is used for wetting the aggregate surface. Here, this limit is estimated at a level below 10 mm of the rim. The recorded value is the slump-flow diameter D_{opt} obtained when the sedimentation limit is reached. When the fluidity of SCC is too low (i.e. when the aggregate water demand is higher than typical), D_{opt} may be adjusted without additional testing.
3. Estimate the proportion between addition and cement (a_d/c) that ensures optimal stability, i.e. the maximum slump flow measured using the Haegermann cone at a defined level of sedimentation. This composition corresponds to maximum viscosity. If the viscosity of fresh concrete is too high, this proportion may be adjusted without repeating the full testing procedure.
4. Estimate the initial SP dosage for SCC testing. Fluidity curves for the given a_d/c ratio with progressively increasing SP content are established. The curves should differ by 15–20% of the maximum acceptable dose of SP. The range of the SP tested should be within 30–100% of this dose. The example is shown in Fig. 3.7. Next, D_{opt} is estimated, and the corresponding SP dosage for a given w/c ratio (corresponding to the tested w/b ratio) is interpolated from the graph. This value represents the initial limit of SP content for SCC testing (to be raised when necessary).

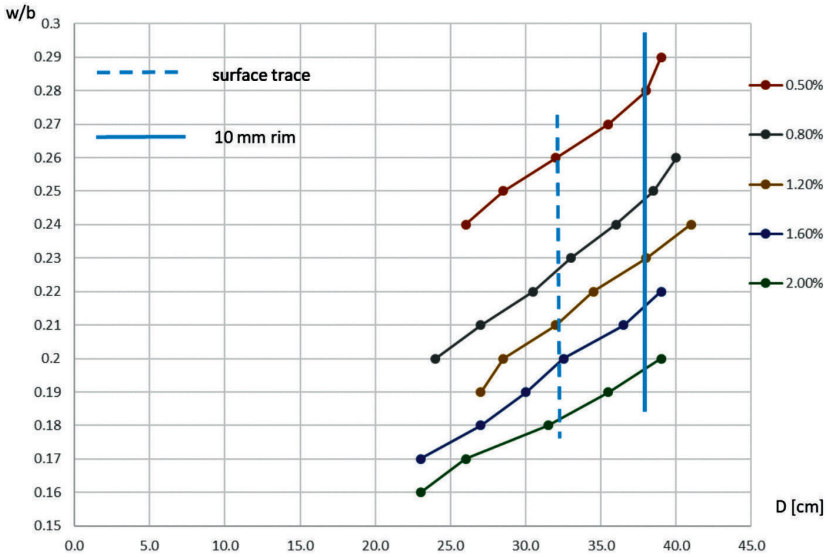

Fig. 3.7. Example plot of SCC binder test

3.5.4.5. THE METHOD OF AGGREGATE TESTING AND OPTIMISATION

The aggregate composition is designed according to the minimum-voids-in-the-loose-state rule by maximising aggregate density in the loose state. The optimum density is typically obtained for a sand-to-aggregate ratio (s/a) between 40 and 50%, with no significant peak observed (see Fig. 3.8). This is beneficial when applying subsequent corrections. From an economic point of view, lower s/a values are preferable (due to lower aggregate water demand). However, from the perspective of passing ability, high values of s/a should be selected.

In order to obtain good passing ability, an additional modification is recommended. As the concrete flow may be blocked by the presence of the coarsest grains, limiting the content of the coarsest fraction is an effective solution. To achieve this, the composition process must be modified by adjusting the main fraction range in the aggregate grading. In conventional concrete, the coarsest fraction is dominant. Here, the mid-size fractions typically constitute the main component. Therefore, the composition process starts from 100% of the mid-size fraction (e.g. 2/8 mm). Next, the coarsest fraction (e.g. 8/16 mm) is added to maximise loose bulk density, while ensuring that its content remains as low as possible (typically less than one-third of the total volume of coarse aggregate). Finally, sand is added to densify the coarse aggregate mixture.

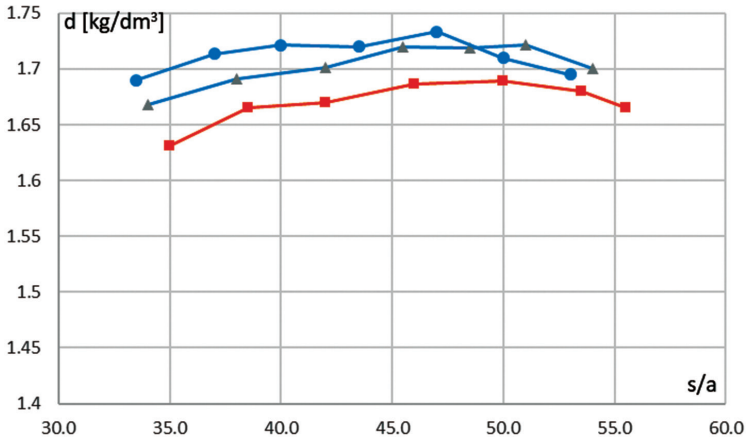

Fig. 3.8. Example result of aggregate optimisation according to maximum density in a loose state

3.5.4.6. THE FINAL SCC OPTIMISATION

1. Aggregate and binder compositions are selected according to the actual design criteria.
2. The aggregate content should be calculated assuming approximately 700 dm^3/m^3. The weighed material is then poured into the main concrete mixer.
3. The binder is prepared separately, as a ready-to-use paste, and poured into a separate bucket. Its content should be calculated assuming at least 400 dm^3/m^3, in order to maintain a sufficient reserve of paste in the bucket, particularly when the paste viscosity is high.
4. The paste is added gradually from the bucket to the aggregate during mixing until the required level of fluidity is achieved.
5. SCC properties are tested, and any necessary adjustments are made.
   - An increase in SP dosage should be considered if:
     – the overfilling level of aggregate voids exceeds 10% for the rounded aggregates and 20% for the crushed aggregates;
     – the viscosity measured in the V-funnel is too high (i.e. > 20 s);
     – the passing ability measured in the L-box is slightly too low (i.e. above 65% and below 80%).
   - An alternative method of reducing viscosity is to return to the binder nomograms and select a paste with lower viscosity (and stability).
   - If the passing ability is significantly too low (i.e. below 65%), the only solution is to alter the aggregate composition by reducing the content of the coarsest fraction and/or increasing the s/a ratio.

3.6. THE HARDENED PROPERTIES OF SCC

Generally, SCC is treated in both EN 1992-1-1 and EN 206 in the same manner as conventional normal-weight concrete. The differences between SCC and typical ready-mixed concrete (RMC) are not greater than those observed in other specialised types of concrete (high-strength concrete, sand concrete, wet-vibrated concrete, etc.) and arise primarily from differences in mixture composition. In the case of SCC, potential minor changes are caused by:

- lower coarse aggregate content,
- higher binder content,
- lower w/b (water to binder) ratio,
- higher water content,
- higher addition content,
- potential susceptibility to segregation or sedimentation.

Assuming a comparable water-to-cement ratio (w/c), these factors may result in:

- a slight decrease in the modulus of elasticity (E) (due to the lower coarse aggregate content); typically, SCC values are close to the lower bound of values calculated according to the rules for normal-density concrete given in EN 1992-1-1;
- an additional reserve of compressive strength when SCC is designed according to methods used for conventional concrete; this is due to the densifying effect of additions, which reduces paste porosity compared with systems having the same w/c ratio without additions, regardless of their type (chemically active or inert);
- potentially improved durability due to lower SCC permeability;
- difficulty in producing low-strength concretes (i.e. C25/30 and below), owing to low w/b ratios;
- higher production costs for low-strength SCC, whereas medium- and high-strength concretes are more comparable in cost;
- local segregation may occur (e.g. due to excessively long free flow within formwork); this may lead to significant variations in the properties of the affected cross-section, much greater than those observed in comparable conventional concrete;
- higher long-term shrinkage may occur in mixtures with high water and cement contents (i.e. when the addition content is relatively low);
- slightly faster strength development at early and intermediate ages may occur due to the self-curing phenomenon (water used for fluidisation of inert additions may be consumed during hydration processes);
- tensile strength may increase, as the microstructure of SCC is more homogeneous and the coarse aggregate content is lower (i.e. the influence of the ITZ is reduced);
- improved adhesion to reinforcement (including prestressing steel) and to existing concrete is observed due to the high viscosity of the mixture.

3.7. SUMMARY

The SCC is a valuable conventional concrete evolution path, aimed at simplifying the process of placing the fresh concrete in formwork. Unfortunately, its proper use requires completely different techniques, concerning both testing and execution stages, when compared to conventional concrete. Therefore, these techniques are described in detail in this chapter, as they are a prerequisite for the proper use of SCC in practice. Similarly, design methods for SCC composition assessment also require a completely different approach to both the aggregate and paste composition optimization procedures. Therefore, these assumptions are highlighted and developed into the detailed procedure enabling the reader to use the described design method in engineering practice. Contrarily, the properties of SCC in hardened state are so similar to those of the corresponding conventional concrete that the description of this otherwise broad topic has been condensed to a list of potential differences that may most frequently occur in practice.

REFERENCES

[1] EN 206. Concrete – Specification, Performance, Production and Conformity.
[2] EN 12350-8. Testing fresh concrete – Part 8: SCC – Slump-flow test.
[3] EN 12350-9. Testing fresh concrete – Part 9: SCC – V-funnel test.
[4] EN 12350-10. Testing fresh concrete – Part 10: SCC – L-box test.
[5] EN 12350-11. Testing fresh concrete – Part 11: SCC – Sieve segregation test.
[6] EN 12350-12. Testing fresh concrete – Part 12: SCC – J-ring test.
[7] ASTM C 1611-09a. Standard Test Method for Slump Flow of Self-Consolidating Concrete.
[8] EN 1015-3. Methods of test for mortar for masonry – Part 3: Determination of consistence of fresh mortar (by flow table).
[9] Daczko J.D.: *Self-Consolidating Concrete – Applying what we know*. CRC Press, 2012.
[10] De Shutter G., Bartos P.J.M., Domone P.L., Gibbs J.: *Self-Compacting Concrete*, Whittles Publishing 2008.
[11] Domone P.L.: *A review of mechanical properties of hardened SCC*. Cem. Concr. Compos. V. 29 (2007), pp. 1–12.
[12] Domone P.L.: *Self-compacting concrete: An analysis of 11 years of case studies*, Cem. Concr. Comp. V. 28 (2006), pp. 197–208.
[13] Shi C., Wu Z., Lv K.X., Wu L.: *A review on mixture design methods for self-compacting concrete*. Constr. Build Mat 84 (2015), pp. 387–398.
[14] Urban M.: *The new conception of self-compacting concrete composition design: theoretical background, evaluation, presentation of procedure and examples of usage*. Mater. Struct. V. 48 (2015), pp. 1321–1341.
[15] Urban M.: *Two limiting lines technique to obtain minimum paste demand of self-consolidating concrete*. ACI Mater. J. V. 116 (2019), pp. 131–138.

[16] Urban M.: *Water Demand (or Specific Surface) of Aggregate as a Dominating Factor for SCC Composition Design.* Appl. Sci. 14 (2024), p. 11108.
[17] EN 1992-1-1. *Eurocode 2: Design of concrete structures – Part 1-1: General rules and rules for buildings.*

4

GEOPOLYMERS

Barbara Kozub

4.1. INTRODUCTION

Geopolymers are inorganic aluminosilicate polymers obtained by the synthesis of aluminium (Al) and silicon (Si) from minerals [1]. Their structure is chemically similar to zeolites, although they have an amorphous microstructure. They are formed from long-chain copolymers of aluminium and silicon oxides stabilised by metal cations such as Na, K, Li, or Ca. This material can coexist with mixed phases, including silicon oxide, an unreacted aluminosilicate substrate, and locally crystalline zeolite forms.

The development of geopolymer research was initiated by observations of polycondensation reactions in systems containing metakaolin and industrial waste materials such as fly ash or blast furnace slag [2]. The term "geopolymer" was introduced in the late 1970s by the French scientist, Professor Joseph Davidovits. The introduction of this term allowed for the classification of the newly discovered geosynthesis, whose products are inorganic polymeric materials. In the initial phase of research, geopolymers were presented as an alternative to thermosetting polymers. This newly discovered class of materials has attracted widespread interest from scientists worldwide [3]. The "depolymerisation-condensation" theory formulated by Davidovits became the foundation for subsequent models describing the mechanisms involved in bond formation in geopolymers.

The term "geopolymer" has become widely used to refer to amorphous and crystalline products formed by the reaction of aluminium silicates with alkali hydroxide/alkali silicate solutions [4]. Other terms commonly used in the literature regarding geopolymer gels and composites include "low-temperature aluminosilicate glass" [5], "alkali-bonded ceramics" [6], "geocement" [7], "alkali-activated cement" [8], "inorganic polymer concrete" [9], and "hydroceramics" [10].

Research indicates that both the type and quality of raw materials and processing conditions significantly affect the properties of the resulting products [3]. The concept of geopolymers has expanded over time to include a variety of starting materials. In addition to pure metakaolin, geopolymers based on fly ash or other mineral wastes are now distinguished [11]. Classification by raw material enables a clearer definition of the material's potential applications and final properties. The choice of precursor is crucial for the system's reactivity and the uniformity of the final product's chemical composition. Metakaolin is characterised by high repeatability of its parameters; however, the use of industrial waste, such as fly ash or slag, helps

mitigate the negative environmental impact of building materials production by reducing CO_2 emissions [12]. However, the chemical composition of mineral waste, even of the same type, can vary significantly by source. This necessitates verifying the physicochemical parameters of the raw material before use [13].

There are several reasons why geopolymers have not yet gained as much popularity as Portland cement. One of the main problems is the limited access to raw materials and the lack of legal regulations in some countries. The lack of established design standards for geopolymers means that, despite achieving strength and durability comparable to or better than traditional Portland cement, their implementation in standard construction applications is limited by technical regulations [14]. Furthermore, in many countries, society still believes that materials produced from waste may be harmful to humans. A significant limitation to the mass production of geopolymers is the variability of raw materials. As is well known, geopolymer technology is highly sensitive to changes in both chemical and phase composition, as well as to the adopted production process parameters. Another limitation is the low repeatability of results, which depends on maintaining consistent process parameters and using raw materials and activating additives with well-controlled compositions. Fluctuations in raw material prices, particularly sodium hydroxide – the main component of the alkaline solution used in geopolymer production – are also hindering the development of mass-scale geopolymer production [15].

The geopolymer formation process results from geopolymerisation, an alkali-activated reaction between a precursor rich in aluminosilicates and a sodium- or potassium-based solution. Factors determining the course of this reaction include the Si/Al ratio, the amount and type of alkaline activator, and the curing conditions of the material [10]. Reducing porosity by the appropriate selection of curing temperature or by lowering water content can improve mechanical properties and chemical resistance.

From an environmental perspective, replacing Portland cement with geopolymer binders is important because it reduces greenhouse gas emissions. The cement industry is estimated to be one of the main emitters of CO_2, and geopolymer technologies can significantly reduce this problem by utilising mineral waste and lowering the energy requirements of the synthesis process [16]. An example of this approach is fly ash geopolymer blocks and bricks, which are characterised by high fire and chemical resistance and reduce energy consumption compared to firing traditional building ceramics [17]. Applications of geopolymers include both engineering structures with high durability requirements and environmental engineering solutions. The porous structure of these materials can be used to adsorb heavy metals or dyes from aquatic environments due to their large specific surface area and chemical stability [18]. It is important to consider the impact of aggressive environmental conditions on the microstructure and macromechanical parameters of these materials. Research on geopolymer technology indicates potential directions of development, including composition optimisation through chemical modifiers,

improving the formulas of aluminosilicate precursors, and refining the material maturation processes to achieve the desired mechanical properties and durability [19]. The literature highlights the special role of Ca ions, derived, for example, from the addition of metallurgical slag, which can be incorporated into the Si–O–Al–O framework, compensating the charges associated with Al atoms while improving strength and limiting the leaching of components from the structure of the finished material [20]. The simultaneous presence of the C-S-H phase coexisting with the geopolymer phase seems to favour achieving very high mechanical parameters, even with a relatively low degree of matrix amorphization [20, 21].

4.2. DEFINITION AND ORIGIN OF GEOPOLYMERS

Geopolymers, a subject of interest in materials chemistry since the late 20th century, are defined as inorganic polymers with an aluminosilicate structure that are synthesised in alkaline or acidic environments using Si- and Al-rich precursors [22]. The key element of their structure is a three-dimensional (2D or 3D) network of Si–O–Al bonds, which may resemble the crystalline system of zeolites but remains amorphous in most cases [23]. Unlike traditional cementitious binders, geopolymers are characterised by a high proportion of covalent bonds between SiO and AlO tetrahedra, forming a stable framework responsible for their mechanical strength and chemical resistance [22].

The term geopolymer refers to a group of inorganic materials formed by the polycondensation of aluminosilicates in a strongly alkaline environment [24]. This reaction involves the rapid dissolution of Si and Al atoms from the source material under the influence of an activator (usually NaOH, KOH, or their silicate derivatives), followed by the condensation of the resulting monomers into polymer structures [25]. The result is a cross-linked matrix whose properties can be shaped by selecting the type of activator and its concentration [26].

Makungu M. Madirisha et al. identify two basic types of geopolymers: alkali-aluminosilicate (AAS), formed through reactions in an alkaline environment, and the less common geopolymers based on acidic activators. In the case of the first type, the process involves steps such as alkalisation of the source material, depolymerisation of silicates and aluminates, and the formation and subsequent polycondensation of an oligo-sialate gel, resulting in the formation of an extensive network of cross-linked chains [22]. This reticulation step leads to the final solid form of the material.

From a chemical perspective, the structure of the geopolymer differs from that of its crystalline natural analogues in that it is predominantly amorphous, exhibiting classical "fuzzy" diffraction in XRD studies [27]. Davidovits also noted the similarity of the geopolymerisation reaction to the synthesis of zeolites [28]. However, the

different reaction conditions result in products exhibiting properties characteristic of glassy or semi-crystalline ceramic binders rather than fully crystalline minerals. This feature opens the possibility of using geopolymers both as structural binders with specific mechanical properties and as sorbents or matrices for immobilising hazardous waste.

The literature also highlights the importance of the type of activator used and the cation present in the alkaline solution. For example, it has been shown that mixtures of potassium silicate and KOH yield materials with better mechanical properties than analogous sodium or mixed K–Na formulations [26]. This can be explained by differences in cation coordination within the cross-linked structure and their impact on gelation.

From a construction technology perspective, the concept of a geopolymer encompasses a wide range of compositions derived from natural raw materials (e.g. metakaolin) or waste materials (e.g. class F fly ash, blast furnace slag). This makes the definition flexible and adaptable both in the field of basic research on aluminosilicate chemistry and in practical industrial applications [29].

Extensive classification by precursor type enables prediction of the potential properties of the final material and targeting its function, from low-temperature cements to high-temperature components of engineering ceramics. It is also important to note that the term "geopolymer" refers not only to cementitious binders used instead of Portland cement. It encompasses a group of materials that can exhibit ion-exchange or pollutant-adsorption capabilities due to the porous macro- and microstructure formed by aluminosilicate gels [30]. This interpretation expands the range of applications far beyond traditional concrete technologies.

A certain definitional difficulty can be noted; the line between "geopolymer" and "alkaline-activated material" is sometimes blurred in technical publications. Some authors use both terms interchangeably, while others prefer to treat geopolymer as a specific subset of chemically bonded products with a high Si–O–Al content and a specific crosslinking mechanism [24]. In laboratory practice, it is important to clarify this scope by describing the phase composition and synthesis conditions.

In summary, a geopolymer is a material category characterised by a common feature: a three-dimensional network of Si and Al atoms bonded by oxygen, forming a coherent chemical framework, most often obtained in an alkaline environment through depolymerisation and polycondensation reactions of aluminosilicate precursors. While this sounds like a purely chemical definition, the technological implications are broad, from the design of modern construction binders to environmental engineering.

4.3. RAW MATERIALS FOR GEOPOLYMER PRODUCTION

Geopolymers can be made from raw materials of natural origin as well as from waste materials. Table 4.1 lists the types of raw materials that can be used to produce geopolymers [31].

Table 4.1. Types of raw materials used for the production of geopolymers [31]

<table>
<tr><th rowspan="2">Natural materials</th><th colspan="3">Waste materials</th></tr>
<tr><th>Municipal waste</th><th>Industrial waste</th><th>Agricultural waste</th></tr>
<tr><td>Kaolin</td><td>Plastic waste</td><td>Fly ash</td><td>Rice husk ash</td></tr>
<tr><td>Metakaolin</td><td>Rubber waste</td><td>Silica fume</td><td>Corn cob ash</td></tr>
<tr><td>Volcanic ash</td><td>Glass wool fibre</td><td>Slag</td><td>Palm oil fuel ash</td></tr>
<tr><td>Zeolite</td><td>Paper waste</td><td>Red mud</td><td>Coconut husk ash</td></tr>
<tr><td>Dolomite</td><td>Effluent waste and sludge</td><td>Industrial recycled glass</td><td rowspan="3">Sawdust ash</td></tr>
<tr><td rowspan="2">Calcined clays</td><td rowspan="2">Cow dung ash</td><td>Waste foundry sand</td></tr>
<tr><td>Tailings</td></tr>
</table>

In principle, any material rich in aluminium and silicon in its composition can be used as a raw material in the geopolymer manufacturing process (Fig. 4.1), so these materials are quite abundant – more than 65% of the Earth's crust consists of Al–Si material, which makes a large and diverse resource available [32–34].

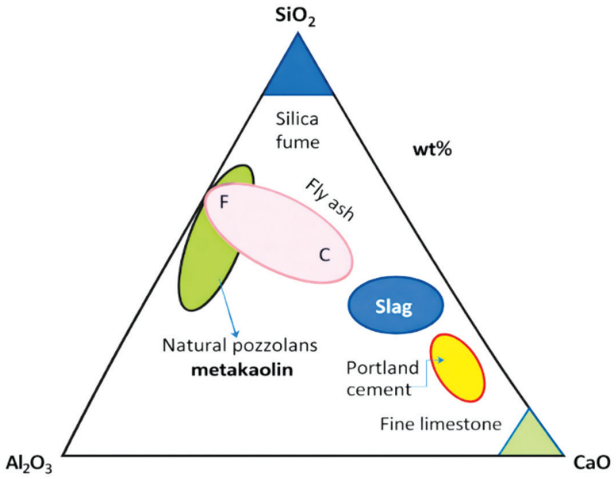

Fig. 4.1. $CaO–Al_2O_3–SiO_2$ ternary diagram of cementitious materials [35]

The first widely used material for geopolymer synthesis was kaolinite [23, 36–38]. In the ensuing years, researchers around the world began to explore new raw materials that are now used to produce geopolymers, including but not limited to: calcined clays [39] or industrial waste (e.g. slag [40], ashes [41], waste glass [42], aluminium mine tailings [43], etc.) and natural silico-aluminates (e.g. pure Al_2O_3–$2SiO_2$ powder) [44], zeolites [45], etc.

Another natural material that has found application in the synthesis of geopolymer materials is volcanic tuff, which enables the production of high-strength geopolymers. Volcanic tuff is a crumbly, pyroclastic rock (ejected by volcanoes in the solid state). In its composition, it very often has an admixture of other crumbly material, which is cemented by a clay or silica binder. A characteristic feature of volcanic tuffs is their high porosity, which consequently results in low density. Fig. 4.2 shows the Filipowice volcanic tuff of Polish origin, whose main component is sanidine [46].

Fig. 4.2. The Filipowice volcanic tuff of Polish origin [46]

There is also a possibility of using waste coming from the processing of crude oil and oil sands, from the incineration of sewage waste, or waste from the paper industry, the latter having in its composition combustible fractions in the form of organic wood, waste paper fibres, or chlorinated organic substances, which is associated with the need for additional processing. Mineral wastes have also found their way into geopolymer manufacturing processes. We can mention waste rock, waste from the processing of chromite ore, iron, tungsten, vanadium, and copper [47].

Bernal et al. [48] presented approximate compositions on CaO–SiO_2–Al_2O_3 three-phase diagrams for selected wastes (Fig. 4.3), which can be applied in the geopolymer manufacturing process.

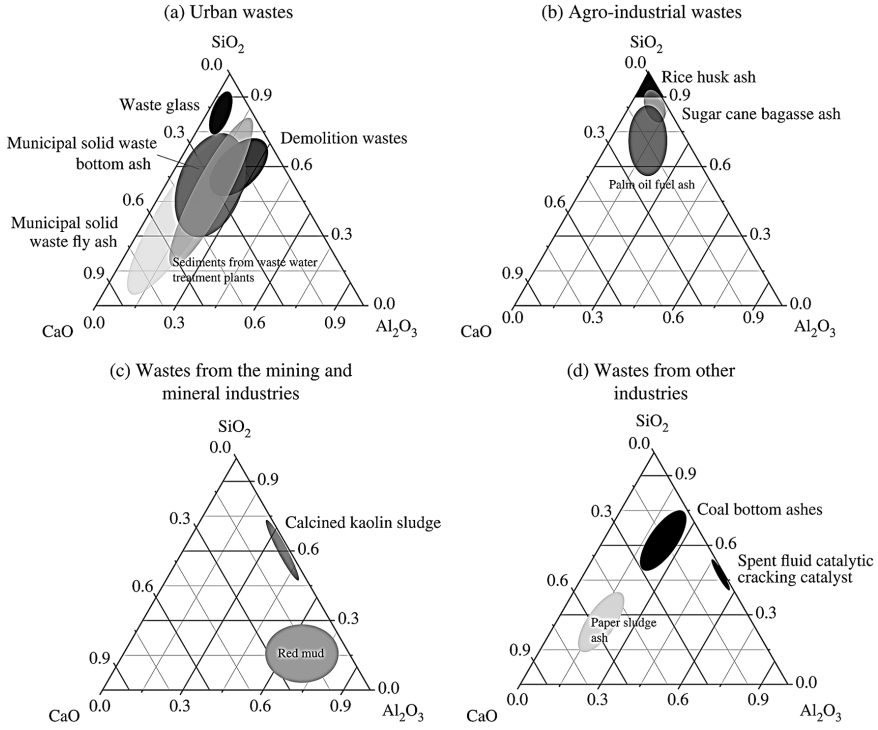

Fig. 4.3. CaO–SiO_2–Al_2O_3 three-phase diagrams for selected wastes that can be used for geopolymer production [48]

4.3.1. METAKAOLIN

Metakaolin is one of the most commonly used raw materials in the synthesis of geopolymers due to its high reactivity and reproducible chemical composition. It is obtained by dehydroxylation of kaolinite, which involves removing chemically bound water by heating to a carefully selected temperature range. This process requires significant energy input because the strong bonding of hydroxyl groups to the aluminosilicate scaffold leads to the disintegration of the ordered crystalline structure [28]. As a result, an amorphous phase is formed, containing silicon oxide and alumina in highly reactive forms, with a significantly larger specific surface area than the starting material. The optimal temperature range for calcining kaolinite to form metakaolin varies in the literature but is typically between 500–800°C [24]. Temperatures below approximately 450°C are insufficient for complete dehydroxylation [28]. However, exceeding the upper threshold of 800–900°C poses the risk of initial recrystallization and the formation of minerals such as mullite or quartz, which reduces the material's reactivity [49]. It has also been shown that a temperature of around 600°C, maintained for approximately two hours, allows the production of a product with high reactivity toward alkaline solutions.

Mineralogically, kaolin consists primarily of pure kaolinite fractions [$Al_2Si_2O_5(OH)_4$], the structure of which is based on SiO_4 tetrahedra connected by octahedral aluminium layers. The thermal activation process removes OH ions from these layers and transforms the regular system into a partially ordered or completely amorphous system, with a high potential for reaction with alkaline activators [26]. This makes metakaolin significantly more reactive in the geopolymerisation process than raw kaolinite [49].

One effect of thermal modification is the increased availability of the reaction surface, which translates into an accelerated dissolution of Si and Al atoms upon contact with a strong base [26]. Differences between individual batches of metakaolin depend on the quality of the starting kaolin and calcination parameters. Natural raw materials may contain additional minerals such as quartz or muscovite, which influence the final product characteristics. An example is the use of metakaolin containing admixtures of muscovite and quartz. In this case, after a day of alkaline activation, the crystal structure of muscovite was observed to disappear, indicating its high reactivity under geopolymerisation conditions, despite the presence of less reactive components [50]. However, the presence of non-reactive phases can act as a structural load or positively influence the so-called grain-packing effect, thereby improving the mechanical properties of the hardened material by reducing porosity [49].

In practical applications, metakaolin is used both on its own as the main geopolymer precursor and in mixtures with other aluminosilicate raw materials – e.g. fly ash or slag – to adjust the rheological properties of the mass and the chemical composition of the resulting binder [51]. Combining metakaolin with such additives allows for control of the Si/Al and Ca/Si molar ratios, which influences the type of gels formed (N-A-S-H or C-(A)-S-H) and the resistance of the finished components to aggressive environments [52].

From an environmental perspective, it is important that metakaolin is not an industrial byproduct or a mineral mined directly for geopolymer purposes. It is produced from kaolin subjected to controlled heat treatment, which requires the consumption of thermal energy, but is often compensated for by high product quality and the stability of the physicochemical properties of commercial batches [51]. Efficient use of metakaolin reduces compositional variability in geopolymer mixtures and enables predictable technological outcomes.

Metakaolin can be considered a prime example of a highly reactive geopolymer precursor: its amorphous nature promotes the rapid release of aluminium and silicon into the alkaline activator solution, while its fine grain size favours the homogeneity of the mixture and, therefore, the even course of the polycondensation process. The role of this raw material was fundamental to the development of the modern definition of geopolymer – research on the synthesis of aluminosilicate binders using metakaolin yielded many key observations on the mechanics of structural cross-linking and the influence of the precursor's morphology on the properties of the cured material.

4.3.2. VOLCANIC ASH

Volcanic ash, considered a natural resource rich in aluminosilicates, has long attracted the attention of researchers as a precursor to geopolymers. Its chemical composition is similar to several other natural pozzolans, such as tuffs and pumice, but its formation is directly related to eruptive processes and the rapid dehydration of lava or magma, resulting in a high content of amorphous silica-alumina phases [50]. This amorphous character largely determines reactivity in alkaline environments and the ability to form a cross-linked geopolymer matrix. The resulting powder is typically characterised by a fine grain size and a variable Si/Al molar ratio, depending on the geological location and parent rock type [53].

The solubility of aluminosilicate fractions of ash in alkaline solutions remains a key issue for geopolymer synthesis. Volcanic ash often contains a mixture of both amorphous and crystalline phases, e.g. sodium anorthite, augite, or ferroan forsterite, which exhibit varying susceptibility to decomposition by NaOH or KOH [50]. During alkaline activation, incomplete dissolution of all minerals is observed, leading to the simultaneous appearance of newly formed phases (such as hydroxyl sodalites) and the persistence of remnants of the original mineral structures in the geopolymer matrix. These remnants can act as microfillers, affecting the mechanical properties of the cured material.

The literature emphasises the specific role of the type of activator used. Sodium systems exhibit a greater ability to release Si and Al monomers than potassium systems, which typically translates into a higher rate of geopolymerisation and better internal cohesion of structures formed from volcanic ash [54]. Potassium activators, on the other hand, can promote the formation of other gel types (K-A-S-H), which offer different thermal or corrosion resistance parameters.

Comparative studies also show that increasing the proportion of more reactive alumina in the mixture – for example, by adding metakaolin – leads to a noticeable increase in final strength compared to mixtures based solely on volcanic ash [13]. The reactivity of volcanic ash is strongly linked to its geological origin. Rocks formed from silica-rich lavas (e.g. rhyolitic) produce ash with a high SiO_2 content in the form of glassy phases that readily react with alkalis. At the same time, products of basaltic eruptions may have a higher proportion of iron and calcium oxides, which changes the reactivity profile [53]. The mineralogical composition can also be a manifestation of local tectonic conditions – the presence of significant amounts of pyroxenes or olivines may extend the time required to develop the full aluminosilicate network due to their slower hydrolysis.

The role of volcanic ash as a precursor to geopolymers is also interesting because of its abundance in seismically active regions and the low cost of extraction in regions where historical or current eruptions have left significant deposits [50, 53]. Such resources are naturally deposited on the ground or on mountain slopes, eliminating the need for deep mining. However, the accumulation of large quantities

of this ash can pose an environmental problem – fine airborne fractions pose health risks to local populations and complicate land reclamation. In this context, its use as a geopolymer raw material offers a way to mitigate negative environmental impacts by transforming waste materials into durable structural components [53].

Techniques for increasing ash reactivity include mechanical grinding to increase surface area and heat treatment to remove moisture or partially alter the crystalline structure [50]. Such treatment can improve the efficiency of the depolymerisation process upon contact with alkali and accelerate the formation of the N-A-S-H gel or its variant, depending on the activator used. In practice, ash blends with other aluminosilicate precursors, e.g. metakaolin or class F fly ash, are also often used to optimise the Si/Al ratio and obtain a material with predictable mechanical properties [54].

One limitation of pure ash formulations is the heterogeneous grain-size distribution and particle shape, which affect the rheology of the fresh geopolymer mass and can lead to uneven distribution of reactive and nonreactive phases. However, proper control of the raw material preparation process minimises these effects. For example, the use of sieving procedures combined with controlled grinding significantly improves the grain uniformity of the input mixture prior to alkaline activation [50].

The use of volcanic ash also raises aesthetic concerns for the finished composites – the raw material's natural colour depends on the oxidation of iron components, allowing for shades ranging from light yellow to dark brown without the need for synthetic pigments. This characteristic may be desirable when designing architectural decorative elements made from geopolymers [53]. It is worth noting that, similarly to type F fly ash with a high Fe_2O_3 content, excessive iron oxides can reduce the available NaOH concentration for aluminosilicate depolymerisation, which is also observed in some volcanic ash batches [13, 55]. In summary, volcanic ash appears to be a valuable natural component for geopolymer technology, offering a favourable cost-reactivity balance and contributing to strategies for the development of local mineral resources. However, its effective use requires consideration of variability in chemical composition across different sources and adjustment of synthesis parameters to the properties of a specific batch of material. Compared to previously analysed high-reactivity precursors, such as metakaolin, they constitute an alternative that offers a wide range of options for shaping the mechanical and aesthetic features of the final products while reducing the negative effects of the eruption on the natural environment [13].

4.3.3. FLY ASH

Fly ash is one of the most commonly used waste raw materials in geopolymer technology, due to both its availability and favourable chemical properties. It is produced as a byproduct of coal combustion in power plants, and its main

components are aluminosilicate phases that form glassy structures during the rapid cooling of mineral particles in the exhaust gases [56]. The dominant amorphous nature of these phases promotes their reactivity in a strongly alkaline environment, making fly ash a good precursor to "N-A-S-H" gel or its variants, depending on the alkaline activators used [54].

Compared to natural raw materials such as metakaolin or volcanic ash, fly ash exhibits greater compositional variability due to the type of coal burned and the combustion conditions [57]. The basic parameters determining its suitability include the Si/Al molar ratio, calcium oxide content, and the presence of iron and magnesium oxides [22]. Fly ash with a low CaO content (class F) is particularly valuable for creating geopolymers with low solubility in acidic environments, while high-calcium fly ash (class C) can generate a mixed "C-(A)-S-H" and "N-A-S-H" matrix, which influences the mechanical profile of the hardened material [16]. However, it should be noted that high calcium content can modify the cross-linking process by preferentially forming phases resembling traditional Portland cement hydration products. Therefore, optimising the mix often involves combining fly ash with other raw materials – for example, blast furnace slag – to ensure the appropriate balance of binder phases and achieve the desired combination of initial strength and long-term durability [58].

From a technical perspective, one of the most important issues is the fineness of the ash particles. Research indicates that using a raw material with a larger specific surface area (e.g. obtained through additional grinding processes) enables faster depolymerisation of glassy phases and more intensive release of sulfur and aluminium monomers into the activator solution [16]. At the same time, reducing grain size reduces the porosity of the final geopolymer by better packing fine fractions between larger particles. This effect translates directly into increased mechanical strength. Particle morphology can also be dependent on the combustion process – the spherical shapes typical of pulverized-fuel combustion ash may behave differently than the irregular grains formed during fluidized-bed combustion.

Fly ash activation typically occurs through contact with NaOH solutions or mixtures of NaOH and sodium/potassium silicate [14]. At elevated temperatures (e.g. 60°C or higher), intense hydrolysis of the Si–O–Al and Si–O–Si bonds present in the glassy ash matrix occurs. Al–OH and Si–OH hydroxyl groups are formed, which then participate in condensation, forming oxygen bridges and a stable three-dimensional geopolymer network [29].

Due to the industrial origin of the raw material, the use of fly ash in geopolymer technology has environmental and economic benefits. It helps reduce the amount of waste sent to landfills and reduces the need for mining natural aluminosilicate raw materials [52]. At the same time, the geopolymer production process generates lower CO_2 emissions than Portland cement production – this difference results from both the absence of a clinkerisation step requiring high temperatures and from the co-use of finished waste materials [59]. It is also estimated that the energy

consumption to obtain a given mass of geopolymer binder is lower than that for the same mass of Portland cement [22, 23].

However, the problem of variable quality of ash obtained from different sources cannot be ignored. Heterogeneity of chemical parameters – e.g. sodium or potassium oxide content – may require adjustment of the activator concentration or the addition of other components controlling the reaction kinetics. Impurities such as unburned carbon can negatively affect polycondensation reactions or the visual properties of the finished product [22]. Therefore, before using each batch of raw material, chemical and mineralogical analysis and laboratory tests simulating the conditions of the target synthesis are recommended.

The aesthetic aspects of using fly ash can also be significant – the material's colour can range from light grey to dark grey or almost black, depending on the iron oxide and unburned fuel content. This colour can enhance the visual appeal of prefabricated geopolymer elements without additional pigmentation.

4.3.4. METALLURGICAL SLAG

Metallurgical slag, particularly in the form of granulated blast furnace slag (GGBFS), is an important waste component used in geopolymer technology. It is a byproduct of the iron smelting process, whereby fused gangue and fluxes form a molten mass that is then rapidly cooled to obtain a glassy-amorphous structure. This water-quenching step preserves the slag's high chemical reactivity by maintaining its oxides in amorphous form [29]. The increased specific surface area and non-crystalline nature of the dominant phases make it responsive to alkaline solutions, forming C-(A)-S-H aluminosilicate-calcium matrices.

A distinguishing feature of GGBFS compared to other aluminosilicate precursors is its high calcium oxide content and lower SiO_2 and Al_2O_3 ratios compared to, for example, class F fly ash [15]. This composition favours the formation of calcium-rich hydration products, which give the geopolymers a character similar to Portland cement in terms of setting speed and initial mechanical strength. The parallel formation of C-(A)-S-H and N-A-S-H phases in mixtures containing slag increases the density of the binding network and thus resistance to environmental factors. The activation mechanism involves the dissolution of Ca^{2+}, Al^{3+}, and Si^{4+} ions under the influence of strong sodium or potassium bases and the condensation of their hydrated forms into a polymeric structure [60].

One known application of blast furnace slag is its synergistic combination with fly ash [29]. In a mixed system, this leads to a correction of the Ca/Si and Si/Al molar ratios to balance the calcium phase, which is responsible for rapid strength gain, and the aluminosilicate phase, which ensures long-term durability. The addition of slag also improves the workability of the fresh mass, thanks to a more favourable rheology resulting from the intensive release of Ca ions already in the early stages of

activation. From a mineralogical perspective, blast furnace slag contains a mixture of glassy phases rich in CaO, along with some crystalline inclusions such as gehlenite and akermanite [61]. The presence of these minerals can modify the rate of the activation reaction; gehlenite is poorly soluble in low NaOH concentrations, while the amorphous fractions undergo rapid alkaline hydrolysis. Compositional variations are related to the type of furnace charge and cooling conditions; these factors determine the reactivity of the raw material.

From an environmental perspective, the use of smelter slag reduces the pressure on the exploitation of natural calcium-silica resources and minimizes the amount of industrial waste destined for landfill [62]. Furthermore, replacing Portland cement with geopolymer binders, incorporating GGBFS, reduces CO_2 emissions; the absence of the clinkerisation process requires lower thermal energy consumption; and the activation reaction itself occurs at temperatures of several dozen degrees Celsius. In this respect, this technology fits into the development strategy for sustainable construction.

However, certain limitations arising from variability in raw materials' origin should be considered. Smelter slag obtained from different plants may contain different amounts of MgO or Fe_2O_3, which affect the colour of the final material and its susceptibility to ionic transport within the polymer network [63]. Magnesium, for example, can stabilise certain forms of hydrated calcium aluminosilicate or influence the viscosity of the fresh geopolymer mass. Using GGBFS as a supplement or the main component of geopolymer mixtures allows tailoring of their properties to specific application needs, from prefabricated infrastructure components requiring high initial strength to protective coatings valued for their microstructural integrity.

4.4. GEOPOLYMERISATION REACTION

Geopolymers consist of long chains (copolymers) of aluminium-silicon and aluminium (repeating sialate monomer units, –Si–O–Al–O–), which are stabilised by bound water and metal cations, e.g. sodium (Na), potassium (K), calcium (Ca), or lithium (Li). The geopolymer structure usually includes other phases, such as silicon oxide, unreacted aluminosilicate substrate, and crystallized aluminosilicates of the zeolite type. To activate aluminosilicate, the following alkaline activators are used:

- sodium hydroxide (NaOH) with a high ability to release silicate and aluminium monomers [4, 64],
- potassium hydroxide (KOH), which has a higher level of alkalinity as compared to NaOH, - sodium silicate (Na_2SiO_3),
- potassium silicate (K_2SiO_3).

An appropriate selection of raw materials and activators enables optimisation of the properties of geopolymers for a specific application. The mechanism of geopolymer formation differs from that of cement-based materials. In Portland cement, bonding

occurs through the hydration of calcium silicates, forming a hydrated C-S-H phase (with the simultaneous release of calcium hydroxide). In the case of geopolymers, the bonding occurs through polycondensation - the reaction takes place between solid aluminosilicate powder and alkali hydroxide/alkali silicate [64, 65] (Fig. 4.4).

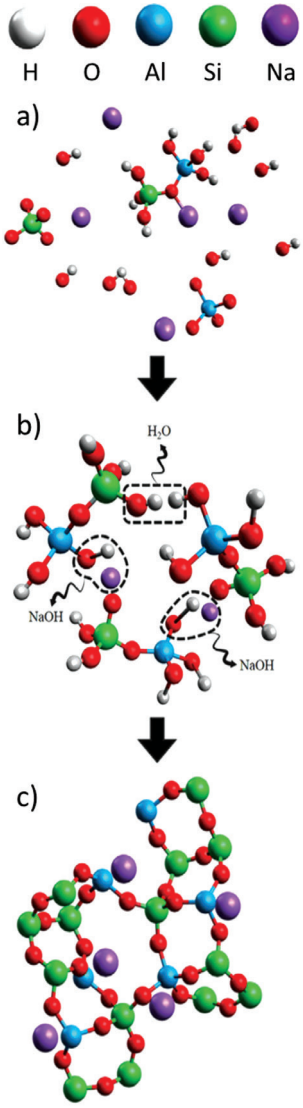

Fig. 4.4. Scheme of geopolymerisation process: a) reorganisation of aluminosilicate, b) gel formation from oligomer condensation, and c) polymerisation [66]

In strongly alkaline aqueous solutions, reactive aluminosilicates are dissolved, and free tetrahedral [SiO4]- and [AlO4]- units are released, which, during polycondensation, join at the corners via free oxygen atoms, forming amorphous or

subcrystalline aluminosilicate space structures. The negative charge of the skeletal structure, containing aluminium, is balanced by the presence of monovalent Na+, K+, or other metal cations. Fig. 4.5 shows a schematic representation of the reactions that occur during the geopolymerisation process [67, 68].

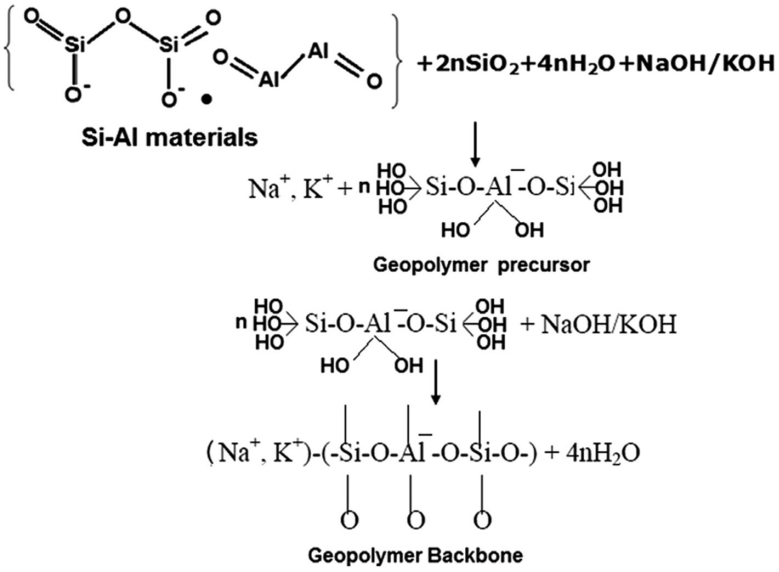

Fig. 4.5. Schematic representation of reactions that take place during the geopolymerisation process [68]

Unlike zeolites, the structure of geopolymers lacks long-range ordering and, depending on the presence of short-range ordering, three basic elementary units of polymer chains can be distinguished [4]:

- PS: poly(sialate) (-Si-O-Al-O-)

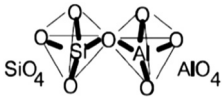

- PSS: poly(sialate-siloxo) (-Si-O-Al-O-Si-O-)

- PSDS: poly(sialate-disiloxo) (-Si-O-Al-O-Si-O-Si-O-)

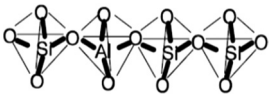

4.4.1. DISSOLVING THE RAW MATERIAL

The dissolution process of the raw material during geopolymerisation is the initiating step that determines the entire subsequent reaction kinetics and properties of the resulting material. Under strongly alkaline conditions, chemical attack occurs on the bonds in the aluminosilicate network of the raw material, both Si–O–Si and Al–O–Al, as well as mixed Si–O–Al bridges, resulting in depolymerisation of the original structure [69]. This bond opening leads to the formation of free units, such as hydroxyl ions or complexes, which serve as precursors to further polycondensation reactions. The influence of the raw material morphology becomes apparent already at this stage: amorphous material dissolves faster than its crystalline counterparts due to the higher density of structural defects [22].

Dissolution is multi-stage, with an initial phase of intense aluminium release. This phenomenon is clearly observed in materials such as metakaolin and the glassy phases of fly ash, where Al is released during the initial contact with the alkali solution [52]. Models describing this process indicate that the predominance of Al in the solution causes the local formation of a gel with a relatively low Si/Al ratio; only the subsequent desorption of silica balances the composition of the resulting matrix [24].

A significant factor is the alkaline activator concentration. High pH solutions, especially those containing additional sodium or potassium silicate, increase the hydrolysis rate and lead to highly supersaturated aluminosilicate solutions [70]. This environment favours the immediate formation of oligomers in the liquid phase, paralleling the dissolution of subsequent layers of the raw material. In laboratory practice, it has been observed that an alkali concentration that is too low limits the disintegration of the aluminosilicate network. In contrast, excessive concentrations can lead to rapid gelation before the dissolution process is complete, disrupting the homogeneity of the resulting material.

The type of activator cation also influences this step. Sodium (Na^+) systems typically demonstrate a greater ability to penetrate the raw material structure and ion exchange with atoms in the network than potassium (K^+) systems, which translates into a higher extraction rate of Si and Al monomers [30].

The surface area available for chemical attack depends on the material's history; grinding or prior thermal treatment can significantly increase the intensity of hydrolysis [51]. For example, metakaolin with a fine grain size provides a larger surface area in contact with the alkali solution, shortening the dissolution stage and accelerating the overall progress of geopolymerisation [69]. A similar effect can be achieved with fly ash by further grinding it.

The dissolution of glassy aluminosilicate phases occurs via a bond-breaking mechanism induced by OH^- ions: nucleophilic attack by the hydroxyl group breaks the oxygen bridges between the SiO_4 or AlO_4 tetrahedra. The resulting –SiOH and –AlOH groups are reactive species ready to participate in condensation during the next phase of the process [71].

If CaO is present (as when using metallurgical slag), there is a parallel release of Ca^{2+} ions into the solution, which can participate in the formation of C-(A)-S-H type hydration products already at the dissolution stage.

It is difficult to define the boundary between the dissolution and condensation stages clearly; both processes overlap in time, especially when the alkali concentration is high, and the process temperature is elevated [71].

To sum up this stage, it can be said that the dissolution of the raw material is a process of chemical-structural destruction controlled by the physicochemical parameters of the system: the activator (its type and concentration), the morphology and mineralogical composition of the raw material, and the reaction conditions, such as temperature or the intensity of mixing of the reaction mass [28].

4.4.2. POLYCONDENSATION

Polycondensation, which follows the raw material dissolution step, is a crucial step in the geopolymerisation process, transforming the reaction system from a solution containing monomers and oligomers into a three-dimensional, cross-linked solid structure. This reaction involves active hydroxyl groups –SiOH and –AlOH, formed during the depolymerisation of the aluminosilicate structure, which combine through oxygen bridges, eliminating water molecules [22].

Depending on the availability of appropriate ions and the pH of the liquid phase, the process proceeds in parallel with the reorganisation of existing tetrahedral SiO_4 and AlO_4 units, leading to gradual thickening of the gel and loss of mobility of its components. Short oligo-sialate chains can form at an early stage of polycondensation, which further elongate and link into branched macrostructures [26]. In the presence of additional anions, such as Al–O–P bonds can form, generating aluminophosphate networks with distinct physical, thermal, and dielectric properties [22].

From a chemical perspective, polycondensation is an exothermic process; the energy released during the formation of covalent oxygen bridges raises the local temperature, which in turn can accelerate the reaction in the surrounding gel regions. Structurally, a transition occurs from the colloidal phase to a coherent amorphous or amorphous-crystalline matrix. Modelling studies indicate that oligomers distributed in solution tend to spatially aggregate according to the principles of energy minimization of intermolecular interactions [72]. This is facilitated by both the diffusion of monomeric units and the increasing medium viscosity resulting from the formation of the first cross-links in the network. In later stages, crystalline structures (e.g. $AlPO_4$ phases) form within the amorphous matrix, resulting in a heterogeneous composite microstructure [22].

A key parameter controlling polycondensation is the Si/Al molar ratio within the reaction mixture. Lower values favor the formation of more ionic Al–O–Si bonds and a higher content of charge-compensating cations, while higher values

promote the development of silicon-rich lattice segments with stronger covalent Si–O–Si bonds. Industrial processes often strive to select this ratio to achieve a compromise between mechanical resistance and chemical stability of the final product. However, excessively high solution alkalinity can be detrimental to oligomers still forming – an excess of OH^- ions promotes their redissolution into free aluminate or silicate ions, thereby delaying the gelation stage [19]. From a kinetic perspective, this process is nonlinear – an induction period is observed, during which the oligomer concentration reaches a critical level enabling the mass formation of cross-links. This is followed by a phase of rapid increases in cross-linking until the mobility of network segments decreases due to densification. Another interesting aspect is the overlap between the polycondensation stage and the final dissolution phases – this means that new monomers can be continuously supplied to the existing network and further densified once the system's first stiffness point is reached [60].

In technological practice, polycondensation is controlled by manipulating the curing temperature and ambient humidity. Higher temperatures increase the kinetic energy of the reactants, intensifying their collisions and improving the statistics of effective condensation reactions [73]. However, excessive heating can cause premature drying of the mass and the development of thermal stresses, resulting in internal microcracks. Therefore, cooling or gradually increasing temperature regimes are often used to support gel maturation without compromising the material's structural integrity. At the end of this stage, the material reaches a quasi-solid state: most of the active hydroxyl groups have been consumed in the formation of oxygen bridges, and the mobility of the remaining molecules within the matrix is limited. Further changes mainly concern the reorganisation of the network's internal segments and the potential growth of secondary crystalline phases during prolonged maturation or exposure to environmental factors [22].

4.5. THE MATURATION PROCESS OF GEOPOLYMERS

The maturation process of geopolymers, defined as the period from the completion of fresh mass formation until the material achieves its intended functional properties, is one of the most sensitive stages of the entire technological cycle. It is during this time that further polycondensation reactions described earlier occur, along with the reorganisation of the gel microstructure and the stabilisation of moisture content in the pores and capillaries. The parameters of the maturation environment – primarily temperature, humidity, and the duration of specific conditions – determine the mechanics of the geopolymerisation process, and thus the density of the aluminosilicate network and the level of structural defects in the finished material.

Temperature is a factor that operates on several levels. Increasing it increases the kinetic energy of the reactants, which accelerates the dissolution of Si and Al precursors and the formation of cross-links in the matrix [59, 68]. For many systems, the optimal range is approximately 50–80°C [29]. In low-calcium materials, such as those based on class F fly ash, moderate heating shortens the time to achieve high mechanical strength by up to several days. However, excessively high temperatures can have the opposite effect – excessive water evaporation causes the formation of micropores and cracks, disrupting gel formation. Especially above 100°C, the risk of loss of structural moisture is high, resulting in a porous material with reduced mechanical resistance and greater susceptibility to carbonation [62].

Humidity in the curing sample's environment acts as a buffer for evaporation and liquid migration within the matrix. Maintaining an appropriate humidity level ensures access to the reaction medium (water), which is necessary for the continued bonding of the tetrahedral silica and aluminium units. An excessively dry atmosphere produces an effect similar to overheating – rapid drying of the surface leads to a moisture gradient between the near-surface zone and the interior of the component, which can result in thermal-hygrometric stresses that initiate cracks. Humid conditions also promote the formation of a homogeneous microstructure in the N-A-S-H or K-A-S-H gel by delaying plasticity loss.

The duration of the maturation stage is an important parameter. In the first hours, reactions forming short oligomer chains and the initial critical points of the network predominate; the following days serve to densify the matrix by replenishing oxygen bridges and spatially reorganizing the skeletal units. Too short a process can leave unbound hydroxyl groups, increasing the material's hygroscopicity and making it more susceptible to alkali leaching. Excessively prolonged periods of maintaining optimal conditions do not always bring additional benefits – once the network reaches saturation, the rate of further changes decreases exponentially [29, 31].

The use of specialised maturation methods allows for control of the final property profile. Geopolymers can be cured in several ways, including [31]:

- **Oven/heat curing**
  During the manufacturing process of geopolymers, water is released through chemical reactions and subsequently evaporates as the curing progresses due to temperature effects [74]. Also, shrinkage during drying becomes negligible because the rigid samples contain only a small amount of water in their pores. Numerous studies have evaluated the effects of annealing time and temperature on selected physical and mechanical properties of geopolymers, as reported [75–78]:
  - Achieving almost perfect geopolymerisation is possible when using curing temperatures in the range of 40–80°C.
  - For alkali-activated fly ash-based geopolymers, the adopted curing temperature has a decisive influence on the strength properties – Singer et al. [30] showed that the higher the curing temperature of such geopolymers, the higher the strength they exhibited.

  - An extension of the curing time also has an impact on the strength of geopolymers; however, it is not as large as in the case of the influence of the curing temperature alone – the extension of the curing time to at least 20 h allows for observing a significant increase in the rate of reaction and accelerated strength of geopolymers [78].
  - The curing time is closely related to the adopted temperature, while the use of high temperatures at the beginning of the process results in the appearance of greater porosity in the material, which negatively affects its strength.
- **Steam curing**

  This curing method has not yet been well described or studied. However, based on results from several publications related to steam curing of geopolymers, it can be observed that:
  - The strength of geopolymers increases with the increase of the adopted steam curing temperature, and a temperature of 80°C is considered the optimum [79].
  - Addition of conventional Portland cement to high-calcium fly ash, by facilitating the hydration process, significantly improves the compressive strength of steam-cured geopolymer [80].
  - For slag-based geopolymers, better strength properties were obtained for samples steam-cured at 80°C compared to samples cured at ambient temperature [81].
  - Hydrothermal steam curing at temperatures above 65°C contributes to the reduction of efflorescence in geopolymers and thus to their strength [77].
- **Ambient curing**

  Ambient-temperature curing of geopolymers is one of the most widely studied methods [31]. As basic observations about this method, the following should be mentioned here:
  - for F class fly ash-based geopolymers activated with an alkaline solution (solution/binder ratio of 0.4), a significant improvement in strength properties occurs, already after five days of curing at ambient temperature, with strength increasing with curing time, and this increase over time is much greater than for samples cured at higher temperatures; nevertheless, considering the final strength values of geopolymers, oven curing is a more effective method [82],
  - in the case of geopolymers for construction applications, manufactured based on fly ash with the addition of conventional Portland cement, the amount of Portland cement used has a decisive influence on the rate of curing at ambient temperature – a smaller amount of cement shortens the setting time while resulting in a faster increase in the strength properties of geopolymers at the initial stage of curing [83],
  - geopolymer composites produced based on fly ash with the addition of slag, cured at ambient temperature, achieve similar setting time, workability,

and initial strength as conventional cement-based concrete – ground granulated blast furnace slag contributes to the release of internal heat, which supports the geopolymerisation process during curing at ambient temperature, which in turn contributes to an increase in strength during the initial period [84].

Therefore, it can be concluded that the main factor hindering the application of geopolymer composites is ambient curing because the structural members cannot be heated and steam-cured in situ. In this regard, further research is needed on the curing scheme of geopolymer composites for its applicability in construction [31].

4.6. PROPERTIES OF GEOPOLYMERS

4.6.1. PHYSICAL PROPERTIES

The most important physical properties of geopolymers include bulk density and porosity, which are closely interdependent and largely determine other material characteristics. Bulk density is related to the geopolymer's microstructure, the degree of solid phase packing, and the proportion of open and closed pores in its structure. The value of this parameter depends primarily on the type of aluminosilicate precursor, the type of alkaline activator, the liquid-to-solid ratio, and the material's curing conditions. An increase in density usually results in a reduction in internal voids and a more compact microstructure, leading to improved mechanical properties [16, 29].

Mineral additives and technological parameters also significantly affect the density of geopolymers. The introduction of heavier fillers, such as basalt or blast furnace slag, can increase the material's density and densify its microstructure. Conversely, the use of low-density additives, such as organic or porous materials, reduces density and may improve the composite's insulating properties. In engineering practice, these properties are intentionally tailored to the material's intended use – from dense, high-density structural materials to lightweight insulating composites [61].

Porosity, defined as the proportion of pore volume in the total volume of the material, is directly related to bulk density. Geopolymers contain both open pores, which influence the transport of liquids and gases, and closed pores, which are responsible for insulating properties. In addition to the total number of pores, their size, shape, and spatial arrangement are also important. Reducing pore size and number leads to a denser microstructure and improved mechanical properties of the material [85].

Higher porosity materials, on the other hand, exhibit lower density and lower strength, but can also exhibit very good thermal insulation properties. A particular

example is foamed geopolymers, whose porosity can exceed 50%, enabling very low thermal conductivity [73]. In such materials, controlling the foaming process, pore size, and pore distribution is crucial to achieving the desired functional properties.

Porosity also significantly impacts the durability of geopolymers, as excessive pore count or size can increase permeability and facilitate the migration of aggressive chemicals. Therefore, designing the microstructure of geopolymers involves not only selecting raw materials but also controlling particle granulation, component ratios, and curing parameters [16, 24].

4.6.2. MECHANICAL PROPERTIES

The mechanical properties of geopolymers are closely related to the structure of their aluminosilicate matrix and to the degree of cross-linking formed during geopolymerisation. The most important mechanical parameter is compressive strength, which determines the material's ability to carry loads without losing structural integrity. In geopolymers, the main strength carriers are N-A-S-H or K-A-S-H gels, whose density and degree of polycondensation determine the material's ultimate resistance [86].

The compressive strength values of geopolymers can vary widely and depend on the chemical composition and synthesis conditions. In materials with a compact microstructure, they can exceed 60 MPa, comparable to the values achieved by high-quality cement concretes [85]. The type of precursor plays a significant role – geopolymers based on metakaolin or fly ash often exhibit stable, high-strength properties. In systems containing blast furnace slag, C-(A)-S-H phases also form, increasing the matrix density and contributing to improved mechanical properties [87].

The molar ratios of the components, especially the Si/Al ratio and the alkaline activator concentration, are also important. A properly selected composition promotes the formation of a dense network of aluminosilicate bonds, whereas excess mixing fluid or excessive porosity can reduce the material's strength [26].

In addition to compressive strength, flexural strength is also important, determining the material's resistance to loads that cause tensile stresses. Geopolymers are typically brittle-ceramic materials, so their flexural strength is sometimes limited. Various reinforcing additives, such as polymer, basalt, or steel fibres, are used to improve these properties. These fibres limit microcrack development and increase the material's ability to absorb energy under load [29, 61].

In recent years, research has also examined the modification of the mechanical properties of geopolymers using nanofillers, such as nano-SiO_2 or carbon nanotubes. These additives enable densification of the microstructure and improved stress transfer within the geopolymer matrix. Mechanical properties also depend on

curing conditions – applying elevated temperatures during the initial curing phase intensifies the polycondensation reaction and leads to a more compact material structure [30].

4.6.3. THERMAL PROPERTIES

One of the significant properties of geopolymers is their high resistance to elevated temperatures. This property results from the presence of a stable Si–O–Al bond network, which exhibits significantly greater thermal resistance than Portland cement hydration products. This allows geopolymers to maintain their structural integrity at high temperatures and exhibit lower mass loss and thermal expansion than traditional cementitious materials [61, 88].

At elevated temperatures, processes related to the removal of physically bound water and microstructural reorganisation can occur within the structure of geopolymers. At temperatures of several hundred degrees Celsius, some decrease in mechanical strength is observed, but the material usually retains its shape and basic structural integrity [69]. At even higher temperatures, new crystalline phases can form, which in some cases can improve the material's thermal stability.

Thanks to these properties, geopolymers are used as fire-resistant materials, protective coatings for steel structures, and components of materials for high-temperature environments. An additional advantage is their non-flammability and the absence of toxic gas emission upon exposure to high temperatures [29].

4.6.4. CHEMICAL AND DURABILITY PROPERTIES

Geopolymers are characterised by high chemical resistance and good environmental durability, two significant advantages over Portland cement-based materials. This is primarily due to the presence of a compact, amorphous aluminosilicate network with low capillary porosity and a large number of Si–O–Al covalent bonds [29]. This structure limits the penetration of aggressive ions and reduces the material's susceptibility to chemical degradation.

Compared to Portland cement, geopolymers exhibit greater resistance to acids, chlorides, and sulfates. In acidic environments, degradation typically begins with ion exchange and partial leaching of aluminium from the structure, but this process occurs much more slowly than in traditional cementitious materials [14]. As a result, geopolymers maintain their structural integrity even in chemically aggressive environments.

Another important characteristic is their resistance to carbonation and limited permeability to carbon dioxide and chloride ions, which is crucial for reinforced

structures. The material's compact microstructure hinders the migration of aggressive agents, allowing corrosion processes to proceed more slowly than in cementitious composites [62].

The environmental durability of geopolymers also includes resistance to freeze-thaw cycles, humidity changes, and atmospheric exposure. The dense microstructure limits the development of damage associated with ice expansion within pores, thereby promoting the long-term preservation of the material's mechanical properties [12]. Geopolymers also exhibit low susceptibility to biological degradation, as their high alkalinity and limited nutrient availability hinder microbial growth.

In summary, geopolymers combine favourable physical, mechanical, thermal, and chemical properties. The ability to shape them through the selection of raw materials, component proportions, and synthesis conditions makes them a group of materials with significant potential for use in modern construction and materials engineering, particularly in the context of durability and resistance to environmental factors.

4.7. GEOPOLYMER COMPOSITES

Nowadays, geopolymer composites play an important role in many sectors of the economy and, consequently, they are finding more and more applications in advanced solutions across industries such as aerospace and automotive. The general division of reinforcements used in composites includes fibres, whiskers [89, 90] and particles (Fig. 4.6), and, as indicated by results reported in the literature [90, 91], their mechanical strength and elastic modulus decrease with increasing diameter [92]. To improve the strength properties and energy absorption, additives such as threads, fibres, whiskers, and nanoparticles are introduced into geopolymer composites [92].

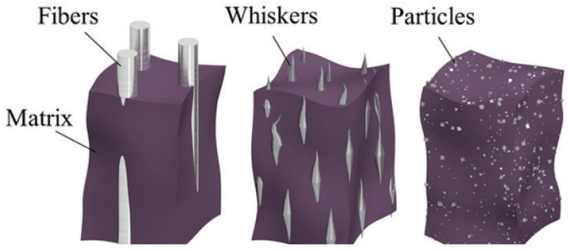

Fig. 4.6. Different types of fibre-reinforced composites based on particle size [92]

The most commonly used reinforcements in geopolymer composites are various types of fibres. Fig. 4.7 shows potential applications of fibre-reinforced geopolymer composites.

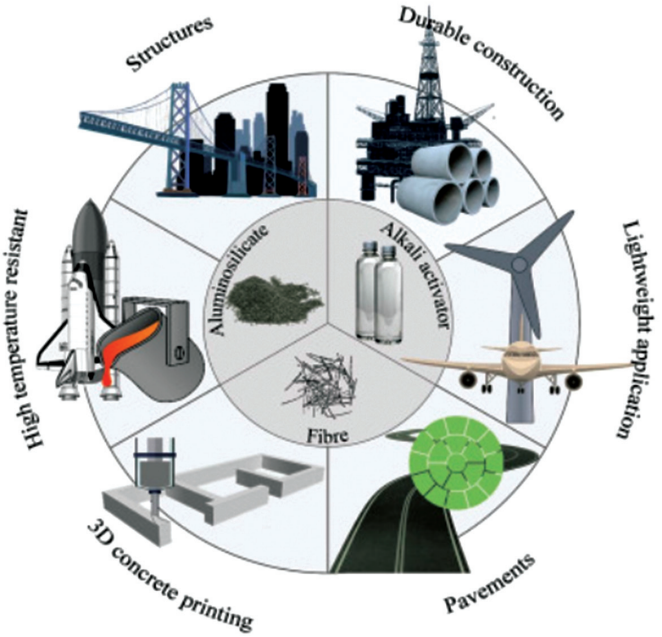

Fig. 4.7. Potential applications of fibre-reinforced geopolymer composites [91]

When choosing this type of reinforcement, several factors must be considered:

- the material must exhibit properties consistent with the application;
- there must be sufficient interaction between the fibre and the matrix to allow proper stress transfer;
- there must be an optimum form factor that will ensure that the composite will behave effectively after a fracture.

As shown in the literature, the type and properties of the fibres used as reinforcement in geopolymer composites have had a greater impact on their final properties than the binder itself [91–96]. Ranjbar et al. [91] in their study divided fibres into five groups:

- Steel fibres, which according to ASTM A820-16 can be divided into five types for different purposes, including:
  - pieces of smooth or deformed cold-drawn wire;
  - smooth or deformed cut sheet;
  - melt-extracted fibres;
  - mill-cut fibres;
  - modified cold-drawn steel fibres.
- Steel fibres are characterised by:
  - density in the range of 7.65–7.85 g/cm^3;
  - a wide tensile strength range of 345–2850 MPa;
  - Young's modulus in the range of 200–210 GPa;
  - ultimate elongation in the range of 0.5–3.5%;

  - corrugated surface (resulting from the manufacturing process), which causes a strong interaction between the fibres and the matrix [97, 98].
- Inorganic fibres, which, depending on the material used, can be processed in a variety of ways, including rod-drawing, hole-passing (melt-spun fibre production), crystal growth from molten solution, or by vapor-liquid-solid techniques, vapor deposition, and chemical reactions [89, 90]. The most commonly used inorganic fibres include:
  - Basalt fibres, obtained from volcanic rocks by melting at temperatures in the range of 1500–1700°C. The advantages of this type of fibre include low cost, high availability, good abrasion resistance, very good strength, and hardness (8–9 on the Mohs scale), durability, and good thermal properties. Basalt fibres show good resistance to acids; unfortunately, they corrode under alkaline conditions [100].
  - Commonly used silica fibres made of high-purity SiO_2 metal oxides, including:
    - electrical glass (E-glass);
    - structural glass (S-glass);
    - chemical glass (C-glass);
    - alkali-resistant glass (AR-glass).
  - Aluminosilicate and alumina fibres, whose composition is also based on metal oxides (silicates + almost 45–60% Al_2O_3), are produced by blowing or spinning molten kaolin or related clays/precursors containing Al_2O_3 and SiO_2.
  - Other fibres based on: boron, boron carbide, boron nitride, zirconia, silicon carbide, or silicon nitride.
- Polymer fibres, whose mechanical properties, stiffness, or environmental stability mainly depend on their degree of crystallinity. Polymer fibres are considered crystalline when their crystallinity exceeds 80%, semi-crystalline when it is in the range of 10–80%, and amorphous when it is below 10% [100, 101]. Depending on the material on the basis of which polymer fibres were produced, they can be divided into synthetic or natural. The most commonly used polymer fibres for geopolymer reinforcements are synthetic fibres based on polypropylene (PP), polyethylene (PE), poly(vinyl alcohol) (PVA), and polyethylene terephthalate (PET). Each of these plastics has unique properties that determine their use; e.g. polypropylene is cheap and reduces the risk of shrinkage and surface cracking, PET is more cost-effective and environmentally friendly, PVA forms very strong bonds with the cement matrix/binding agent but has a tendency to break fibres, which negatively affects tensile strength, polyethylene is non-hygroscopic and has good tensile strength and resistance to light chemicals [101–103].
- Natural fibres, whose popularity has been steadily increasing in recent years, are considered environmentally friendly and can be an alternative to synthetic fibres. Unfortunately, for natural fibres, there are still obstacles to the production of geopolymers. The most difficult obstacle to eliminate is the decomposition

of certain chemical components of the fibre, which results in the weakening of the bond between the fibre and the matrix – the type, form, and properties of the chosen natural fibre are decisive here. Natural fibres have properties that facilitate their use as reinforcements in a variety of composite materials, including plastics and concrete. Their major advantages include, but are not limited to, reproducibility of raw materials, relatively low production costs, and in many cases, relatively short "production" times (short plant vegetation cycles). Compared to chemical fibres, they are characterised by low density and high specific strength, are non-toxic to the human body and environmentally friendly, and are usually easy to process [104–109]. Natural fibres used in the production of geopolymer composites include monofilament cellulosic fibres such as jute, hemp, kenaf, bagasse, and sisal [110]. These fibres exhibit several advantages:

- easy availability;
- low cost;
- low density;
- reduced thermal conductivity;
- acceptable mechanical properties.

However, it is also important to mention the disadvantages of natural fibres, which include:

- low durability;
- poor performance at high fibre content, which reduces the workability of the fresh composite;
- inconsistent material properties;
- poor interaction with the matrix [110–112].

- Carbon fibres and nanofibres (approximately 0.5–1.5 μm in diameter), known for their exceptionally high strength and low weight among reinforcement fibres, are widely used in advanced composites. They are characterised by retaining high tensile strength and Young's modulus at high temperatures. PAN fibres obtained in the process of polyacrylonitrile conversion belong to the most commonly used ones, due to their favourable price-to-strength ratio. Less frequently used are packing fibres (a by-product of crude oil processing) and artificial silk fibres. Among nanofibres, nanotubes are the most commonly used. In the literature, one can find a division of fibres into different categories [113, 114]:
  - division according to Young's modulus:
    - low modulus below 200 GPa;
    - standard modulus about 230 GPa;
    - medium modulus about 300 GPa;
    - high modulus over 350 GPa;
    - very high modulus exceeding 600 GPa.
  - division taking into account geometrical features:
    - continuous fibres;
    - carbon fibres.

4.8. GEOPOLYMER APPLICATIONS

One of the most important applications of geopolymers is construction, where these materials are considered an alternative to traditional Portland cement-based composites. Their use stems from their favourable mechanical properties, high chemical resistance, and good thermal stability, as well as from their ability to utilise waste materials such as fly ash or blast furnace slag [29]. Compared to traditional cement concretes, geopolymers are characterised by a different microstructure based on a three-dimensional network of Si–O–Al aluminosilicate bonds, which facilitates the formation of a compact matrix with limited porosity and low permeability to aggressive environmental factors. This allows for the achievement of high mechanical strength relatively quickly after the elements are formed [27].

In engineering practice, geopolymers are used to produce various structural elements, such as load-bearing beams, floor slabs, tunnel segments, and prefabricated facade panels. These materials can be produced from both natural precursors, such as metakaolin, and aluminosilicate waste materials. In many cases, mixed systems are used, such as fly ash and blast furnace slag (FA–GGBFS), which produce a synergistic effect resulting from the coexistence of geopolymerisation reactions and the hydration of calcium phases. This increases the matrix density and improves the material's mechanical properties [29].

A significant aspect of geopolymers' structural applications is their high resistance to chemical agents, such as chlorides and sulfates, which often lead to the degradation of cement concretes. A properly designed material microstructure limits the penetration of aggressive ions and slows down corrosion processes in structures exposed to marine environments, salinity, or aggressive de-icing agents [18]. For this reason, geopolymers are considered materials for infrastructure applications, including bridges, transportation elements, and structures exposed to moisture and fluctuating temperatures.

Another important characteristic of geopolymers is their high resistance to fire and elevated temperatures. Unlike cementitious materials, they do not rapidly degrade with temperature increases, and their structure remains stable even at temperatures of several hundred degrees Celsius. In many cases, they maintain structural integrity even at temperatures up to 800–1000°C, making them attractive materials for the design of structural elements with increased fire-safety requirements [114, 115]. As a result, they can be used as steel cladding, fire-resistant panels, or structural components exposed to high temperatures.

Designing geopolymer structural elements requires appropriate control of the material's bulk density and porosity. High density increases mechanical strength and reduces the permeability of liquids and aggressive gases, while moderate porosity can reduce the dead weight of precast elements and improve their insulating properties. For elements operating primarily in compression, such as columns or foundation blocks, achieving the most compact possible

microstructure by optimising the chemical composition and granulation of the components is crucial. However, elements subjected to bending, such as slabs or beams, often require additional reinforcement in the form of fibres or continuous reinforcement, which increases the material's resistance to crack formation and propagation [116].

The potential of geopolymer technology is also confirmed by industrial-scale examples. One such example is the use of geopolymer concrete, Earth Friendly Concrete (EFC), in infrastructure structures, including airport and road elements. Operational observations indicate that such materials are less susceptible to chemical corrosion, salt efflorescence, and environmental degradation compared to traditional Portland cement concretes [62].

Another significant argument for using geopolymers in construction is their favourable environmental footprint. Their production eliminates the need for clinkerisation, which is a major source of CO_2 emissions in the cement industry. Furthermore, the ability to utilise byproducts from the energy and metallurgical industries helps reduce waste and the carbon footprint of construction projects [22]. As a result, geopolymers can be a significant element of sustainable construction strategies.

Another important application of geopolymers in construction is insulation materials. The ability to shape the material's porous structure plays a key role here, allowing for low thermal conductivity while maintaining adequate mechanical stability. The geopolymer structure allows the incorporation of lightweight, highly porous fillers, such as cork granules, perlite, or pumice, into the mix, thereby reducing the material's density and enhancing its thermal insulation properties [18].

The nature of porosity also plays a significant role in insulating properties. Closed pores reduce thermal conductivity by trapping air within the material structure, while open pores primarily influence the transport of water vapor and liquids. Geopolymer technology enables control of pore structure through the use of foaming agents, surfactants, and the appropriate selection of mixing and curing parameters [16]. As a result, materials with an optimised pore structure can be obtained, combining good thermal insulation properties with sufficient mechanical strength.

An additional advantage of geopolymer insulating materials is their high fire resistance. Unlike many polymeric materials, they do not melt or release toxic gases when heated, and their structure remains stable even at temperatures reaching approximately 1000°C [29]. This allows them to be used not only as thermal insulation for building envelopes but also as a protective layer for structural elements exposed to fire.

In the case of foamed geopolymers, it is possible to obtain materials with very low density, often below 500 kg/m^3, and thermal conductivity below 0.15 W/(m·K). However, achieving these parameters requires precise control of the foaming process, including the viscosity of the fresh mass, the reaction time of the blowing

agent, and the material's curing conditions [68]. Properly designed geopolymer-based insulation systems can compete with traditional mineral and polymer-based construction materials.

In summary, the use of geopolymers in construction encompasses both structural elements and insulation materials. Their high mechanical strength, chemical and thermal resistance, and the ability to use waste raw materials make them a promising alternative to traditional building materials, especially given growing requirements for structural durability and efforts to limit the impact of construction on the natural environment.

REFERENCES

[1] Błaszczyński, T.Z.; Król, M.R. Geopolymers in Construction. *Civil and Environmental Engineering Reports* **2015**, *16*(1), 25–40. https://doi.org/10.1515/ceer-2015-0002.

[2] Xu, J.; Mi, Z.; Zhao, D.; Zhong, G.; Sun, Y.; Hu, X.; Sun, J.; Li, X.; Zhu, W.; Li, M.; et al. Research and Application Progress of Geopolymers in Adsorption: A Review. *Nanomaterials* **2022**, *12*, 3002. https://doi.org/10.3390/nano12173002.

[3] Davidovits, J. Geopolymer Cement: A Review. In *Geopolymer Science and Technics*; Technical Paper No. 21; Geopolymer Institute: Saint-Quentin, France, **2013.**

[4] Duxson, P.; Fernández-Jiménez, A.; Provis, J.L.; Lukey, G.C.; Palomo, A.; van Deventer, J.S.J. Geopolymer Technology: The Current State of the Art. *J. Mater. Sci.* **2007**, *42*, 2917–2933. https://doi.org/10.1007/S10853-006-0637-Z.

[5] Rahier, H.; Simons, W.; van Mele, B.; Biesemans, M. Low-Temperature Synthetized Aluminosilicate Glasses: Part III. Influence of the Composition of the Silicate Solution on Production, Structure and Properties. *J. Mater. Sci.* **1997**, *32*, 2237–2247. https://doi.org/10.1023/A:1018563914630/METRICS.

[6] Mallicoat, S.; Sarin, P.; Kriven, W.M. Novel, Alkali-Bonded, Ceramic Filtration Membranes. *Ceram. Eng. Sci. Proc.* **2008**, *37*, 37–44. https://doi.org/10.1002/9780470291283.CH5.

[7] V., K.P. Alkaline Cements. *Proceedings of the 1st International Conference on Alkaline Cements and Concretes, Kyiv, Ukraine,* **1994**, *1*, 11–129.

[8] Palomo, A.; López de la Fuente, J.I. Alkali-Activated Cementitious Materials: Alternative Matrices for the Immobilisation of Hazardous Wastes. Part I: Stabilisation of Boron. *Cement and Concrete Research* **2003**, *33*(2), 281–288.

[9] Sofi, M.; van Deventer, J.S.J.; Mendis, P.A.; Lukey, G.C. Engineering Properties of Inorganic Polymer Concretes (IPCs). *Cement and Concrete Research* **2007**, *37*(2), 251–257.

[10] Bao, Y.; Grutzeck, M.W.; Jantzen, C.M. Preparation and Properties of Hydroceramic Waste Forms Made with Simulated Hanford Low-Activity Waste. *Journal of the American Ceramic Society* **2005**, *88*(12), 3287–3302.

[11] Škvára, F. Alkali Activated Materials or Geopolymers? *Ceramics–Silikáty* **2007**, *51*(3), 173–177.

[12] Sbahieh, S.; McKay, G.; Al-Ghamdi, S.G. Comprehensive Analysis of Geopolymer Materials: Properties, Environmental Impacts, and Applications. *Materials* **2023**, *16, 7363*. https://doi:10.3390/MA16237363.

[13] Mehta, A.; Siddique, R. An Overview of Geopolymers Derived from Industrial By-Products. *Constr. Build. Mater.* **2016**, *127*, 183–198. https://doi:10.1016/J.CONBUILDMAT.2016.09.136.
[14] Nawaz, M.; Heitor, A.; Sivakumar, M. Geopolymers in Construction – Recent Developments. *Constr. Build. Mater.* **2020**, *260*. https://doi:10.1016/J.CONBUILDMAT.2020.120472.
[15] Łach, M.; Quesada, E.; Harja, M. Geopolymer Foams – Will They Ever Become a Viable Alternative to Popular Insulation Materials? – A Critical Opinion. *Materials* **2021**, *14*, 3568. https://doi:10.3390/MA14133568.
[16] Chen, S.; Ruan, S.; Zeng, Q.; Liu, Y.; Zhang, M.; Tian, Y.; Yan, D. Pore Structure of Geopolymer Materials and Its Correlations to Engineering Properties: A Review. *Construction and Building Materials,* **2022**, *328, 127064*. https://doi:10.1016/J.CONBUILDMAT.2022.127064.
[17] Arain, A.M.; Aziz, S.; Soomro, S.A.; Iqbal, A.; Laghari, A.Q. Optimization of Geopolymer Synthesis Using Coal Fly Ash for Enhancement in Properties as Sustainable and Durable Construction Material. *Journal of Ecological Engineering* **2026**, *27(2)*, 199–209. https://doi:10.12911/22998993/211245.
[18] Kudłacik-Kramarczyk, S.; Drabczyk, A.; Figiela, B.; Korniejenko, K. Geopolymers: Advanced Materials in Medicine, Energy, Anticorrosion and Environmental Protection. *Materials* **2023**, *16, 7416*. https://doi:10.3390/MA16237416.
[19] Alhawat, M.; Ashour, A.; Yildirim, G.; Aldemir, A.; Sahmaran, M. Properties of Geopolymers Sourced from Construction and Demolition Waste: A Review. *Journal of Building Engineering* **2022**, *50*, 104104. https://doi:10.1016/J.JOBE.2022.104104.
[20] Škvára, F.; Kopecký, L.; Nemecek, J.; Bittnar, Z. Microstructure of Geopolymer Materials Based on Fly Ash. *Ceramics – Silikáty* **2006**, *50*, 208–215.
[21] Ettahiri, Y.; Samuel, D.M.; Bouna, L.; Khali, A.; Ayoub Aziz; Benlhachemi, A.; Pérez-Villarejo, L.; Kriven, W.M. Comparative Study of Physicochemical Properties of Geopolymers Prepared by Four Moroccan Natural Clays. *Journal of Building Engineering* **2023**, *80*, 108021. https://doi:10.1016/J.JOBE.2023.108021.
[22] Madirisha, M.M.; Dada, O.R.; Ikotun, B.D. Chemical Fundamentals of Geopolymers in Sustainable Construction. *Materials Today Sustainability* **2024**, *27*, 100842. https://doi:10.1016/J.MTSUST.2024.100842.
[23] Burduhos Nergis, D.D.; Abdullah, M.M.A.B.; Vizureanu, P.; Mohd Tahir, M.F. Geopolymers and Their Uses: Review. *IOP Conf. Ser. Mater. Sci. Eng.* **2018**, *374*, 012019. https://doi:10.1088/1757-899X/374/1/012019.
[24] Mira, Ş.; Schiopu, A.-G.; Oproescu, M.; Modan, E.M. Comparative Assessment of Functionalized Geopolymers. *Applied Sciences* **2026**, *16*(3), 1513.
[25] Jwaida, Z.; Dulaimi, A.; Mashaan, N.; Othuman Mydin, M.A. Geopolymers: The Green Alternative to Traditional Materials for Engineering Applications. *Infrastructures* **2023**, *8*, 98. https://doi:10.3390/INFRASTRUCTURES8060098.
[26] Castillo, H.; Collado, H.; Droguett, T.; Sánchez, S.; Vesely, M.; Garrido, P.; Palma, S. Factors Affecting the Compressive Strength of Geopolymers: A Review. *Minerals* **2021**, *11*, 1317. https://doi:10.3390/MIN11121317.
[27] Davidovits, J. Properties of Geopolymer Cements. In *Proceedings of the First International Conference on Alkaline Cements and Concretes*; Kyiv, Ukraine, 1994; pp. 131–149.
[28] Dahal, S. Synthesis of Alkali Activated Geopolymer Cement from Clay. **2022**. https://doi:10.37421/2165-784X.22.12.455.

[29] Petermann, J.C.; Saeed, A.; Hammons, M.I. Alkali-Activated Geopolymers: A Literature Review. **2010**. https://doi:10.21236/ADA559113.
[30] Jeyasehar, A.; Salahuddin, M.; Thirugnanasambandam, S. Development of fly ash based geopolymer concrete precast elements. **2013**.
[31] Yang, H.; Liu, L.; Yang, W.; Liu, H.; Ahmad, W.; Ahmad, A.; Aslam, F.; Joyklad, P. A Comprehensive Overview of Geopolymer Composites: A Bibliometric Analysis and Literature Review. *Case Studies in Construction Materials* **2022**, *16*. https://doi:10.1016/J.CSCM.2021.E00830.
[32] Mucsi, G.; Ambrus, M. Raw Materials for Geopolymerisation. **2018**. https://doi:10.26649/MUSCI.2017.008.
[33] Xu, H.; Van Deventer, J.S.J. The Geopolymerisation of Alumino-Silicate Minerals. Int. J. Miner. Process. 2000, 59, 247–266. https://doi:10.1016/S0301-7516(99)00074-5.
[34] Mucsi, G.; Kumar, S.; Csoke, B.; Kumar, R.; Molnár, Z.; Rácz, Á.; Mádai, F.; Debreczeni, Á. Control of Geopolymer Properties by Grinding of Land Filled Fly Ash. *Int. J. Miner. Process.* **2015**, *143*, 50–58. https://doi:10.1016/J.MINPRO.2015.08.010.
[35] Khatib, J.M. (Ed.) *Sustainability of Construction Materials*, 2nd ed.; Woodhead Publishing: Cambridge, UK, 2016.
[36] Vizcaíno, C.; de Gutiérrez, R.M.; Castello, R.; Rodríguez, E.; Guerrero, C.E. Pozzolan Obtained by Mechanochemical and Thermal Treatments of Kaolin. *Applied Clay Science* **2010**, *49*(4), 405–413.
[37] Duxson, P.; Provis, J.L.; Lukey, G.C.; Mallicoat, S.W.; Kriven, W.M.; van Deventer, J.S.J. Understanding the Relationship between Geopolymer Composition, Microstructure and Mechanical Properties. *Colloids and Surfaces A: Physicochemical and Engineering Aspects* **2005**, *269*(1–3), 47–58.
[38] Balczár, I.; Korim, T.; Kovács, A.; Makó, É. Mechanochemical and Thermal Activation of Kaolin for Manufacturing Geopolymer Mortars–Comparative Study. *Ceramics International* **2016**, *42*(14), 15367–15375.
[39] Tuyan, M.; Andiç-Çakir, Ö.; Ramyar, K. Effect of Alkali Activator Concentration and Curing Condition on Strength and Microstructure of Waste Clay Brick Powder-Based Geopolymer. *Composites Part B: Engineering* **2018**, *135*, 242–252.
[40] Alcamand, H.A.; Borges, P.H.R.; Silva, F.A.; Trindade, A.C.C. The Effect of Matrix Composition and Calcium Content on the Sulfate Durability of Metakaolin and Metakaolin/Slag Alkali-Activated Mortars. *Ceram. Int.* **2018**, *44*, 5037–5044. https://doi:10.1016/J.CERAMINT.2017.12.102.
[41] El-Wafa, M.A.; Fukuzawa, K. Early-Age Strength of Alkali-Activated Municipal Slag–Fly Ash–Based Geopolymer Mortar. *Journal of Materials in Civil Engineering* **2018**, *30*. https://doi:10.1061/(ASCE)MT.1943-5533.0002234.
[42] Tho-In, T.; Sata, V.; Boonserm, K.; Chindaprasirt, P. Compressive Strength and Microstructure Analysis of Geopolymer Paste Using Waste Glass Powder and Fly Ash. *Journal of Cleaner Production* **2018**, *172*, 2892–2898.
[43] Lemougna, P.N.; Wang, K.; Tang, Q.; Cui, X. Study on the Development of Inorganic Polymers from Red Mud and Slag System: Application in Mortar and Lightweight Materials. *Construction and Building Materials* **2017**, *156*, 486–495.
[44] Ducman, V.; Korat, L. Characterization of Geopolymer Fly-Ash-Based Foams Obtained with the Addition of Al Powder or H_2O_2 as Foaming Agents. Materials Characterization **2016**, *113*, 207–213.

[45] Papa, E.; Medri, V.; Amari, S.; Manaud, J.; Benito, P.; Vaccari, A.; Landi, E. Zeolite–Geopolymer Composite Materials: Production and Characterization. *Journal of Cleaner Production* **2018**, *171*, 76–84.
[46] Available online: http://alsitech.pl/wp-content/uploads/2016/01/Geopolimery-z-tufu-wulkanicznegoa.pdf (accessed May 19, 2022).
[47] Figiela, B.; Korniejenko, K. The Possibility of Using Waste Materials as Raw Materials for the Production of Geopolymers. *Acta Innovations* **2020**, 48–56. https://doi:10.32933/ACTAINNOVATIONS.36.4.
[48] Bernal, S.A.; Rodríguez, E.D.; Paula Kirchheim, A.; Provis, J.L. Management and Valorisation of Wastes through Use in Producing Alkali-Activated Cement Materials. *Journal of Chemical Technology and Biotechnology 91*, https://doi:10.1002/jctb.4927.
[49] Zain, H.; Abdullah, M.M.A.B.; Hussin, K.; Ariffin, N.; Bayuaji, R. Review on Various Types of Geopolymer Materials with the Environmental Impact Assessment. *MATEC Web of Conferences* **2017**, *97*, 01021. https://doi:10.1051/MATECCONF/20179701021.
[50] Tomek, S.; Nana, A.; Tchakouté, H.K.; Temuujin, J.; Rüscher, C.H. Mineralogical Evolution of Raw Materials Transformed to Geopolymer Materials: A Review. *Ceram. Int.* **2024**, *50*, 35855–35868. https://doi:10.1016/J.CERAMINT.2024.07.024.
[51] Dal Poggetto, G. *Synthesis of Geopolymers with Industrial Waste: Chemical and Microstructural Characterization.* Ph.D. Thesis, University of Modena and Reggio Emilia, Modena, Italy, **2016**.
[52] Provis, J.; Duxson, P.; Lukey, G.C.; Deventer, J. Modelling the Formation of Geopolymers. Department of Chemical and Biomolecular Engineering, The University of Melbourne, Melbourne, Australia, **2006**.
[53] Servadei, F.; Cotineau, N.; Medri, V.; Murri, A.N.; Papa, E.; Valdrè, G.; Landi, E. Co-Valorisation of Construction and Demolition Waste and Basalt Powder as Raw Materials in Geopolymers. *Construction and Building Materials* **2025**, *414*, 135656.
[54] Bhardwaj, P.; Gupta, R.; Salamamal, S.T.; Dhand, C.; Mishra, D. Recent Trends in Mechanochemical Processing of Fly Ash Aluminosilicate Materials (Geopolymers): Advancement, Challenges, and Opportunities. *J. Mater. Cycles Waste Manag.* **2024**, *26*, 1–1955.
[55] Hidavati, R.E.; Esarabadilla, F.S.; Dadang, D.; Harmelia, L.; Nurlina, N.; Prasetiyoko, E.; Fansuri, H. Setting Time and Compressive Strength of Geopolymers Made of Three Indonesian Low-Calcium Fly Ash with Variation of Sodium Silicate Additi56.
[56] Asim, N.; Alghoul, M.; Mohammad, M.; Amin, M.H.; Akhtaruzzaman, M.; Amin, N.; Sopian, K. Emerging Sustainable Solutions for Depollution: Geopolymers. *Constr. Build. Mater.* **2019**, *199*, 540–548. https://doi:10.1016/J.CONBUILDMAT.2018.12.043.
[57] Ichimiya, K.; Hatanaka, S.; Atarashi, D.; Kunieda, M.; Goda, H.; Harada, K. Technical Committee on Application of Geopolymer Technology to Construction Field. *Journal of Advanced Concrete Technology* **2015**, *13*(6), 321–340.
[58] Wijesekara, K.K.D.A.; Sadique, M.; Carnacina, I.; Fielding, A.; Bojczuk, G.C. Mechanical and Durability Analysis of Geopolymer Concrete Made with Recycled Silicate Activator for Low Carbon Breakwaters. *Cleaner Waste Systems* **2025**, *11*. https://doi:10.1016/J.CLWAS.2025.100322.

[59] Vigvash; Raj, S.; Shazaman, M.; Rawat, D.K. Geopolymer as Alternate Cementitious Material: An Overview. *Journal of Emerging Technologies and Innovative Research (JETIR)* **2025**, *12*, L727–L739.
[60] Provis, J.L.; Van Deventer, J.S.J. Industrialization of Geopolymers: An Overview of Key Concepts. In *Alkali Activated Materials: State-of-the-Art Report, RILEM TC 224-AAM*; Springer: Dordrecht, **2014**; pp. 1–15.
[61] Łach, M.; Kozub, B.; Bednarz, S.; Bąk, A.; Melnychuk, M.; Masłoń, A. The Influence of the Addition of Basalt Powder on the Properties of Foamed Geopolymers. *Materials* **2024**, *17*, 2336. https://doi:10.3390/MA17102336.
[62] de Oliveira, L.B.; de Azevedo, A.R.G.; Marvila, M.T.; Pereira, E.C.; Fediuk, R.; Vieira, C.M.F. Durability of Geopolymers with Industrial Waste. *Case Studies in Construction Materials* **2022**, *16*, e00839. https://doi:10.1016/J.CSCM.2021.E00839.
[63] Kriven, W.M.; Leonelli, C.; Provis, J.L.; Boccaccini, A.R.; Attwell, C.; Duxson, P.; Ferrone, C.; Rossignol, S.; Luukkonen, T.; Van Deventer, J.S.J.; et al. Why Geopolymers and Alkali-Activated Materials Are Key Components of a Sustainable World: A Perspective Contribution. **2024**. https://doi:10.1111/jace.19828.
[64] Singh, B.; Ishwarya, G.; Gupta, M.; Bhattacharyya, S.K. Geopolymer Concrete: A Review of Some Recent Developments. *Constr. Build. Mater.* **2015**, *85*, 78–90. https://doi:10.1016/J.CONBUILDMAT.2015.03.036.
[65] Davidovits, J. *Geopolymers: Inorganic Polymeric New Materials.* Journal of Thermal Analysis **1991**, *37*, 1633–1656.
[66] Davidovits, J. Geopolymeric Cement Based on Low-Cost Geologic Materials. In *Proceedings of the Second International Conference on Geopolymers*; Saint-Quentin, France, **1999**; pp. 1–16.
[67] El Hafid, K.; Hajjaji, M.; El Hafid, H. Influence of NaOH Concentration on Microstructure and Properties of Cured Alkali-Activated Calcined Clay. *Journal of Building Engineering* **2017**, *12*, 212–218.
[68] Singh, N.B.; Middendorf, B. Geopolymers as an Alternative to Portland Cement: An Overview. *Construction and Building Materials* **2020**, *237*, 117455.
[69] Zhong, H.; Zhang, M. 3D Printing Geopolymers: A Review. *Cement and Concrete Composites* **2022**, *130*, 104527.
[70] Soutsos, M.; Boyle, A.P.; Vinai, R.; Hadjierakleous, A.; Barnett, S.J. Factors Influencing the Compressive Strengths of Fly Ash Based Geopolymers Factors Influencing the Compressive Strength of Fly Ash 1 Based Geopolymers. **2016**. https://doi:10.1016/j.conbuildmat.2015.11.045.
[71] Provis, J.L. Geopolymers and Other Alkali Activated Materials: Why, How, and What? *Materials and Structures/Materiaux et Constructions* **2014**, *47*, 11–25. https://doi:10.1617/S11527-013-0211-5.
[72] Ricciotti, L.; Apicella, A.; Perrotta, V.; Aversa, R. Geopolymer Materials for Extrusion-Based 3D-Printing: A Review. *Polymers* **2023**, *15*, 4688. https://doi:10.3390/POLYM15244688.
[73] Hardjito, D.; Rangan, B.V. *Development and Properties of Low-Calcium Fly Ash-Based Geopolymer Concrete.* Research Report GC1; Curtin University of Technology: Perth, Australia, 2005.
[74] Heah, C.Y.; Kamarudin, H.; Mustafa Al Bakri, A.M.; Binhussain, M.; Luqman, M.; Khairul Nizar, I.; Ruzaidi, C.M.; Liew, Y.M. Effect of Curing Profile on Kaolin-

Based Geopolymers. *Phys. Procedia* **2011**, *22*, 305–311. https://doi:10.1016/J.PHPRO.2011.11.048.

[75] Perera, D.S.; Uchida, O.; Vance, E.R.; Finnie, K.S. Influence of Curing Schedule on the Integrity of Geopolymers. *J. Mater. Sci.* **2007**, *42*, 3099–3106. https://doi:10.1007/S10853-006-0533-6.

[76] Kani, E.N.; Allahverdi, A. Effects of Curing Time and Temperature on Strength Development of Inorganic Polymeric Binder Based on Natural Pozzolan. *J. Mater. Sci.* **2009**, *44*, 3088–3097. https://doi:10.1007/S10853-009-3411-1.

[77] Rovnaník, P. Effect of Curing Temperature on the Development of Hard Structure of Metakaolin-Based Geopolymer. *Constr. Build. Mater.* **2010**, *24*, 1176–1183. https://doi:10.1016/J.CONBUILDMAT.2009.12.023.

[78] Yewale, V. V; Shirsath, M.N.; Hake, S.L. Evaluation of Efficient Type of Curing for Geopolymer Concrete. *International Journal of New Technologies in Science and Engineering* **2016**, *3*.

[79] Pangdaeng, S.; Phoo-ngernkham, T.; Sata, V.; Chindaprasirt, P. Influence of Curing Conditions on Properties of High Calcium Fly Ash Geopolymer Containing Portland Cement as Additive. *Mater. Des.* **2014**, *53*, 269–274. https://doi:10.1016/J.MATDES.2013.07.018.

[80] Yunsheng, Z.; Wei, S.; Qianli, C.; Lin, C. Synthesis and Heavy Metal Immobilization Behaviors of Slag Based Geopolymer. *J. Hazard. Mater.* **2007**, *143*, 206–213. https://doi:10.1016/J.JHAZMAT.2006.09.033.

[81] Vijai, K.; Kumutha, R.; Vishnuram, B.G. Effect of Types of Curing on Strength of Geopolymer Concrete. *International Journal of the Physical Sciences* **2010**, *5*(9), 1419–1423.

[82] Nath, P.; Sarker, P.K. Use of OPC to Improve Setting and Early Strength Properties of Low-Calcium Fly Ash Geopolymer Concrete Cured at Room Temperature. *Cement and Concrete Composites* **2015**, *55*, 205–214.

[83] Nath, P.; Sarker, P.K. Effect of GGBFS on Setting, Workability and Early Strength Properties of Fly Ash Geopolymer Concrete Cured in Ambient Condition. *Construction and Building Materials* **2014**, *66*, 163–171.

[84] Pławecka, K.; Bazan, P.; Lin, W.T.; Korniejenko, K.; Sitarz, M.; Nykiel, M. Development of Geopolymers Based on Fly Ashes from Different Combustion Processes. *Polymers* **2022**, *14*, 1954. https://doi:10.3390/POLYM14101954.

[85] Ramesh, V.; Srikanth, K. Mechanical Properties and Mix Design of Geopolymer Concrete – A Review. *E3S Web of Conferences* **2020**, *184*, 01091.

[86] Cheng, Y.; Hongqiang, M.; Hongyu, C.; Jiaxin, W.; Jing, S.; Zonghui, L.; Mingkai, Y. Preparation and Characterization of Coal Gangue Geopolymers. *Constr. Build. Mater.* **2018**, *187*, 318–326. https://doi:10.1016/J.CONBUILDMAT.2018.07.220.

[87] He, R.; Dai, N.; Wang, Z. Thermal and Mechanical Properties of Geopolymers Exposed to High Temperature: A Literature Review. *Advances in Civil Engineering* **2020**, 7532703.

[88] Sun, Q.; Li, W. *Inorganic-Whisker-Reinforced Polymer Composites: Synthesis, Properties and Applications.* CRC Press: Boca Raton, FL, USA, 2015.

[89] Cooke, T.F. Inorganic Fibres—A Literature Review. *Journal of the American Ceramic Society* **1991**, *74*, 2959–2978. https://doi:10.1111/J.1151-2916.1991.TB04289.X.

[90] Bowen, D.H. Fibre-Reinforced Ceramics. *Fibre Science and Technology* **1968**, *1*, 85–112. https://doi:10.1016/0015-0568(68)90001-8.

[91] Ranjbar, N.; Zhang, M. Fibre-Reinforced Geopolymer Composites: A Review. *Cem. Concr. Compos.* **2020**, *107*. https://doi:10.1016/J.CEMCONCOMP.2019.103498.
[92] Aulia, T.B. Effects of Polypropylene Fibres on the Properties of High-Strength Concretes. Ph.D. Thesis, Institute for Massivbau and Baustofftechnologie, University of Leipzig, Leipzig, Germany, **2002**.
[93] Mastali, M.; Dalvand, A.; Sattarifard, A.R.; Abdollahnejad, Z.; Illikainen, M. Characterization and Optimization of Hardened Properties of Self-Consolidating Concrete Incorporating Recycled Steel, Industrial Steel, Polypropylene and Hybrid Fibres. *Compos. B Eng.* **2018**, *151*, 186–200. https://doi:10.1016/J.COMPOSITESB.2018.06.021.
[94] Sukontasukkul, P.; Pongsopha, P.; Chindaprasirt, P.; Songpiriyakij, S. Flexural Performance and Toughness of Hybrid Steel and Polypropylene Fibre Reinforced Geopolymer. *Constr. Build. Mater.* **2018**, *161*, 37–44. https://doi:10.1016/J.CONBUILDMAT.2017.11.122.
[95] Bhutta, A.; Borges, P.H.R.; Zanotti, C.; Farooq, M.; Banthia, N. Flexural Behavior of Geopolymer Composites Reinforced with Steel and Polypropylene Macro Fibres. *Cem. Concr. Compos.* **2017**, *80*, 31–40. https://doi:10.1016/J.CEMCONCOMP.2016.11.014.
[96] Farooq, M.; Bhutta, A.; Banthia, N. Tensile Performance of Eco-Friendly Ductile Geopolymer Composites (EDGC) Incorporating Different Micro-Fibres. *Cem. Concr. Compos.* **2019**, *103*, 183–192. https://doi:10.1016/J.CEMCONCOMP.2019.05.004.
[97] Wang, X.H.; Jacobsen, S.; Ying He, J.; Liang Zhang, Z.; Lee, S.F.; Lein, H.L. Application of Nanoindentation Testing to Study of the Interfacial Transition Zone in Steel Fibre Reinforced Mortar. **2009**. https://doi:10.1016/j.cemconres.2009.05.002.
[98] Yin, J.; D'Haese, C.; Nysten, B. Surface Electrical Properties of Stainless Steel Fibres: An AFM-Based Study. *Appl. Surf. Sci.* **2015**, *330*, 65–73. https://doi:10.1016/J.APSUSC.2014.12.188.
[99] Wei, B.; Cao, H.; Song, S. Tensile Behavior Contrast of Basalt and Glass Fibres after Chemical Treatment. *Mater. Des.* **2010**, *31*, 4244–4250. https://doi:10.1016/J.MATDES.2010.04.009.
[100] Ko, Y.H.; Ahart, M.; Ko, J.H.; Song, J. Investigation of Polymorphism for Amorphous and Semi-Crystalline Poly (-Ethylene Terephthalate-) Using High-Pressure Brillouin Spectroscopy. *Journal of the Korean Physical Society* **2017**, *70*, 382–388. https://doi:10.3938/JKPS.70.382.
[101] Kozub, B.; Bazan, P.; Mierzwiński, D.; Korniejenko, K. Fly-Ash-Based Geopolymers Reinforced by Melamine Fibres. *Materials* **2021**, *14*, 400. https://doi:10.3390/MA14020400.
[102] Bazan, P.; Kozub, B.; Łach, M.; Korniejenko, K. Evaluation of Hybrid Melamine and Steel Fibre Reinforced Geopolymers Composites. *Materials* **2020**, *13*, 5548. https://doi:10.3390/MA13235548.
[103] Kozub, B.; Castro-Gomes, J. An Investigation of the Ground Walnut Shells' Addition Effect on the Properties of the Fly Ash-Based Geopolymer. *Materials* **2022**, *15*, 3936. https://doi:10.3390/MA15113936.
[104] Alomayri, T.; Low, I.M. Synthesis and Characterization of Mechanical Properties in Cotton Fibre-Reinforced Geopolymer Composites. *Journal of Asian Ceramic Societies* **2013**, *1*, 30–34. https://doi:10.1016/J.JASCER.2013.01.002.
[105] Alomayri, T.; Shaikh, F.U.A.; Low, I.M. Characterisation of Cotton Fibre-Reinforced

Geopolymer Composites. *Compos. B Eng.* **2013**, *50*, 1–6. https://doi:10.1016/J.COMPOSITESB.2013.01.013.

[106] Pacheco-Torgal, F.; Jalali, S. Cementitious Building Materials Reinforced with Vegetable Fibres: A Review. *Constr. Build. Mater.* **2011**, *25*, 575–581. https://doi:10.1016/J.CONBUILDMAT.2010.07.024.

[107] Korniejenko, K.; Frączek, E.; Pytlak, E.; Adamski, M. Mechanical Properties of Geopolymer Composites Reinforced with Natural Fibres. *Procedia Eng.* **2016**, *151*, 388–393. https://doi:10.1016/J.PROENG.2016.07.395.

[108] Alomayri, T.; Shaikh, F.U.A.; Low, I.M. Thermal and Mechanical Properties of Cotton Fabric-Reinforced Geopolymer Composites. *J. Mater. Sci.* **2013**, *48*, 6746–6752. https://doi:10.1007/S10853-013-7479-2.

[109] Ardanuy, M.; Claramunt, J.; Toledo Filho, R.D. Cellulosic Fibre Reinforced Cement-Based Composites: A Review of Recent Research. *Constr. Build. Mater.* **2015**, *79*, 115–128. https://doi:10.1016/J.CONBUILDMAT.2015.01.035.

[110] Azwa, Z.N.; Yousif, B.F.; Manalo, A.C.; Karunasena, W. A Review on the Degradability of Polymeric Composites Based on Natural Fibres. *Mater. Des.* **2013**, *47*, 424–442. https://doi:10.1016/J.MATDES.2012.11.025.

[111] Chen, R.; Ahmari, S.; Zhang, L. Utilization of Sweet Sorghum Fibre to Reinforce Fly Ash-Based Geopolymer. *J. Mater. Sci.* **2014**, *49*, 2548–2558. https://doi:10.1007/S10853-013-7950-0.

[112] Bunsell, A.R., Ed. *Handbook of Tensile Properties of Textile and Technical Fibres*, 2nd ed.; Woodhead Publishing: Cambridge, UK, **2009**.

[113] Chung, D.D.L. *Carbon Composites: Composites with Carbon Fibres, Nanofibres, and Nanotubes*, 2nd ed.; Butterworth-Heinemann: Oxford, UK, **2017**.

[114] Ridtirud, C.; Chindaprasirt, P.; Pimraksa, K. Factors Affecting the Shrinkage of Fly Ash Geopolymers. *International Journal of Minerals, Metallurgy and Materials* **2011**, *18*(1), 100–104.

[115] Gourley, J.T. Geopolymers in Australia. *Journal of the Australian Ceramic Society* **2014**, *50*(2), 102–110.

[116] Goode, M. *Fire Protection of Structural Steel in High-Rise Buildings.* Arup Fire: London, UK, **2004**.

5

3D PRINTING OF CEMENTS AND CONCRETES

Szymon Gądek

5.1. INTRODUCTION

Additive Manufacturing (AM), commonly referred to as 3D printing, is a manufacturing process in which physical objects are produced directly from digital models through layer-by-layer material deposition. In contrast to conventional manufacturing methods based on material removal or mould forming, additive manufacturing builds structures only where material is required, enabling optimised material usage and geometric freedom [1].

In construction engineering, additive manufacturing represents a significant technological transition toward automation and digitalisation of the building process. The integration of computer-aided design, robotics, and advanced materials allows construction elements to be fabricated with minimal manual intervention [1].

Initially developed for rapid prototyping, additive manufacturing has evolved into a production technology applied across multiple industries, including aerospace, medicine, automotive engineering, and civil engineering [2].

5.2. HISTORICAL DEVELOPMENT OF ADDITIVE MANUFACTURING

5.2.1. POLYMER-BASED ADDITIVE MANUFACTURING

The concept of layered fabrication predates modern digital technologies. Early concepts related to automated layered construction appeared in the twentieth century; however, practical implementation became possible only after the development of computer-controlled manufacturing systems.

A major milestone occurred in 1984 when Charles Hull introduced stereolithography (SLA), enabling fabrication of objects using digital layer data and establishing the STL file format standard.

Since then, additive manufacturing technologies have developed rapidly. Initially limited by cost and complexity, they have become increasingly accessible due to advances in computing power, robotics, and materials science. Today, additive manufacturing is considered one of the fastest-growing technological fields worldwide.

In construction, successful implementations of printed buildings and infrastructure elements demonstrate the beginning of a technological transformation sometimes described as a **new industrial revolution** in building technology [2].

5.2.2. ADDITIVE MANUFACTURING IN CONSTRUCTION

The concept of layer-based fabrication using construction materials emerged significantly earlier than in 1984. One of the earliest known examples of large-scale additive construction was developed by the American inventor William E. Urschel, who in 1939 created a device known as the Wall Building Machine.

Urschel's machine may be regarded as an analogue precursor to contemporary construction 3D printers. The system deposited concrete horizontally in successive layers, forming walls without the need for conventional formwork. The process resembled slip forming; however, it introduced automation and continuous material placement, which are now recognised as defining characteristics of modern additive manufacturing.

A distinctive feature of the Wall Building Machine was its radial operation around a central axis, conceptually similar to contemporary robotic construction systems and gantry-based printers. The machine required only minimal formwork and enabled rapid wall construction while significantly reducing labour demand. Urschel also explored geometric freedom, integration of reinforcement, and the use of locally available concrete mixtures—concepts that closely align with current research directions in large-scale additive manufacturing.

Furthermore, Urschel's system incorporated mechanical smoothing mechanisms designed to improve surface quality and reduce post-processing requirements. He also proposed integrated reinforcement placement during the construction process, anticipating modern approaches to automated reinforcement deposition in additively manufactured concrete structures.

Despite its innovative character, Urschel's technology did not become an industrial standard, primarily due to technological limitations of the time, including the absence of digital control systems and advanced material formulations. Nevertheless, many principles developed during the 1930s and 1940s re-emerged decades later in modern Large-Scale Additive Manufacturing (LSAM) systems.

More than eighty years after Urschel's prototypes, the same key advantages—geometric freedom, rapid fabrication, and reduced labour intensity—remain the primary drivers behind the development of construction 3D printing technologies. This historical perspective demonstrates that contemporary additive construction should not be viewed as an entirely new invention, but rather as a technological continuation of earlier engineering concepts that have become feasible today through digital tools, automation, and advanced materials [3].

5.3. PRINCIPLES OF ADDITIVE MANUFACTURING

5.3.1. DIGITAL WORKFLOW

Additive manufacturing connects digital design directly with physical fabrication. The standard workflow includes:

1. Creation of a 3D model using CAD software,
2. Conversion to STL or equivalent format,
3. Slicing into layers,
4. Automated deposition of material.

Integration with Building Information Modeling (BIM) systems enables continuous data flow from architectural concept to construction execution [2].

5.3.2. DIFFERENCE BETWEEN ADDITIVE AND TRADITIONAL MANUFACTURING

Traditional construction relies on casting, formwork, and manual assembly. Additive manufacturing eliminates many intermediate stages and allows automated fabrication.

Key differences include:

- material addition instead of removal,
- reduced waste generation,
- higher geometric complexity,
- digital process control.

Research indicates that additive construction may reduce material waste by up to 30–60% and construction time by up to 70% depending on application conditions [1].

5.4. ADDITIVE MANUFACTURING TECHNOLOGIES USED IN CONSTRUCTION

Additive manufacturing technologies can be classified according to the standardised terminology introduced in ISO/ASTM 52900:2021, which defines the fundamental process categories used across industrial and research applications. The standard distinguishes seven primary additive manufacturing process categories based on the method of material deposition and consolidation [4].

5.4.1. STANDARDISED PROCESS CATEGORIES

1. Binder Jetting (BJT) is an additive manufacturing process in which a liquid bonding agent is selectively deposited to join powder particles. The bonding agent locally solidifies regions of a powder bed, forming the geometry layer by layer.
2. Directed Energy Deposition (DED) is a process in which focused thermal energy is used to fuse materials as they are being deposited. The energy source may include a laser, electron beam, or plasma arc, which melts feedstock material during placement.
3. Material Extrusion (MEX) is an additive manufacturing process in which material is selectively dispensed through a nozzle or orifice. The deposited material solidifies after extrusion, forming successive layers.
4. Material Jetting (MJT) involves selective deposition of droplets of feedstock material, typically photopolymers or waxes. The material is deposited similarly to inkjet printing and subsequently solidified.
5. Powder Bed Fusion (PBF) is a process in which thermal energy selectively fuses regions of a powder bed. Energy sources such as lasers or electron beams locally melt or sinter powder particles.
6. Sheet Lamination (SHL) is an additive manufacturing process in which sheets of material are bonded layer by layer to form a part. Bonding may occur through adhesives, ultrasonic welding, or thermal processes.
7. Vat Photopolymerisation (VPP) is a process in which liquid photopolymer resin contained in a vat is selectively cured using light-induced polymerisation. Technologies such as stereolithography (SLA) and digital light processing (DLP) belong to this category.

5.4.2. RELEVANCE OF PROCESS CATEGORIES TO CONSTRUCTION 3D PRINTING

Although ISO/ASTM 52900 defines seven additive manufacturing categories, only a subset plays a major role in construction engineering. Among them, Material Extrusion (MEX) is the most significant for large-scale additive construction, as it enables continuous deposition of cementitious materials with relatively low energy demand and scalable equipment design.

Other categories support construction indirectly by enabling fabrication of tools, moulds, reinforcement components, or architectural prototypes. Consequently, modern construction additive manufacturing should be understood as a hybrid technological ecosystem combining multiple AM processes rather than relying on a single method.

These technologies are not always directly applicable. Some studies indicate that additive manufacturing processes other than material extrusion can also play

a role in construction applications. In particular, binder jetting has been identified as one of the most promising alternative technologies for the construction industry. This process allows the use of various mineral materials, including gypsum, cementitious mixtures, geopolymers, clay, and sand, followed by curing and post-processing to achieve the required mechanical properties. Unlike extrusion-based systems, the surrounding powder acts as a natural carrier medium, enabling the production of complex architectural elements without additional formwork. Current research highlights the scalability potential of binder jetting technology as well as its suitability for sustainable construction, particularly in the production of custom-made building components and large prefabricated elements [5].

Fig. 5.1. An example of using the Material Extrusion technique to print an element from a concrete mixture

5.4.3. CONCRETE 3D PRINTING SYSTEMS AND PRINTING APPROACHES

Additive manufacturing in construction is implemented using several technological approaches that differ in material delivery method, printer architecture, and application scale. Although multiple additive manufacturing categories are defined in ISO/ASTM standards, only selected processes are currently suitable for cementitious materials and large-scale construction applications.

1. Extrusion-Based Concrete Printing

Extrusion-based printing is the most widely used method in construction-scale additive manufacturing. In this approach, a cementitious or geopolymer mixture is

pumped through a nozzle and deposited layer by layer to form structural elements. The material must exhibit controlled rheological properties, allowing flow during pumping while maintaining shape stability after deposition.

Two major extrusion-based approaches are commonly distinguished:

- Contour Crafting (CC) – an early large-scale construction printing technology based on automated layer deposition using gantry systems, enabling rapid wall construction with limited formwork.
- Concrete Printing (CP) – developed mainly for prefabricated components, providing improved geometric control and flexibility in producing complex shapes.

Due to scalability and relatively low energy demand, extrusion printing currently represents the dominant technology for concrete 3D printing.

2. Powder-Based Printing

Powder-based additive manufacturing creates elements by selectively depositing a liquid binder onto layers of powder material. The surrounding powder acts as a natural support, enabling fabrication of complex geometries without additional formwork.

However, due to material handling and post-processing requirements, powder-based systems are typically applied to architectural elements and research-scale structures rather than full building construction.

Fig. 5.2. Example of an architectural print made using the Binder Jetting method (TUF-Germany)

3. Robotic and Gantry Printing Systems

Construction printers are commonly implemented as either gantry-based systems or robotic arm platforms. Gantry printers provide large working volumes and are therefore frequently used for on-site building fabrication. Robotic arm systems offer greater geometric flexibility and are particularly suitable for complex architectural forms and experimental applications.

Historical automated construction devices, such as early radial wall-building systems, demonstrated principles similar to modern printing technologies, including continuous material deposition and reduced dependence on formwork [1].

In practice, extrusion-based systems dominate structural applications, while powder-based and robotic approaches complement construction workflows by enabling complex geometries and specialised components. Modern additive construction increasingly combines automated printing with conventional construction techniques, forming hybrid manufacturing processes.

5.5. MATERIALS FOR 3D PRINTING IN CONSTRUCTION

Printable construction materials must satisfy specific rheological and mechanical requirements:

- pumpability,
- extrudability,
- buildability,
- shape stability after deposition.

Compared to conventional concrete, printable mixtures often contain higher binder content to ensure adequate cohesion and early strength development.

Printed layers must undergo a controlled transition from a semi-fluid (fresh) state to a load-bearing solid state. This transition should occur rapidly enough to ensure structural buildability, yet not so quickly that interlayer bonding is compromised. Proper adhesion between successive layers requires sufficient open time, allowing partial diffusion and mechanical interlocking at the interface.

Fig. 5.3. An example of a poorly selected 3D printing material – too high viscosity

An additional challenge is related to gravitational loading and the cumulative mass of the deposited material. Previously printed layers must exhibit adequate early-age mechanical strength, often referred to as green strength, to sustain the weight of subsequently deposited layers without excessive deformation or collapse. In practical applications, the printing process is frequently paused and resumed only after the lower layers have achieved sufficient stiffness and yield stress to maintain geometric stability under increasing structural load.

However, increased cement usage raises sustainability concerns, since Portland cement production accounts for approximately 8% of global CO_2 emissions [1].

5.6. GEOPOLYMERS AS SUSTAINABLE PRINTING MATERIALS

Geopolymers are inorganic aluminosilicate binders formed through alkaline activation of silicon- and aluminium-rich materials. Developed in the 1970s, they are considered environmentally friendly alternatives to Portland cement.

Advantages of geopolymers include:

- reduced carbon footprint,
- high early strength,
- fire resistance,
- chemical durability,
- excellent adhesion properties.

Studies demonstrate that geopolymer materials can be successfully adapted for additive manufacturing technologies while maintaining sufficient mechanical performance and interlayer bonding.

Copper-slag-based geopolymer materials, for example, achieved compressive strengths above 40 MPa after curing, confirming their structural potential [1].

5.7. ADVANTAGES OF ADDITIVE MANUFACTURING IN CONSTRUCTION

Additive manufacturing introduces several advantages compared to traditional construction methods:

- reduction of labour requirements,
- improved workplace safety,
- decreased material waste,
- design flexibility,
- automation of production processes.

Automation reduces the number of accidents on construction sites and improves efficiency through precise digital control.

Additionally, additive manufacturing enables fabrication in harsh environments, including underwater and extraterrestrial conditions [6].

5.8. ADVANCED APPLICATIONS OF ADDITIVE MANUFACTURING

- Underwater Construction
  Additive manufacturing enables automated fabrication in underwater environments, improving safety and reducing environmental impact. Although still experimental, underwater printing shows strong potential for marine infrastructure and repair operations [1].

- Space Construction
  3D printing is a key technology for lunar and Martian habitats. Using local materials significantly reduces transportation costs and energy consumption.
  Geopolymer composites are particularly promising due to their mechanical performance and resistance to extreme environmental conditions [7].

5.9. CHALLENGES AND LIMITATIONS

Despite rapid development, additive construction faces several challenges:

- absence of standardised regulations,
- certification difficulties,
- high equipment costs,
- variability of printable materials,
- anisotropic mechanical properties caused by layered deposition.

Printed elements may show lower mechanical properties compared to traditionally cast materials if process parameters are not optimized [1].

5.10. FUTURE TRENDS

Future research directions include:

- development of sustainable binders,
- optimisation of geopolymer mixtures,

- robotic automation,
- integration with artificial intelligence,
- multifunctional and smart materials.

Additive manufacturing is currently transitioning from experimental research toward industrial implementation and large-scale application [2].

5.11. CONCLUSIONS

Additive manufacturing represents a paradigm shift in construction engineering by integrating digital design, automated fabrication, and advanced materials. The technology enables sustainable construction through reduced waste, optimised material use, and improved efficiency.

Geopolymer-based materials further enhance sustainability by lowering environmental impact while maintaining mechanical performance. Rather than replacing conventional construction entirely, additive manufacturing is expected to complement traditional techniques, creating hybrid construction systems combining automation and material innovation.

REFERENCES

[1] Kozub B, Sitarz M, Gądek S, Ziejewska C, Mróz K, Hager I, Upscaling of Copper Slag-Based Geopolymer to 3D Printing Technology Materials 2024, 17, 5581.
[2] Hager I, Rewolucja technologiczna w budownictwie – druk 3d budynków i obiektów inżynieryjnych, Politechnika Krakowska, May 2018.
[3] Curth A, Slip Forming to Construction 3D Printing: The early history of Large-Scale Additive Manufacturing, , ICI Jurlan, July-September 2022.
[4] ISO/ASTM 52900:2021(en) – ASTM, Standard terminology for additive manufacturing—general principles. part 1: Terminology.
[5] Shako P, Chu S H, Puzatova A, Dini E, Review of binder jetting 3D printing in the construction industry, Progress in Additive Manufacturing 7 (4), January 2022.
[6] Korniejenko K, Gądek S, Dynowski P, Tran D, Rudziewicz M, Pose S, Grab T, Additive Manufacturing in Underwater Applications, Appl. Sci. 2024, 14, 1346.
[7] Korniejenko K, Pławecka K, Kozub B, An Overview for Modern Energy-Efficient Solutions for Lunar and Martian Habitats Made Based on Geopolymers Composites and 3D Printing Technology, Energies 2022, 15, 9322.

6

FIRE BEHAVIOUR TESTING OF BUILDING MATERIALS

Katarzyna Mróz

6.1. FUNDAMENTALS OF FIRE BEHAVIOUR

Understanding fire behaviour is a prerequisite for interpreting any fire test result related to building materials. Fire behaviour testing does not attempt to reproduce real fires in their full complexity; instead, it isolates selected physical and chemical phenomena that govern fire initiation and early fire development. This lecture establishes the technical baseline required to understand what is measured during reaction-to-fire testing and why such measurements are relevant for building safety.

Fire is not a singular phenomenon, but a coupled process involving heat transfer, chemical reactions, material decomposition, and fluid flow. Consequently, the fire behaviour of a material depends not only on its chemical composition but also on its physical form, geometry, and interaction with surrounding conditions.

6.1.1. COMBUSTION OF SOLID MATERIALS

Combustion of solid materials is a complex process that involves several sequential physical and chemical phenomena occurring before visible burning takes place. Understanding the stages of pyrolysis, ignition, and flame spread is essential for explaining how materials contribute to fire development and how their behaviour is evaluated in fire testing.

Pyrolysis – solid materials do not burn directly. Before combustion can occur, the material undergoes pyrolysis, which is the thermal decomposition of a solid under the influence of heat. During pyrolysis, complex molecules break down into smaller compounds, which can ignite in the presence of oxygen. Pyrolysis may occur in oxygen-rich or oxygen-poor environments and often begins far before visible flames appear. The rate of pyrolysis is influenced by external heat flux, material composition, density, thickness, and thermal conductivity of the material. In many fire tests, the observed burning behaviour is primarily a function of how quickly pyrolysis products are generated rather than the intrinsic flammability of the solid material itself.

Ignition – occurs when the concentration of pyrolysis gases and the local temperature reach conditions sufficient for sustained combustion. Two principal ignition mechanisms are distinguished: piloted ignition, which requires an external ignition source such as a spark or flame, and auto-ignition, which occurs solely due to elevated temperature. In building fires, piloted ignition is common, whereas

laboratory tests may involve both mechanisms, depending on the test method. Ignition temperature is not a single material constant but depends on environmental conditions, heat transfer, and surface characteristics. Therefore, ignition behaviour measured in standardised tests should be interpreted as comparative rather than absolute.

Flame spread – once ignition has occurred, flame spread describes the propagation of combustion across a material surface. Flame spread is governed by heat feedback from the flame to the unburnt material, which accelerates further pyrolysis. Radiation is typically the dominant heat transfer mechanism driving this process. In reaction-to-fire testing, flame spread is a critical indicator of early fire growth. Rapid flame spread can lead to flashover conditions even when individual materials release relatively modest amounts of energy.

6.1.2. HEAT TRANSFER MECHANISMS IN FIRES

Fire behaviour is controlled by three fundamental heat transfer mechanisms: conduction, convection, and radiation. Each plays a distinct role in fire development and material response.

Conduction is the transfer of heat through a material due to temperature differences. In fire scenarios, conduction determines the rise in temperature within building components and influences the depth of carbonisation of wood and the softening of polymers. Materials with low thermal conductivity can delay the penetration of heat, whereas highly conductive materials can rapidly transfer it to adjacent elements.

Convection is the process by which heat is transferred through the movement of hot gases. In enclosed spaces, such as those affected by fires, convective heat transfer dominates, with buoyant hot gases accumulating near ceilings and spreading laterally. Convective heat exposure is particularly important for vertical flame spread and for heating materials that are not directly exposed to flames.

Radiation is the most critical mechanism of heat transfer in fire growth. Flames and hot smoke layers emit thermal radiation that can initiate the combustion of materials at a distance, without direct contact. Radiation largely governs flame spread rates and the ignition of secondary objects. Most standardised reaction-to-fire tests implicitly measure how materials respond to radiative heat exposure, even when the test description does not explicitly refer to radiation.

6.1.3. REACTION TO FIRE VERSUS FIRE RESISTANCE

In fire safety engineering, a fundamental distinction is made between reaction to fire and fire resistance.

Reaction to fire describes how a material or product contributes to the development of a fire, particularly in its early stages. This encompasses ignitability, flame spread, heat release, smoke production, and the formation of burning droplets or particles. Reaction-to-fire tests generally focus on fire growth rather than structural performance and are conducted on materials or products.

Fire resistance describes the ability of a building element to maintain its load-bearing capacity, integrity and thermal insulation for a defined period under standardised fire exposure. Fire resistance testing is applied to systems or assemblies rather than individual materials.

Misinterpreting these two concepts can have serious consequences. For example, a material with excellent reaction-to-fire performance may still fail rapidly under load in a fire, while a structurally fire-resistant system may contain combustible components that behave poorly in a fire.

6.1.4. CONCLUDING REMARKS

The aim of fire behaviour testing is to quantify how materials behave under fire exposure, particularly during the early stages of a fire. These tests provide comparative data to support classification, regulation, and engineering judgement. However, it should be noted that they do not replicate real fires and should not be interpreted as direct predictors of fire safety performance in all scenarios.

To interpret fire test results correctly and appreciate both their value and their limitations, it is essential to have a clear understanding of combustion processes, heat transfer mechanisms, and material-specific responses.

6.2. REGULATORY FRAMEWORK AND CLASSIFICATION SYSTEMS (REACTION-TO-FIRE)

Fire behaviour testing has little practical value unless it is embedded within a regulatory framework that defines how the results are used, how products are classified, and how compliance is demonstrated. In the building materials and construction products market, fire tests are carried out to facilitate market access, obtain regulatory approval, and inform design decisions.

Within the European Union, the placing of construction products on the market is governed by the Construction Products Regulation (CPR) [1]. The CPR establishes harmonised conditions for marketing construction products by defining how their performance in relation to essential characteristics must be declared.

Fire behaviour is one of these essential characteristics. The CPR does not specify the level of fire performance that products must achieve. Instead, it establishes

a common technical language that enables Member States to define their own minimum requirements while ensuring the comparability of product performance across the internal market.

A key principle of the CPR is that products must be tested and classified using harmonised methods, ensuring that products tested in one country can be assessed and accepted in another.

CE marking indicates that a construction product complies with the applicable harmonised technical specifications under the Construction Products Regulation (CPR). It is not a quality mark, nor does it imply that a product is suitable for a specific application. Instead, it shows that the manufacturer has followed the required procedures for assessing and verifying performance.

For fire behaviour, CE marking confirms that the product has been tested according to the relevant harmonised fire test standards, the results have been classified using the European fire classification system, and that the declared performance is also traceable and legally accountable.

CE marking enables transparency and comparability but does not replace engineering judgement or regulatory approval at a national level.

The Declaration of Performance (DoP) is the key legal document linking fire tests to regulatory compliance. In the DoP, the manufacturer declares the performance of a product with respect to its essential characteristics, including reaction to fire.

For reaction to fire, the DoP typically includes:

– The fire class (e.g. A2-s1,d0);
– Reference to the applicable harmonised standard;
– The intended use of the product.

The DoP is legally binding. Incorrect or misleading declarations can result in regulatory, civil and criminal consequences. For engineers and designers, the DoP is the main source of information for verifying whether a product meets fire safety requirements.

6.2.1. EUROPEAN FIRE CLASSIFICATION OF CONSTRUCTION PRODUCTS

The European fire classification system, commonly referred to as the Euroclass system [2], translates complex fire test results into a standardised classification label. This label enables non-specialists to compare products and allows authorities to define minimum performance requirements in building regulations.

The Euroclass system focuses on reaction to fire, i.e. how a material or product contributes to fire development during the early stages of a fire.

Reaction to fire is classified into seven main classes:
A1 – non-combustible materials with no contribution to fire;
A2 – very limited contribution to fire;
B, C, D – increasing contribution to fire;
E – limited fire performance, typically based on ignitability;
F – no determined performance.

The classes are hierarchical: a higher class implies better fire performance under the conditions defined by the test methods.

It is essential to recognise that these classes do not describe fire resistance or behaviour in fully developed fires. They are indicators of early fire growth potential.

In addition to the main reaction-to-fire class, Euroclasses include a smoke production classification:
s1 – low smoke production;
s2 – limited smoke production;
s3 – no limitation on smoke production.

Smoke classification addresses visibility and evacuation conditions rather than combustibility alone. Two materials with identical reaction-to-fire classes may differ significantly in smoke production, leading to very different safety outcomes in real fire scenarios.

The third component of the Euroclass label concerns the formation of flaming droplets or particles:
d0 – no flaming droplets or particles;
d1 – limited occurrence;
d2 – no performance determined or significant occurrence.

Flaming droplets can ignite secondary materials and accelerate fire spread. This parameter is particularly relevant for thermoplastic materials and layered products.

6.2.1.1. HOW TO READ THE EUROCLASS LABEL?

A complete Euroclass classification combines all three components. Understanding this notation is essential for interpreting product documentation and verifying regulatory compliance with design requirements.

For example, the designation:

A2-s1,d0

indicates a material with very limited contribution to fire (A2), low smoke production (s1), and no flaming droplets or particles (d0).

6.2.2. COMPARISON WITH INTERNATIONAL APPROACHES

The European approach emphasises a harmonised classification system that integrates multiple fire behaviour parameters into a single label. This facilitates regulatory use and market transparency.

The Euroclass system is particularly suited to prescriptive regulatory frameworks, where minimum classes are specified in building codes. ASTM- and ISO-based approaches are more commonly used in performance-based design, where test data are interpreted within a broader fire engineering analysis.

It is important to recognise that these systems are not directly interchangeable. A product classified under the Euroclass system cannot be assumed to have an equivalent classification under ASTM-based schemes without additional testing and analysis.

6.2.3. CONCLUDING REMARKS

Fire classification systems serve as the interface between laboratory testing and real-world regulation. In Europe, the CPR, CE marking, and the Euroclass system together create a harmonised framework that allows fire behaviour to be assessed, declared, and regulated consistently across the internal market.

However, classifications are simplifications of complex phenomena. They enable comparison and compliance but do not replace engineering judgement or a holistic understanding of fire behaviour.

6.3. REACTION-TO-FIRE TESTS – METHODS AND EQUIPMENT

Fire behaviour testing aims to quantify how construction materials and products respond to fire exposure under controlled and repeatable conditions. Standardised fire tests are essential because they provide a consistent basis for classification, regulatory compliance, and comparison between products.

Reaction-to-fire testing focuses primarily on the early stages of fire development, where the contribution of materials to ignition, flame spread, heat release, and smoke production is most critical. To capture these phenomena, testing methods are performed at different scales. Small-scale tests investigate fundamental combustion

characteristics, medium-scale tests evaluate fire growth behaviour of products, and large-scale tests attempt to simulate realistic fire scenarios.

This lecture introduces the most important standardised tests used in European classification systems and discusses how these tests are performed, what parameters they measure, and how the results should be interpreted.

6.3.1. SMALL-SCALE REACTION-TO-FIRE TESTS

Small-scale tests are designed to measure intrinsic properties of materials related to combustibility and potential energy release. They provide basic information that contributes to the determination of high reaction-to-fire classes.

Non-Combustibility Test (ISO 1182:2020, [3]) classes A1-A2

The non-combustibility test evaluates whether a material contributes to combustion when exposed to high temperature in a controlled furnace environment.

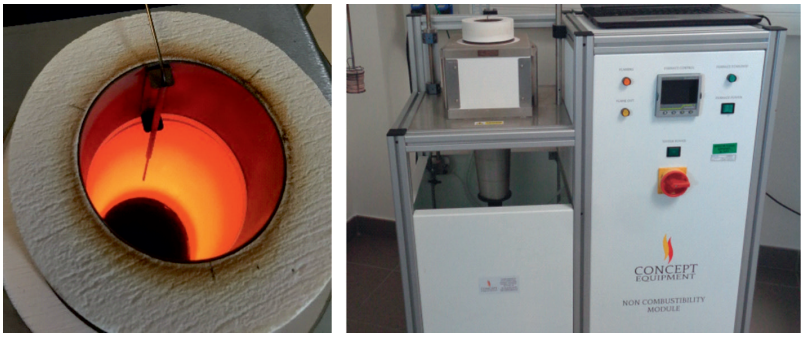

Fig. 6.1. Experimental setup for the non-combustibility test [4]

In this test, a small cylindrical specimen is inserted into a vertical tube furnace maintained at approximately 750°C. The specimen is exposed to the hot environment without an external flame, and several parameters are monitored during the test.

The main quantities measured include:

- Temperature increase within the furnace
- Duration and occurrence of flaming
- Mass loss of the specimen

A material is considered non-combustible if it does not produce sustained flaming and does not cause a significant temperature increase within the furnace. Materials such as mineral wool, concrete, ceramics, and many mineral-based products typically meet the criteria for non-combustibility.

Typical failure modes include sustained flaming or excessive temperature rise caused by oxidation or decomposition reactions within the specimen.

Heat of Combustion (ISO 1716:2018 [5]), classes A1-A2

The heat of combustion represents the total amount of energy that a material can release when completely burned. This property is measured using a bomb calorimeter, a sealed pressure vessel in which a small sample is combusted in a pure oxygen atmosphere.

Fig. 6.2. Experimental setup for the non-combustibility test [6]

The test measures the temperature rise of the surrounding water bath, which is used to calculate the calorific value of the material.

The key parameter obtained from this test is the heat of combustion (PCS) expressed in megajoules per kilogram (MJ/kg).

This parameter represents the theoretical maximum energy that could be released by the material. Materials with low calorific values, such as mineral products, are less likely to contribute significantly to fire growth.

6.3.2. MEDIUM-SCALE REACTION-TO-FIRE TESTS

While small-scale tests focus on fundamental properties, medium-scale tests evaluate the behaviour of products under conditions that more closely resemble real fire scenarios. These tests provide the primary data used for reaction-to-fire classification in the European system.

Single Burning Item (SBI) Test (EN 13823:2022, [7]), classes A2-D

The Single Burning Item test is the central test method used for classification of construction products in Euroclasses A2 to D.

In this test, two rectangular specimens are mounted in a corner configuration that simulates the intersection of two walls. A gas burner located at the base of the corner produces a defined heat release rate that represents a burning wastebasket or similar localized ignition source.

The fire exposure lasts for twenty minutes, during which multiple parameters are continuously recorded.

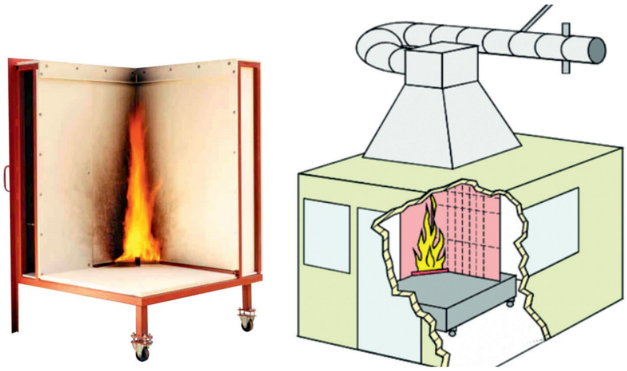

Fig. 6.3. Experimental setup for the non-combustibility test [8, 9]

The most important parameters derived from the SBI test include:

- FIGRA (Fire Growth Rate Index) – an indicator of how rapidly heat release increases during the test
- THR (Total Heat Release) – the cumulative amount of energy released by the specimen
- SMOGRA (Smoke Growth Rate) – the rate at which smoke production increases
- LFS (Lateral Flame Spread) – the extent to which flames spread across the specimen surface

FIGRA is one of the most important classification parameters because it characterizes the potential for rapid fire growth.

Smoke production is determined through optical measurements of the exhaust gases in the test hood, allowing calculation of the smoke production rate.

Failure modes observed during the SBI test may include rapid flame spread across the specimen, detachment of burning fragments, or intense smoke production. Materials containing thermoplastic components may also exhibit dripping behaviour.

Ignitability Test (EN ISO 11925-2 [10]), classes B-E

The ignitability test evaluates how easily a material ignites when exposed to a small flame. This test is typically used to determine the lowest reaction-to-fire classes.

The specimen is mounted vertically and exposed to a small standardised flame for a defined duration. The flame is applied either to the surface of the specimen or to its edge.

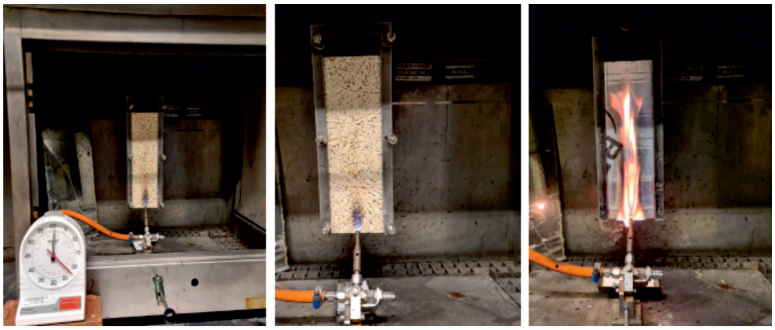

Fig. 6.4. Ignitability test at the Efectis laboratory [9]

During the test, the following observations are made:

– Whether ignition occurs,
– The height of flame spread on the specimen surface,
– Whether flaming droplets ignite the filter paper placed below the specimen.

The test is relatively simple but provides critical information about a product's susceptibility to ignition under small flame exposure.

Typical failure occurs when flames propagate beyond a specified height or when burning droplets ignite the filter paper.

6.3.3. CONCLUDING REMARKS

Standard fire behaviour tests provide a structured and reproducible way to evaluate how construction materials respond to fire exposure. Small-scale tests measure fundamental combustion properties, while medium-scale tests assess the fire growth behaviour of products.

Together, these methods form the experimental foundation of fire classification systems and regulatory frameworks.

6.4. FIRE RESISTANCE TESTS – PRINCIPLES AND METHODS

While reaction-to-fire tests evaluate how materials contribute to the development of a fire, fire resistance tests assess the ability of building elements to maintain their function during fire exposure. In real buildings, the failure of structural or separating elements can lead to rapid fire spread, collapse, or loss of safe evacuation routes. For this reason, fire resistance is a fundamental requirement in building regulations worldwide.

Fire resistance testing evaluates the performance of complete building elements, rather than individual materials. These elements may include load-bearing walls, floors, columns, beams, doors, or service penetrations. The objective is to determine how long such elements can withstand exposure to fire while continuing to perform their intended functions.

During standardised fire resistance testing, specimens are exposed to controlled thermal conditions in large furnaces that simulate the temperature of a developing fire. Their performance is then evaluated against defined criteria relating to structural stability, integrity and insulation.

6.4.1. STANDARD FIRE EXPOSURE

Fire resistance tests are generally conducted using a standard temperature–time curve, which represents a simplified model of fire development in a compartment.

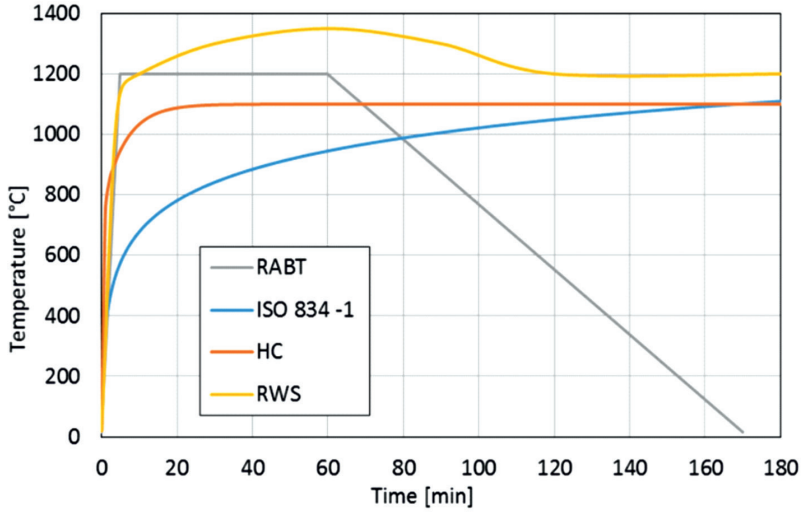

Fig. 6.5. Different fire scenarios used in standard fire resistance tests

The most widely used curve is defined in the International Organization for Standardization (ISO) standard ISO 834 [11] and in equivalent European standards. The curve describes how furnace temperature increases over time during the test.

The following fire scenarios are commonly used (Fig. 6.5):

- ISO 834-1 – the specimens of construction purposes – it reflects the burning rate of the general building materials and contents.
- Hydrocarbon (HC) – in buildings of risk of burning car fuel tankers, petrol or another chemical tanker.
- RWS – for laboratory testing of tunnel concrete, as a result of studies carried out in Netherlands and Norway.
- RABT – developed based on a series of research program performed in Germany.

The purpose of this standardised exposure is not to reproduce a specific real fire but to create consistent and reproducible conditions under which different construction elements can be compared. Because the heating curve is predefined, the measured fire resistance time reflects the ability of the element to withstand severe thermal exposure under controlled conditions.

6.4.2. FIRE RESISTANCE PERFORMANCE CRITERIA

Fire resistance performance is assessed using several criteria that describe different aspects of structural and thermal behaviour. These criteria are commonly expressed using the letters **R**, **E**, and **I**.

Load-bearing capacity (R) – The criterion R represents the ability of a structural element to maintain its load-bearing capacity during fire exposure. Failure occurs when the element collapses or deforms to such an extent that it can no longer safely support the applied load.

Load-bearing capacity is relevant for structural components such as columns, beams, floors, and load-bearing walls. During the fire test, the mechanical load is typically applied to the testing element to simulate real structural conditions while it is exposed to furnace heating.

Integrity (E) – The criterion E, or integrity, refers to the ability of an element to prevent the passage of flames and hot gases from the fire-exposed side to the unexposed side.

Integrity failure may occur through cracks, openings, or joint failures that allow flames to penetrate the separating element. In fire resistance tests, integrity is evaluated using visual observation and specific indicators, such as cotton pad tests that detect the passage of hot gases capable of igniting combustible materials.

Insulation (I) – The criterion I, or thermal insulation, refers to the ability of an element to limit the temperature rise on the unexposed side of the construction.

Insulation failure occurs when temperatures on the unexposed surface exceed specified limits. Typically, the average temperature rise must not exceed approximately 140°C above the initial temperature, and local temperatures must not exceed a higher specified limit.

Fire resistance performance is expressed as a time classification combined with the relevant performance criteria, for example: **REI 30, R 60, REI 120.**

These classifications indicate that the tested element maintained its required performance criteria for 30, 60, or 120 minutes under standardised fire exposure.

The combination of letters depends on the type of element and its function. A structural column may be classified only in terms of load-bearing capacity (R), while a compartment wall may require all three criteria (REI).

Fire resistance classifications are widely used in building regulations to define the minimum fire performance required for different building elements.

6.4.3. FIRE RESISTANCE TEST SETUP

Fire resistance tests are conducted in large-scale furnaces capable of reaching temperatures exceeding 1000°C while maintaining controlled heating conditions.

The test specimen is installed in a frame that replicates its intended position within a building, such as a wall or floor assembly. The furnace exposes one side of the specimen to the standard fire curve, while the opposite side remains accessible for temperature measurements and visual inspection.

Thermocouples are installed on the unexposed surface to monitor temperature rise. Additional instrumentation may measure deflection, displacement, or structural deformation during the test.

When load-bearing elements are tested, hydraulic systems apply mechanical loads to simulate structural conditions. These loads are maintained throughout the test until failure occurs or the required fire resistance period is reached (Fig. 6.6).

6.4.4. TYPICAL BEHAVIOUR OF BUILDING MATERIALS IN FIRE RESISTANCE TESTS

During fire exposure, building materials undergo a range of physical and chemical transformations that influence the performance of the entire assembly.

Steel elements may lose strength rapidly as temperature increases, leading to significant deformation or collapse unless protected by fire-resistant coatings or insulation systems.

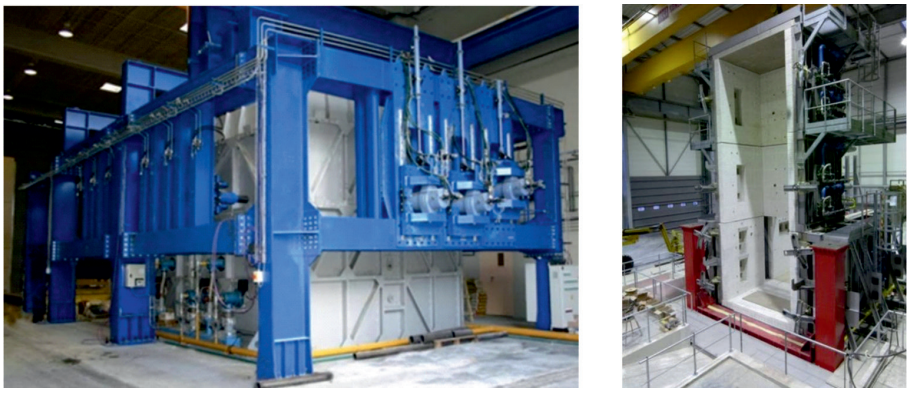

Fig. 6.6. Full-scale furnaces. Left: Promethee (CERIB, France); right: VULCAIN (CSTB, France)

Concrete elements generally exhibit good fire resistance due to their low thermal conductivity and high thermal mass. However, at high temperatures, they may experience spalling, where fragments of concrete detach violently from the surface, exposing reinforcement bars to direct heat.

Timber structures behave differently from steel or concrete. When exposed to fire, timber forms a char layer on its surface. This char layer acts as an insulating barrier that slows further degradation of the underlying material. As a result, large timber elements may maintain load-bearing capacity for extended periods despite gradual cross-sectional reduction.

Composite or layered systems may experience delamination, where layers separate under thermal stress. This can expose previously protected materials to direct flame exposure and accelerate failure.

Fire resistance testing plays a crucial role in ensuring that building elements can maintain structural stability and compartmentation during fire exposure. By evaluating load-bearing capacity, integrity, and insulation under standardised conditions, these tests provide a consistent basis for classification and regulatory control.

6.4.5. CONCLUDING REMARKS

Fire resistance tests are intended to assess the performance of construction elements in terms of their load-bearing and fire-separating properties, collectively referred to as fire resistance, for their regulated use in buildings. Fire resistance classifications should be viewed as part of a broader fire safety strategy that includes material behaviour, structural design, and fire protection measures.

In addition to standardised tests, the non-standardised laboratory tests of building materials aim to investigate their behaviour at high temperatures. These

tests are performed on specimens of different sizes and shapes. During testing, various measurements are taken to better describe the processes occurring in building materials during heating. These parameters include temperature, vapour pore pressure development, thermal strains, and specimen deflection. Generally, we can distinguish two main categories of non-standardised testing methods for high-temperature behaviour investigations: small-scale and medium-scale.

6.5. NON-STANDARDISED METHODS FOR THE ASSESSMENT OF FIRE BEHAVIOUR OF BUILDING MATERIALS

Standardised fire tests, such as reaction-to-fire classification tests or fire resistance tests, play a crucial role in regulatory frameworks and product certification. However, these tests often provide only limited insight into the underlying physical processes occurring within materials during fire exposure. For this reason, research laboratories frequently employ non-standardised experimental methods to study the behaviour of building materials subjected to elevated temperatures.

These experimental techniques aim to investigate fundamental material responses, including thermal strains, pore pressure development, moisture migration, cracking, and degradation of mechanical properties. Such knowledge is essential for understanding the mechanisms that govern material performance in fire and for developing improved materials with enhanced fire resistance.

Non-standardised testing methods can generally be divided into small-scale laboratory tests and medium-scale furnace tests. Small-scale tests focus primarily on intrinsic material properties and thermo-mechanical behaviour, while medium-scale tests attempt to reproduce more realistic fire exposure conditions on larger specimens.

6.5.1. SMALL-SCALE TESTS

Small-scale tests are designed to investigate the behaviour of materials exposed to elevated temperatures under controlled laboratory conditions. These experiments typically involve small specimens in the form of prisms, cubes, or cylinders, usually with volumes not exceeding approximately 3400 cm^3.

The specimens are heated using electrically controlled furnaces that provide stable and uniform temperature conditions. Heating rates are generally relatively low, typically between 1 and 5°C per minute, and the heating scenario is often linear. Such controlled heating allows researchers to study temperature-dependent changes in physical and mechanical properties.

Small-scale experiments enable detailed investigation of phenomena such as:
- thermal strains and deformations,
- development of pore vapour pressure,
- temperature gradients inside the material,
- degradation of mechanical properties,
- cracking processes induced by thermal stresses.

In many experimental setups, specimens are placed in a mechanical loading frame, allowing the application of compressive or tensile stresses during heating. This configuration enables the investigation of thermo-mechanical coupling effects that occur in structural materials exposed to fire.

Following the classification proposed by researchers such as Phan, three main approaches can be distinguished: stressed tests, unstressed tests, and unstressed residual tests.

In the stressed test method, the specimen is loaded before heating. Typically, a compressive load corresponding to approximately 10–50% of the ultimate compressive strength is applied at room temperature and maintained during heating. Once the target temperature is reached, the specimen is further loaded until failure while still at elevated temperature. This method simulates the behaviour of structural materials subjected simultaneously to mechanical loads and high temperatures during a fire.

The unstressed method differs in that the specimen is heated without external load until the desired temperature is reached. Mechanical loading is applied only after the target temperature is achieved. This approach allows researchers to evaluate material strength under high temperature without the influence of mechanical stresses during heating.

The unstressed residual method is used to evaluate post-fire performance. In this approach, the specimen is first heated to the target temperature without load and then allowed to cool down to room temperature. After cooling, mechanical loading is applied until failure. The results provide information about the residual strength and stiffness of materials after fire exposure, which is essential for assessing structural safety after a fire event.

Small-Scale Experimental Setups

Advanced measurement systems have been developed to monitor deformation, temperature distribution, and internal pressure within heated specimens.

One such system was developed at the Centre Scientifique et Technique du Bâtiment (CSTB) in France (Fig. 6.7). In this setup, cylindrical specimens with dimensions of approximately 104 mm in diameter and 300 mm in height are placed inside a cylindrical furnace capable of reaching temperatures up to about 600°C.

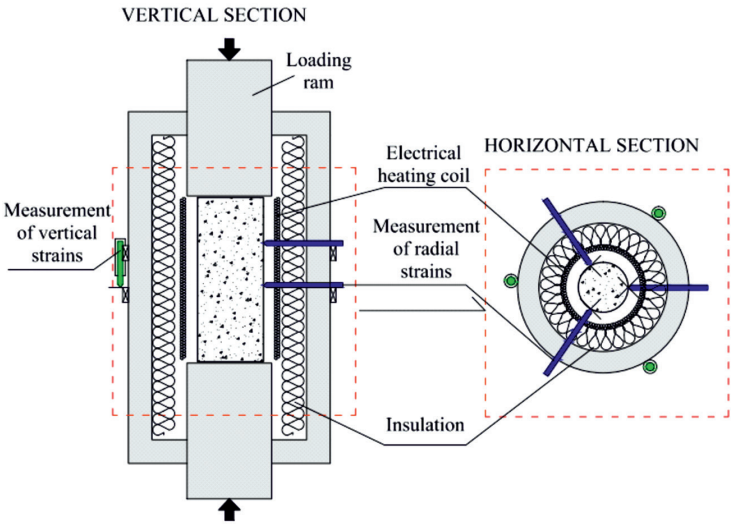

Fig. 6.7. Measurement system for radial and longitudinal deformation of small cylindrical specimen, after [12, 13]

The furnace is equipped with several independently controlled heating elements to minimise thermal gradients within the specimen. The entire system is integrated into a mechanical testing machine that can apply loads.

Thermal strains and deformations are measured using extensometers mounted outside the furnace. These extensometers are connected to the specimen via thin rods, enabling the measurement of vertical and radial deformation during heating.

Additional measurement devices have been developed to monitor radial expansion. These use metallic rods arranged around the specimen at equal angular intervals. The rods transmit radial displacement from the specimen surface to sensors located outside the furnace. High-precision displacement sensors enable radial strains to be measured with micrometre accuracy.

Temperature measurements are obtained using thermocouples placed directly on the specimen's surface. This system enables the simultaneous measurement of temperature, deformation, and applied load, providing detailed information about thermo-mechanical behaviour.

Restrained Ring Tests

Another experimental method used to investigate thermal strain behaviour involves the ring test configuration.

In this setup, circular specimens are cast within steel rings that restrain their thermal expansion during heating. The specimen may have a diameter of approximately 284 mm and a thickness of about 100 mm. Two steel rings surrounding the specimen provide confinement and allow indirect measurement of the material's thermal strain (Fig. 6.8).

During heating, the restrained specimen attempts to expand, inducing stress in the steel rings. Strain gauges attached to the external surface of the rings measure the resulting deformation. Because the mechanical properties of the steel rings are known, the measured strain can be used to calculate the thermal strain of the specimen.

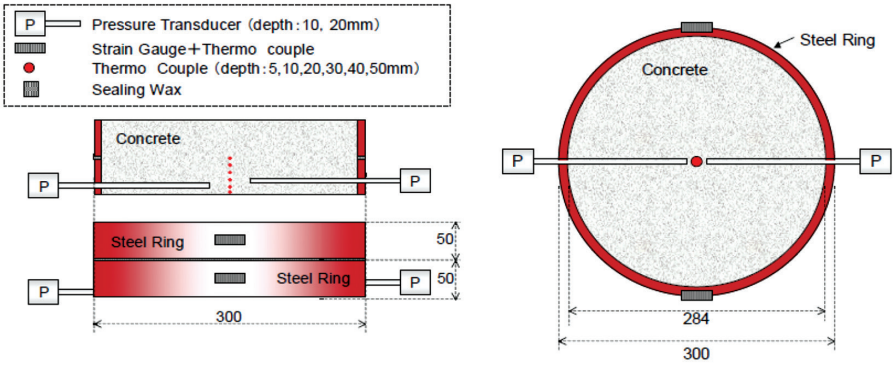

Fig. 6.8. Schematic representation of the ring test [14]

The test setup is often instrumented with thermocouples placed at various depths within the specimen to measure the internal temperature profile. In addition, pore pressure sensors may be embedded within the material to monitor vapour pressure development during heating.

This type of experiment is particularly useful for studying moisture-related phenomena, such as the build-up of pore pressure that can lead to explosive spalling in concrete exposed to fire.

PTM Method (Pressure-Temperature-Mass)

One of the most advanced experimental approaches used in fire research is the PTM method, which simultaneously measures pressure, temperature, and mass loss within a heated specimen (Fig. 6.9).

In this test, prism-shaped specimens are exposed to radiant heating from an electric heater. The heating is typically quasi-unidirectional, meaning that one surface is directly exposed to heat while the remaining surfaces are insulated.

The specimen may contain several embedded gauges consisting of sintered metal plates connected to thin tubes extending outside the specimen. These tubes are connected to pressure transducers that measure internal pore pressure during heating. Thermocouples inserted into the same measurement system allow simultaneous recording of internal temperature.

The PTM test enables researchers to monitor several key parameters simultaneously:

– internal temperature development,
– pore pressure evolution,

– mass loss due to moisture evaporation,
– moisture migration within the material.

This technique provides valuable insight into the mechanisms responsible for thermal damage and explosive spalling in cementitious materials exposed to fire.

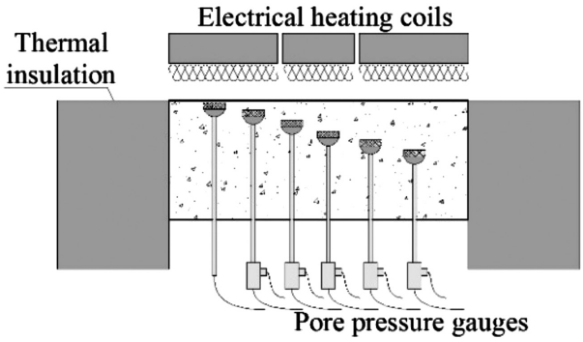

Fig. 6.9. Experimental setup of the PTM test [15].

6.5.2. MEDIUM-SCALE FURNACE TESTS

Medium-scale tests represent an intermediate step between small-scale laboratory experiments and full-scale fire resistance tests. These tests are often used as screening tools to evaluate the fire performance of different material mixtures or structural configurations before conducting expensive full-scale tests.

Medium-scale tests typically involve specimens such as slabs or panels exposed to fire in laboratory furnaces. These furnaces may be heated using propane burners or oil burners and can reproduce different fire scenarios.

In laboratory fire research, several standard fire curves are commonly used to simulate different fire conditions. The most frequently used curve is the ISO 834 standard fire curve, which represents typical fire development in buildings.

Other fire curves may also be used in research depending on the expected fire scenario. For example, hydrocarbon fire curves simulate rapid fire growth typical of fuel fires, while tunnel fire curves such as RWS or RABT represent severe fires in tunnel environments.

Unloaded Medium-Scale Tests

In unloaded tests, specimens are exposed to fire without additional mechanical loading. Typically, a slab specimen is placed horizontally above a furnace opening and supported along its edges.

During heating, thermocouples embedded within the specimen record temperature development at different depths. Additional thermocouples placed near the exposed surface measure furnace temperature.

These tests allow researchers to observe phenomena such as cracking, spalling, and temperature distribution within the material. Because no external load is applied, the test primarily examines thermal damage mechanisms.

Loaded Medium-Scale Tests

In many cases, it is necessary to study the behaviour of materials under combined thermal and mechanical loading. Medium-scale experimental setups therefore often include loading frames capable of applying compressive forces during fire exposure.

Load can be applied using several methods, including post-tensioning bars, hydraulic flat jacks, or external loading frames. These systems enable the application of uniaxial or biaxial compression while the specimen is heated.

For example, the Dragon furnace, developed at the Cracow University of Technology (Fig. 6.10), is a medium-scale furnace designed for such experiments. The furnace chamber contains a fireproof lining and can expose specimens through an opening of approximately 600 × 600 mm. The heating system uses a gas burner capable of delivering thermal power of about 140 kW.

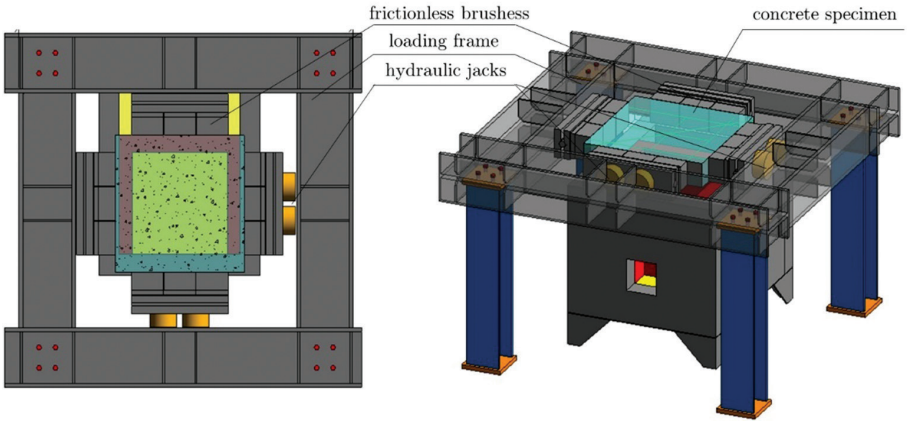

Fig. 6.10. Experimental setup for testing unloaded and loaded slabs under fire condition at medium-scale (Cracow University of Technology, Poland)

Specimens are mounted above the furnace opening and may be subjected to external loading using a specially designed loading frame. Flat hydraulic jacks distribute compressive forces through steel loading shoes equipped with brushes to reduce friction and ensure uniform stress distribution.

During the test, various parameters may be monitored, including temperature development within the specimen, deformation, and cracking behaviour.

These experiments allow researchers to evaluate the combined effects of thermal exposure and mechanical loading, providing valuable insight into structural performance during fire.

6.5.3. CONCLUDING REMARKS

Non-standardised fire testing methods play an essential role in fire research because they provide detailed information about the physical processes that occur within materials exposed to high temperatures. While standardised tests are necessary for classification and regulatory purposes, they often cannot capture complex phenomena such as pore pressure development, moisture migration, or thermo-mechanical damage.

Small-scale laboratory experiments allow precise investigation of intrinsic material properties and failure mechanisms. Medium-scale furnace tests provide a bridge between laboratory experiments and full-scale fire resistance tests by enabling more realistic fire exposure conditions.

Together, these experimental approaches contribute to a deeper understanding of material behaviour in fire and support the development of safer and more fire-resistant construction materials.

6.6. FINAL CONCLUSIONS

Testing of the building materials' fire behaviour is a fundamental component of modern fire safety engineering. Understanding the physical and chemical processes involved in combustion, such as pyrolysis, ignition, and flame spread, provides a scientific basis for interpreting fire test results and evaluating how materials contribute to the development of fires. These processes are governed by heat transfer mechanisms (conduction, convection, and radiation), which determine how fire interacts with materials and spreads within the built environment.

Standardised fire testing methods offer a structured, reproducible approach to evaluating the fire performance of construction materials and building components.

Reaction-to-fire tests focus on the initial stages of fire development, evaluating parameters such as ignitability, heat release, flame spread, smoke production, and flaming droplets. The results of these tests form the basis of classification systems such as the European Euroclass system. This system translates complex experimental results into clear performance categories, supporting regulatory compliance and product comparison within the framework of the Construction Products Regulation.

Fire resistance tests evaluate the ability of complete building elements to maintain their structural function during fire exposure. These tests determine how long structural and separating elements can perform their intended role during a fire by assessing load-bearing capacity, integrity, and thermal insulation under standardised temperature–time conditions. Such classifications are essential for ensuring structural stability, compartmentation, and safe evacuation in buildings.

Although standardised tests are important for regulation and product certification, they represent simplified scenarios and cannot fully capture the complexity of real fires. For this reason, non-standardised experimental methods are widely used in research to investigate detailed behaviour of materials at high temperatures. These methods allow the study of thermal strains, pore pressure development, moisture migration, cracking and thermo-mechanical degradation, and provide deeper insight into the mechanisms that govern material behaviour in fire conditions.

The combined use of standardised testing and advanced research methods provides a comprehensive framework for understanding and evaluating fire behaviour in construction materials. This knowledge supports the development of safer building materials, informs engineering design and contributes to improving fire safety regulations. Ultimately, effective fire testing and classification systems play a vital role in reducing fire risk and improving the resilience of building facilities and infrastructure.

REFERENCES

[1] PE/12/2024/REV/1, *Regulation (EU) 2024/3110 of the European Parliament and of the Council of 27 November 2024*, 2024.
[2] PN-EN 13501-2:2016-07, *Fire classification of construction products and building elements – Part 2: Classification using data from fire resistance tests, excluding ventilation services – Polish version*, 2017.
[3] ISO 1182:2020, *Reaction to fire tests for products — Non-combustibility test*, 2020.
[4] Concept Equipment. [Online]. Available: https://concept-e.co.uk/products/non-combustibility-system/, 09/03/2026.
[5] ISO 1716:2018, *Reaction to fire tests for products — Determination of the gross heat of combustion (calorific value)*, 2018.
[6] Parr. [Online]. Available: https://www.parrinst.com/products/oxygen-bomb-calorimeters/6100-compensated-jacket-calorimeter/, 09/03/2026.
[7] EN 13823:2020+A1:2022, *Reaction to fire tests for building products - Building products excluding floorings exposed to the thermal attack by a single burning item*, 2022.
[8] Fire Testing Technology. [Online]. Available: https://www.fire-testing.com/single-burning-item-sbi/, 09/03/2026.
[9] Efectis. [Online]. Available: https://efectis.com/, 05/03/2026.
[10] ISO 11925-2:2026, *Reaction to fire tests — Ignitability of products subjected to direct impingement of flame Part 2: Single-flame source test*, 2026.
[11] ISO 834-1:1999, *Fire-resistance tests — Elements of building construction — Part 1: General requirements*, 1999.
[12] Hager I., *Comportement à haute température des bétons à haute performance - évolution des principales propriétés mécaniques, Thèse Dr.*, 2004.
[13] Mindeguia J. C., *Contribution Expérimentale A La Compréhension Des Risques D'instabilité Thermique Des Bétons*, Universitè de Pau et des Pays de l'adour, 2009.

[14] Tanibe T., Ozawa M., Lustoza D. R., Kikuchi K., Morimoto H., *Explosive spalling behaviour of restrained concrete in the event of fire*, Proceedings of 2nd international RILEM workshop on concrete spalling due to fire exposure, October 2011, 319–326.
[15] Kalifa P., Chéné G., Gallé C., *High-temperature behavior of HPC with polypropylene fibers from spalling to microstructure*, Cement and Concrete Research., vol. 31, no. 10, 2001, 1487–1499.

7

INVESTIGATION OF AGEING PROCESSES IN BUILDING MATERIALS

Aleksander Kozak

7.1. THERMODYNAMICS AND KINETICS OF MATERIAL DEGRADATION

Building materials used across diverse structures and environmental conditions are subjected to aggressive gaseous and liquid media. This exposure precipitates gradual degradation, ultimately compromising their structural integrity and operational safety. Consequently, durability – defined as a structure's capacity to maintain its performance parameters throughout its design life – plays a fundamental role in ensuring safe long-term operation. It is imperative to acknowledge a foundational tenet of materials science: most construction materials exist in a metastable state. The manufacture of steel, cement and polymers is a highly energetic process in which energy is imparted to raw materials to engineer specific properties. In accordance with the Second Law of Thermodynamics, spontaneous processes in isolated systems proceed towards maximum entropy, which, in physicochemical terms, denotes the maximum dispersion of energy and matter (an increase in the number of accessible microstates). The corrosion of steel is fundamentally the reversion of iron to its naturally stable ore state (oxides, hydroxides, or carbonates). Similarly, while cement hydration is an exothermic process progressing towards a lower energy state, subsequent carbonation represents a continued drive towards environmental equilibrium. Materials engineers cannot suspend thermodynamic laws; they can merely retard the kinetics of these processes. Thermodynamics unequivocally dictates that a system will gravitate towards the lowest Gibbs free energy, G. A negative change in this energy, $\Delta G < 0$, is the prerequisite for process spontaneity.

The spontaneity of degradation processes, such as corrosion or carbonation, is governed by the following equation:

$$\Delta G = \Delta H - T\Delta S$$

where:

ΔH – change in enthalpy (heat of reaction)
T – absolute temperature
ΔS – change in entropy (measure of energy and matter dispersion within the system)

In degradation mechanisms, such as the electrochemical corrosion of steel in concrete, ΔG is negative. As previously established, this indicates a thermodynamic drive for the steel to revert to its more stable ore configuration. Consider the electrochemical corrosion of steel reinforcement: it is a spontaneous process in the presence of oxygen and moisture because the Gibbs free energy change for rust formation ($Fe_2O_3 \cdot nH_2O$) is highly negative. Steel embedded in concrete remains

protected not because thermodynamic principles cease to apply, but because the passive layer provides a robust kinetic barrier. Upon a reduction in pH (carbonation) or the ingress of chlorides, this barrier is compromised, and thermodynamic forces prevail. A further illustration is the alkali-silica reaction (ASR). Reactive (amorphous) silica possesses a higher free energy than its crystalline counterpart (quartz). In a highly alkaline environment, hydroxyl ions, OH^-, attack the siloxane bonds (Si-O-Si) of the amorphous silica, inducing depolymerisation and the subsequent formation of a hygroscopic alkali-silicate gel. The driving force for the ensuing structural distress (swelling) is the osmotic pressure generated as this gel absorbs water. The primary objective of materials engineers is to fabricate kinetic barriers that decelerate such phenomena. It is crucial to recognise that a kinetic barrier encompasses not only the activation energy of chemical reactions, E_a, but, predominantly, the mass transport resistance of the material matrix. In civil engineering, most degradation processes are mass-transport limited. Before a reduction in the system's free energy can occur, chloride ions or CO_2 molecules must traverse the tortuous capillary pore network of the concrete. Therefore, from an engineering perspective, microstructural optimisation (e.g. by reducing the water-to-cement ratio or incorporating pozzolanic additions) constitutes the most efficacious strategy for artificially maintaining the system in a metastable state, thereby prolonging the time required for aggressive agents to reach the critical zone.

Ageing is intrinsically an increase in the system's entropy. The degradation of a polymer structure under ultraviolet (UV) irradiation or elevated temperatures, or the deterioration of the C-S-H phase due to external factors, invariably leads to the dispersion of energy and matter. Having established the thermodynamic inevitability of material degradation, the subsequent challenge is to devise laboratory methodologies that induce these degradation tendencies within a timeframe viable for research and investment cycles.

Acknowledging the thermodynamic certainty of degradation, the focus shifts to its rate, thereby entering the domain of chemical kinetics. In both research and forensic engineering, Service Life Prediction (SLP) is of paramount importance. To forecast operational lifespan, deterministic or probabilistic models are employed. These models facilitate estimating the precise moment when a specific parameter (e.g. carbonation depth) exceeds a permissible threshold, defined as the durability limit state. The probabilistic approach further incorporates the statistical distribution of material properties and the variability of environmental conditions, enabling the determination of the probability of failure at a given time. This methodology is rigorously delineated in the international standard ISO 15686 (Buildings and constructed assets – Service life planning), which establishes the framework for assessing structural durability. According to the standard, reliable durability forecasting requires a thorough understanding of degradation mechanisms under specific environmental conditions. For concrete structures, the fib Model Code 2010 and its updated version, the fib Model Code 2020, serve as pivotal documents,

introducing advanced durability verification procedures based on reliability theory. Consequently, SLP functions as an indispensable tool for scheduling maintenance inspections and optimising Life Cycle Costing (LCC). Most degradation processes (e.g. polymer hydrolysis, corrosion, diffusion) accelerate with elevated temperatures, a relationship described by the Arrhenius equation:

$$k = A \times \exp\left(-\frac{E_a}{RT}\right)$$

where:

k – reaction rate constant
A – pre-exponential factor (collision frequency)
E_a – activation energy [J/mol]
R – universal gas constant
T – absolute temperature [K]

The activation energy, E_a, represents the energetic barrier to the process. A high E_a value denotes a strong temperature dependence (e.g. the thermal degradation of polymers). Conversely, diffusion-controlled processes (such as chloride transport in concrete) typically exhibit a lower apparent activation energy (approximately 35–50 kJ/mol) compared to chemical reactions (often >80 kJ/mol). Nevertheless, they still demonstrate significant temperature dependence, which is a critical consideration when designing structures for diverse climatic zones. In photochemical processes (e.g. UV-induced polymer degradation), the energy barrier for the initiation stage is overcome by photon energy rather than by the system's thermal energy. Consequently, the initiation phase itself is virtually independent of the ambient temperature.

When analysing the degradation kinetics of building materials via the Arrhenius equation, it must be acknowledged that in complex, porous matrices (such as concrete or polymer composites), the true activation energy of a single chemical reaction is rarely determined. Instead, the concept of apparent activation energy, $E_{a\text{app}}$, is utilised. It is a macroscopic parameter that aggregates the energetic barriers of multiple constituent processes: the diffusion of aggressive agents through the pore solution, the kinetics of chemical binding (e.g. chloride-binding isotherms by the AFm phase), and the dissolution of solid phases. Furthermore, under actual operational conditions, degradation processes seldom occur in isolation. Structures are typically subjected to coupled degradation; for instance, mechanical loading induces microcracking, which drastically reduces the matrix's diffusion resistance, thereby shifting the rate-controlling mechanism from diffusion to capillary suction. Under such circumstances, classical models predicated solely on Fick's laws and the Arrhenius equation prove inadequate, necessitating the implementation of advanced multiphysics modelling in modern Service Life Prediction.

7.1.1. SURFACE AND BULK DEGRADATION

In materials science, surface degradation refers to processes in which structural deterioration is confined to or strictly controlled by the outer layer. A classic example is the photodegradation of organic materials (polymers, resins, and bituminous binders) under UV radiation. High-energy photons initiate photo-oxidation, leading to chain scission and the formation of carbonyl groups. This process occurs exclusively within a thin near-surface layer, resulting in chalking, microcracking, and a loss of gloss, whereas the material core remains intact for an extended period. In metals, atmospheric corrosion is also typically a surface phenomenon, although it may propagate deeper into the substrate over prolonged exposure.

In the context of cementitious composites, the boundary between the surface and the bulk is more complex owing to their porosity. Although aggressive chemical agents originate from the external environment, their destructive impact manifests within the structure once the diffusion barrier is breached:

- Carbonation: This entails the diffusion of carbon dioxide into the matrix, precipitating a pH reduction in the pore solution across the entire volume encompassed by the reaction front, ultimately leading to reinforcement depassivation.
- External Sulphate Attack (ESA): Although sulphate ions permeate from the exterior (e.g. from groundwater), their reaction with aluminates contained in the cementitious matrix leads to the formation of secondary, expansive ettringite. This process results in crystallisation within the capillary pores of the concrete, generating internal stresses that lead to a global loss of matrix cohesion and subsequent internal bursting.

Bulk degradation refers to processes in which destructive agents are present throughout the material mass from its inception. The most prominent example in concrete technology is the alkali–silica reaction (ASR). In this instance, reactive silica in the aggregate reacts with alkalis in the pore solution, forming an expansive gel throughout the element; this generates osmotic pressure that causes expansion, cracking, and disintegration of the material.

7.1.2. THERMAL AND CHEMICAL DEGRADATION OF POLYMERIC COATINGS

Polymeric protective coatings exhibit entirely different degradation kinetics. Elevated temperature is a key factor driving their degradation, as it accelerates the diffusion of oxygen and water into the coating. Furthermore, the type and colour of the material significantly influence infrared radiation absorption. It is generally accepted that white coatings maintain temperatures approximately 10°C–15°C lower–and in extreme cases, up to 30°C lower–than black coatings. Consequently, coatings with higher absorption are subjected to substantially greater thermal stresses.

It must be emphasised that the maximum temperature to which a polymer is exposed in a natural environment is typically too low to induce direct homolysis of the main polymer chain bonds. However, it is entirely sufficient to cause the thermal decomposition of hydroperoxides (ROOH) formed during the UV initiation phase, thereby drastically accelerating the propagation of radical reactions. In certain polyvinyl chloride (PVC)-based polymers, elevated temperatures additionally induce the migration and volatilisation of the plasticiser, resulting in a severe increase in brittleness. Conversely, extremely low temperatures induce the glass transition of protective coatings, increasing their susceptibility to mechanical damage.

Rain, dew, and high humidity drive polymer hydrolysis and the leaching of additives (pigments and stabilisers), whereas freeze–thaw cycles generate stresses at the coating–substrate interface, leading to a loss of adhesion. In urban and industrial environments, coatings are additionally subjected to chemical aggression. The presence of sulphur oxides (SO_2) and nitrogen oxides (NO_x) leads to the formation of acids (e.g. H_2SO_4). While these acids aggressively etch mineral and metallic substrates, in the case of polymeric coatings, gases such as NO_x and atmospheric ozone (O_3) act primarily as potent oxidants. They engage in synergistic reactions with UV radiation, accelerating the cross-linking or degradation of macromolecular chains.

7.2. NATURAL TESTING METHODOLOGY

Dating back approximately a century, coatings manufacturers observed that the environmental stressors prevalent in South Florida and the Arizona desert caused extreme degradation of their products. These geographic locations served as natural laboratories for evaluating material performance, subsequently facilitating the development of enhanced durability profiles. South Florida provides a unique, year-round synergistic environment of high-intensity solar radiation, elevated temperatures, and substantial moisture. Conversely, the arid Arizona desert climate is defined by intense irradiance and thermal extremes, coupled with negligible precipitation and low relative humidity.

Notwithstanding its reliability, the natural weathering process remains inherently time-intensive, often requiring years of exposure to yield representative data for long-term durability interpolation. To mitigate these temporal constraints while maintaining outdoor exposure conditions, sophisticated solar concentration systems were developed. These apparatuses utilise a ten-mirror array designed to reflect and concentrate natural solar radiation onto test specimens. Furthermore, exposure efficiency is maximised by an automated dual-axis tracking mechanism that continuously aligns the system with the sun's azimuth and elevation throughout the diurnal cycle.

7.3. ACCELERATED TESTING METHODOLOGY – ENVIRONMENTAL SIMULATION

Service Life Prediction (SLP) of polymers and protective coatings in the construction sector relies on the rigorous simulation of environmental conditions. Two fundamental standards in this domain are EN ISO 4892-2 (xenon-arc lamps) and EN ISO 4892-3 (fluorescent UV lamps). The selection of the appropriate standard dictates the reliability of the correlation between laboratory results and actual degradation under natural conditions.

EN ISO 4892-2 defines the methods for exposing plastics to laboratory light sources using xenon-arc lamps, which simulate the full solar spectrum (290–800 nm: UV + VIS + IR). This standard is applied to evaluate the durability of façade coatings, roofing membranes, and exterior PVC profiles. Xenon test chambers are equipped with borosilicate-filtered lamps, providing an irradiance of 0.51–1.0 W/m^2 at 300 nm. Key parameters include water spray, relative humidity control (RH 30–95%), and a Black Standard Temperature (BST) of 38–89°C. The standard specifies several methods, among which Method A serves as the benchmark for construction materials (cycle: 102 minutes of dry irradiation / 18 minutes of irradiation with water spray). An example of such a weathering chamber is shown in Fig. 7.1 below.

Fig. 7.1. Q-SUN Xe-3-HSE weathering chamber, Q-Lab (xenon-arc radiation with water spray)

EN ISO 4892-3 details exposure to fluorescent UV lamps (UVA-340/UVB-313), typically employed for rapid screening tests. These chambers emit radiation within a narrow spectral band (e.g. 295–365 nm for UVA). The ageing cycle generally comprises alternating periods of UV irradiation at elevated temperatures and moisture condensation in the dark (e.g. 8 hours of UV at 60°C followed by 4 hours of condensation at 50°C). An example of such a weathering chamber is presented in Fig. 7.2.

Fig. 7.2. QUV/spray/RP weathering tester, Q-Lab (UV radiation with water spray)

7.4. CORRELATION BETWEEN NATURAL AND ARTIFICIAL WEATHERING

Establishing a correlation between laboratory results and natural weathering presents a formidable challenge. Under natural conditions, materials are simultaneously subjected to a multitude of factors: UV radiation, fluctuating temperatures, moisture, rain, hail, ozone, and microorganisms. Ageing chambers typically simulate only a select few of these (e.g. UV radiation combined with water spray or elevated temperatures), neglecting the complex, synergistic interactions between them that accelerate degradation in nature. Standard laboratory tests generally fail to account for the presence of ozone (a potent oxidant), sulphur and nitrogen oxides (the precursors to acid rain), and the impact of bacteria and fungi. The degradation

products of additives, such as plasticisers or stabilisers, can serve as a nutrient source for microorganisms in the natural environment, thereby further altering the material's deterioration mechanism. Climatic conditions vary drastically depending on the geographical location, and even at the same site over the years. It is exceedingly difficult to establish a stable correlation model for phenomena that are inherently variable and unrepeatable in nature; studies demonstrate that natural exposure experiments conducted in different years can yield divergent results. Consequently, correlating laboratory data with natural weathering is regarded as one of the most complex tasks in material durability research, as the conditions within ageing chambers significantly oversimplify the highly dynamic natural environment.

The transition from 'laboratory hours' to 'years in service' requires the application of complex acceleration factors (AFs). It is crucial for researchers to acknowledge that a standard cycle – while providing a baseline for quality assurance – is a simplified model of the stochastic nature of the outdoor environment. Consequently, advanced lifetime prediction models often integrate these standardised results with probabilistic methods to better estimate the reliability of structures in specific macroclimatic zones. The transition from raw experimental data to robust scientific conclusions requires a sophisticated statistical framework. A frequent oversight in materials science is the overreliance on the coefficient of determination, R^2, as the sole indicator of correlation between artificial and natural weathering. While a high R^2 suggests a strong linear relationship, it does not inherently account for non-linear degradation kinetics or the heteroscedasticity often observed in long-term field data. Certain studies postulate that an exposure period of 2,000–4,000 hours in a test chamber simulates several years of service life (typically 3–5 years) under the most severe natural conditions. To correlate both ageing modalities, the Total Radiant Exposure derived from regional annual meteorological data is evaluated, allowing for the calculation of the equivalent chamber hours required to match this intensity.

7.5. EVALUATION AND DIAGNOSTIC METHODS

To empirically verify these thermodynamic transformations, a multi-scale analytical approach is indispensable. Scanning Electron Microscopy (SEM), frequently coupled with Energy-Dispersive X-ray Spectroscopy (EDS), facilitates the high-resolution visualisation of microstructural alterations and the identification of localised chemical gradients. An example of an SEM instrument is depicted in Fig. 7.3.

Fig. 7.4 presents a representative SEM micrograph of the polymeric material following one year of exposure in Kraków.

Fig. 7.3. EVO MA 10 scanning electron microscope (Carl Zeiss)

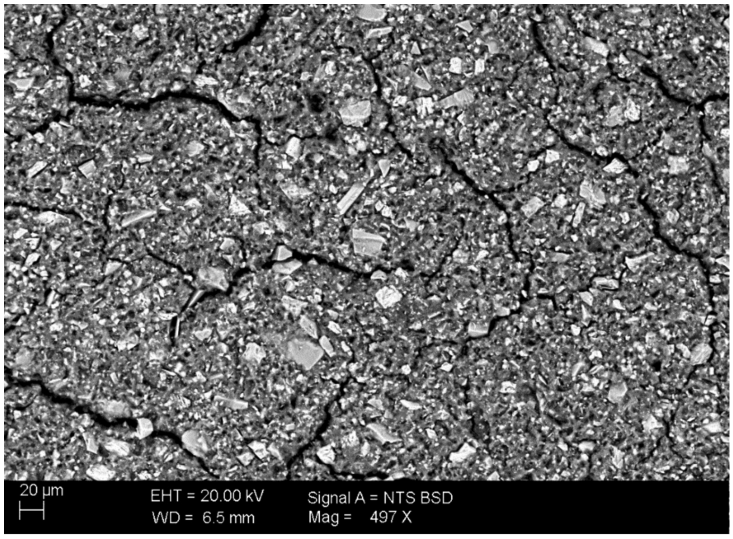

Fig. 7.4. Polymeric coating after one year of exposure in Kraków

While SEM provides insights into the morphology of degradation products—for instance, through the visual examination of the bulk polymeric material and

elemental analysis via EDS, or, in the case of mineral building materials such as concrete, the identification of expansive ettringite formation and porosity alterations within the interfacial transition zone—Fourier-Transform Infrared (FTIR) spectroscopy serves as a critical tool for molecular characterisation. FTIR enables the detection of specific functional groups, making it particularly effective for monitoring the carbonation progress in cementitious matrices or the oxidative degradation of polymer-based additives by analysing characteristic vibrational bands. In the engineering of building materials and polymers (e.g. bitumens, resins, and coatings), the Carbonyl Index (CI) is a pivotal parameter that describes the degree of photo-oxidation or thermal ageing. Monitoring this index using the Attenuated Total Reflectance FTIR (FTIR-ATR) technique involves analysing changes in the absorption spectrum of the specimen, specifically focusing on the formation of carbonyl groups.

Formation of carbonyl groups: Ageing processes induce the scission and oxidation of polymer chains. Consequently, carbonyl groups (C=O) emerge within the material's structure. These groups exhibit strong absorption in the wavenumber range of approximately 1700–1750 cm^{-1}. To ensure the result is reliable and independent of the specimen's thickness, the intensity (peak area or height) of the carbonyl band is referenced against a stable band that remains unaltered during ageing (e.g. the vibrations of CH_2 or CH_3 groups around 1450–1460 cm^{-1} or 2900 cm^{-1}). The index is typically defined as the ratio of the carbonyl peak area to the reference peak area. The growth kinetics of this index serve as a quantitative measure of the progression of photo-oxidation.

An example of an FTIR spectrometer is presented in Fig. 7.5.

Fig. 7.5. Jasco FT/IR-6700 spectrometer

An example of an FTIR spectrum is shown in Fig. 7.6.

When evaluating polymeric materials subjected to degradation factors, assessing the tensile properties is of paramount importance; this is tested in accordance with the EN ISO 527-3 standard. The test specimen, the standard geometry of which is illustrated in Fig. 7.7, is secured within the grips of a universal testing machine

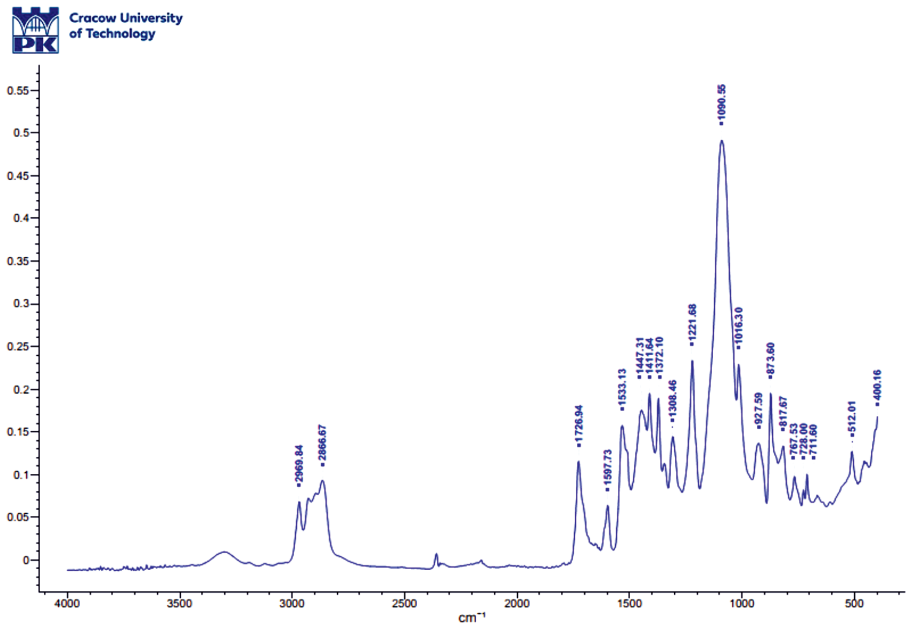

Fig. 7.6. Representative FTIR spectrum

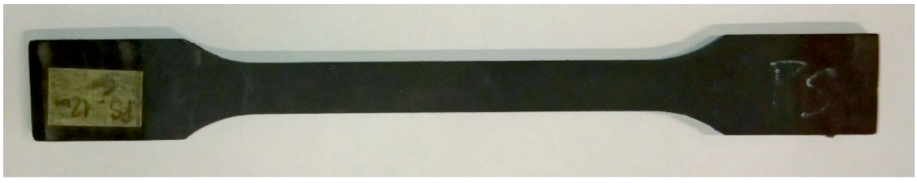

Fig. 7.7. Specimen for mechanical testing

(e.g. ZwickRoell). This method facilitates the determination of tensile strength, elongation at break, and the energy to failure.

To evaluate the adhesion of a coating to concrete, the EN 1542 standard is applied, which specifies the procedure for conducting pull-off adhesion tests and outlines the assessment criteria. Adhesion is expressed in MPa; for flexible systems without traffic loads, it must exceed 0.8 MPa, whereas for flexible systems subjected to traffic loads, this requirement increases to 1.5 MPa. The failure mode is also reported—cohesive failure is considered optimal, as it indicates that the coating is stronger than the underlying substrate.

Crack-bridging ability: Concrete is an inherently brittle material susceptible to cracking (due to plastic shrinkage, dynamic loads, and thermal gradients). The function of a flexible protective coating is to 'bridge' these cracks, thereby preventing the penetration of carbon dioxide and chlorides into the reinforcement. The testing

standard EN 1062-7 defines two primary test methods that simulate different structural operating conditions: static crack-bridging and dynamic crack-bridging.

Salt spray simulation aims to replicate a highly corrosive environment characterised by elevated salinity and humidity. The EN ISO 9227:2023-02 standard specifies the procedures for conducting tests in a sprayed salt solution. An example of such testing is the evaluation of the corrosion resistance of rail fastening systems that secure railway tracks to sleepers. Fig. 7.8 illustrates the appearance of such a chamber.

Fig. 7.8. Salt fog chamber, model Corrosionbox C200400E

In the case of building materials, visual assessment using an optical microscope – capable of achieving magnifications of, for example, ×200 – is also widely employed for testing both mineral and polymeric materials.

Another diagnostic parameter utilised for evaluating coatings or films is the testing of vapour permeability, which determines the so-called equivalent air layer thickness, S_d, expressed in metres. This value represents the diffusion resistance of the coating. These tests are conducted for both water vapour and carbon dioxide. For water vapour S_d value below 5 m indicates that the coating is vapour-permeable, whereas for carbon dioxide, S_d value exceeding 50 m demonstrates that the coating will effectively protect the concrete against carbonation.

The assessment of chalking involves measuring the quantity of loose powder (degraded binder and pigment) on the surface, which serves as visual evidence of the coating's deterioration under UV exposure.

7.6. CONCLUSIONS AND FUTURE PERSPECTIVES

Testing ageing processes in building materials has evolved from simple outdoor exposure into a sophisticated, multi-instrumental science. As demonstrated in the preceding chapters, the degradation of polymers and the corrosion of steel are complex phenomena that cannot be fully captured by a single test. The integration of Accelerated Weathering and Cyclic Corrosion Testing remains the cornerstone of service life prediction, providing a necessary, albeit imperfect, bridge between laboratory research and real-world durability. In the context of the European Green Deal and global sustainability goals, ageing studies transcend mere durability assessments; they are now pivotal to the circular economy. Understanding how recycled polymers or low-carbon cements age compared with their conventional counterparts is essential for the widespread adoption of green building materials. Currently, testing protocols are being adapted to evaluate the re-ageing potential of materials following their initial life cycle.

7.7. SUMMARY

This comprehensive study investigates the thermodynamic and kinetic mechanisms governing the degradation of building materials, alongside the methodologies employed for service life prediction. Acknowledging the inherent metastability of construction materials, the research delineates between surface-level deterioration, such as the photo-oxidation of polymeric coatings, and bulk degradation processes, including carbonation and alkali–silica reactions. The synergistic impact of ultraviolet radiation, thermal stress, and chemical oxidants on material integrity is critically examined. Furthermore, the study evaluates the efficacy of natural weathering versus accelerated environmental simulation, employing xenon-arc and fluorescent UV apparatuses. It highlights the formidable challenges in correlating artificial testing with stochastic natural environments, advocating for advanced probabilistic models over simple linear correlations. To empirically quantify degradation, a multi-scale diagnostic framework is presented, encompassing Scanning Electron Microscopy (SEM), Fourier-Transform Infrared (FTIR) spectroscopy for Carbonyl Index monitoring, and rigorous mechanical testing. Ultimately, the research underscores a paradigm shift in materials science: transitioning from fundamental durability assessments to evaluating the re-ageing potential of low-carbon and recycled materials, thereby aligning with the circular economy objectives of the European Green Deal.

REFERENCES

[1] Andrady A. L., Heikkilä A. M., Pandey K. K., Bruckman L. S., White C. C., Zhu M., Zhu L., *Effects of UV radiation on natural and synthetic materials*, Photochemical & Photobiological Sciences, 22, 2023, 1177–1202.

[2] Atkins P., de Paula J., Keeler J., *Atkins' Physical Chemistry (11th ed.)*, Oxford University Press, Oxford 2018.

[3] Bochen J., *Durability assessment of building materials exposed to atmospheric agents by testing in simulated environment*, Architecture Civil Engineering Environment, 1/2013, 17–25.

[4] Bochen J., *Weathering effects on physico-chemical properties of external plaster mortars exposed to different environments*, Construction and Building Materials, 79, 2015, 192–206.

[5] Celina M., Gillen K. T., Assink R. A., *Accelerated ageing and lifetime prediction: Review of non-Arrhenius behaviour due to two competing processes*, Polymer Degradation and Stability, 90(3), 2005, 395–404.

[6] Cristoforetti A., Rossi S., Deflorian F., Fedel M., *Comparative study between natural and artificial weathering of acrylic-coated steel, aluminium, and galvanised steel*, Materials and Corrosion, 74(10), 2023, 1429–1438.

[7] Friedrich D., *Comparative study on artificial and natural weathering of wood–polymer compounds: A comprehensive literature review*, Case Studies in Construction Materials, 9, 2018, e00196.

[8] Jelle B. P., *Accelerated climate ageing of building materials, components and structures in the laboratory*, Journal of Materials Science, 47, 2012, 6475–6496.

[9] Jelle B. P., Nilsen T. N., Hovde P. J., Gustavsen A., *Accelerated climate ageing of building materials and application of the attenuated total reflectance (ATR) Fourier transform infrared (FTIR) radiation experimental method*, Proceedings of the 8th Symposium on Building Physics in the Nordic Countries, Volume 1, Copenhagen 2008, 951–958.

[10] Jones M. S., Effects of UV radiation on building materials, available at: https://niwa.co.nz/sites/default/files/2025-06/Jones.pdf

[11] Klakegg O. J., Kjølle K. H., Mehang C. G., Olsson N. O. E., Shiferaw A. T., Woods R. (Ed.), *Proceedings of the 7th Nordic Conference on Construction Economics and Organisation 2013: Green Urbanisation – Implications for Value Creation*, Akademika Publishing, Trondheim 2013.

[12] Kozak A., *Multi-criteria assessment of an acrylic coating exposed to natural and artificial weathering*, Procedia Engineering, 108, 2015, 664–672.

[13] Kržišnik D., Lesar B., Thaler N., Humar M., *Influence of natural and artificial weathering on the colour change of different wood and wood-based materials*, Forests, 9(8), 2018, 488.

[14] Phillipson M. C., Emmanuel R., Baker P. H., *The durability of building materials under a changing climate*, Wiley Interdisciplinary Reviews: Climate Change, 7(4), 2016, 590–599.

[15] Q-Lab Corporation, *Test Services Brochure*, available at: https://www.q-lab.com/weathering/weathering-exposure-testing-services

[16] Ribeiro M. C. S., Ferreira A. J. M., Marques A. T., *Effect of natural and artificial weathering on the long-term flexural performance of polymer mortars*, Mechanics of Composite Materials, 45(5), 2009, 515–526.

[17] Taylor H. F. W., *Cement Chemistry (2nd ed.)*, Thomas Telford Publishing, London 1997.

[18] ASTM G154-23, *Standard Practice for Operating Fluorescent Ultraviolet (UV) Lamp Apparatus for Exposure of Materials*.
[19] ASTM G155-21, *Standard Practice for Operating Xenon Arc Light Apparatus for Exposure of Materials*.
[20] EN 1062-6:2002, *Paints and varnishes — Coating materials and coating systems for exterior masonry and concrete — Part 6: Determination of carbon dioxide permeability*.
[21] EN 1062-7:2004, *Paints and varnishes — Coating materials and coating systems for exterior masonry and concrete — Part 7: Determination of crack-bridging properties*.
[22] EN 1542:1999, *Products and systems for the protection and repair of concrete structures — Test methods — Measurement of bond strength by pull-off*.
[23] EN ISO 7783:2018, *Paints and varnishes — Determination of water-vapour transmission properties — Cup method*.
[24] EN ISO 9227:2023, *Corrosion tests in artificial atmospheres — Salt spray tests*.
[25] fib, *Model Code for Concrete Structures 2010*, fib Bulletins 65 & 66, Ernst & Sohn, Lausanne 2013.
[26] fib, *Model Code for Concrete Structures 2020*, fib Bulletins 108 & 109, Lausanne 2023.
[27] ISO 4628-6:2011, *Paints and varnishes — Part 6: Assessment of degree of chalking by tape method*.
[28] ISO 4892-2:2013, *Plastics — Methods of exposure to laboratory light sources — Part 2: Xenon-arc lamps*.
[29] ISO 4892-3:2016, *Plastics — Methods of exposure to laboratory light sources — Part 3: Fluorescent UV lamps*.
[30] ISO 527-3:2018, *Plastics — Determination of tensile properties — Part 3: Test conditions for films and sheets*.
[31] ISO 15686-1:2011, *Buildings and constructed assets — Service life planning — Part 1: General principles and framework*.
[32] ISO 15686-2:2012, *Buildings and constructed assets — Service life planning — Part 2: Service life prediction procedures*.

8

NON-DESTRUCTIVE TESTING OF CEMENT AND GEOPOLYMER CONCRETE STRUCTURES

Mateusz Sitarz

8.1. INTRODUCTION

8.1.1. THE ROLE OF NON-DESTRUCTIVE TESTING IN CONCRETE STRUCTURE

Concrete structures are frequently examined after hardening to verify whether they meet the requirements assumed at the design stage and during service. In engineering practice, it is desirable that such assessments do not impair the structural integrity of the element being tested. For this reason, **non-destructive testing (NDT)** has become an essential component of contemporary concrete diagnostics.

Methods used to evaluate concrete can be classified according to the extent of damage they introduce. **Fully non-destructive techniques allow for testing without any physical alteration of the material**, whereas partially destructive and destructive methods, such as core drilling or pull-out and pull-off tests, require local damage and subsequent repair. Between these two categories, there are techniques that cause only limited surface disturbance. Whenever feasible, non-destructive methods are preferred, as they enable structural assessment while preserving the original condition of the concrete.

Non-destructive and semi-destructive techniques make it possible to evaluate a broad range of concrete properties. These include basic material characteristics such as density, elastic modulus, and strength, as well as surface properties like hardness and absorption. In addition, NDT methods can be applied to locate reinforcement, estimate its size, and determine the thickness of the concrete cover. Certain techniques also support the assessment of construction quality and structural integrity through the identification of internal defects, including cracks, voids, honeycombing, and delamination.

Non-destructive testing is applicable to both newly constructed and existing concrete structures. In new structures, it is primarily used for quality control and resolving uncertainties related to materials or construction procedures. In existing structures, NDT is most often employed to assess their safety, serviceability, and overall structural condition. Exclusive reliance on destructive testing is usually impractical, as such methods are costly, time-consuming, and limited in number, which may result in non-representative data. Consequently, **non-destructive testing is commonly used as an initial assessment tool to identify critical zones that may require further detailed investigation.**

Typical applications of non-destructive testing in the concrete structures include:

- quality control of precast elements and in-situ concrete construction,
- verification of material alignment with technical specifications,
- monitoring strength development to support decisions related to formwork removal, prestressing, or load application,
- detection and evaluation of internal defects such as cracks, voids, and honeycombing,
- assessment of concrete uniformity prior to core sampling or load testing,
- determination of reinforcement location, quantity, and condition,
- increasing the reliability of a limited number of destructive tests,
- evaluation of material variability to select representative testing locations,
- identification of concrete deterioration caused by mechanical, chemical, thermal, or environmental factors,
- assessment of concrete durability and long-term performance,
- providing data to support planned modifications or changes in structural use.

8.1.2. AN OVERVIEW OF COMMON NON-DESTRUCTIVE TESTING METHODS FOR CONCRETE STRUCTURES

A variety of non-destructive testing methods are available for the evaluation of concrete structures, each providing different types of information related to material properties, structural condition, and durability. **In engineering practice, the selection of an appropriate method depends on the nature of the structure, the type of suspected problem, and the objectives of the investigation**. In most cases, the non-destructive testing is preceded by a thorough visual inspection, which plays a fundamental role in planning further diagnostic activities.

Table 8.1. Common Non-Destructive Testing Methods for Concrete Structures

NDT Method	Basic Principle	Main Applications
Visual Inspection	Direct observation of surface features and defects	Preliminary assessment; identification of cracks, discoloration, spalling; selection of further NDT methods
Rebound Hammer Test	Measurement of surface rebound related to concrete hardness	Estimation of surface hardness and approximate compressive strength
Ultrasonic Pulse Velocity (UPV)	Measurement of ultrasonic wave propagation speed	Assessment of concrete quality, uniformity, and compressive strength
Impact Echo Testing	Analysis of stress wave reflections caused by mechanical impact	Detection of delamination, voids, and internal flaws

Gas Permeability – Torrent Permeability Test	Measuring the rate of air flow through the concrete surface	Assessing the quality and durability of concrete cover, evaluating surface permeability
Water Permeability Test (GWT)	Water penetration assessment	Surface water permeability of concrete

8.2. VISUAL INSPECTION

Visual inspection is **the most basic and essential non-destructive method** used in the assessment of concrete structures. It allows an experienced engineer to identify surface features related to workmanship, structural performance, and material degradation. It is often the **first technique used to identify visible features** that may require further investigation and, therefore, forms the foundation of any diagnostic programme. **Common indicators include cracks, spalling, discoloration, weathering, surface defects, and lack of uniformity**.

This method provides a preliminary evaluation of structural condition and forms the basis for selecting appropriate subsequent testing techniques. **Visual inspection should consider not only the structure itself but also surrounding elements and environmental conditions.** Despite its simplicity, careful observation is critical, as overlooked details may lead to incorrect assessment.

8.2.1. TOOLS AND EQUIPMENT FOR VISUAL INSPECTION

Visual inspection of concrete structures requires appropriate tools to ensure accurate observation and reliable documentation. **Basic equipment includes measuring tapes or rulers, markers, and simple instruments for recording environmental conditions, such as thermometers.**

Where direct access to structural elements is limited, optical aids such as binoculars, telescopes, and inspection scopes (borescopes or endoscopes) are used to examine inaccessible areas without damaging the structure. For detailed surface assessment, crack width gauges, or microscopes and magnifying tools are applied to measure and examine fine cracks and surface defects.

Photographic documentation is an essential component of visual inspection. A digital camera with suitable zoom or macro capabilities enables systematic recording of the observed defects, while colour charts support the identification of variations in the concrete appearance. The inspection process should be supported by relevant structural drawings, which allow for precise location and consistent recording of observations.

8.2.2. GENERAL PROCEDURE OF VISUAL INSPECTION

Visual inspection should begin with a **review of all available documentation**, including structural drawings, technical specifications, construction records, and previous inspection reports. This step allows the engineer to understand the structure, its history, and its intended use.

The inspection should be carried out systematically, covering visible defects, structural usage, adjacent structures, and environmental conditions. **All defects must be identified, their severity assessed, and their probable causes considered.** Attention should be given to the distribution and pattern of damage, as well as comparisons between similar structural elements.

Surface features such as cracking, spalling, honeycombing, deflection, and discoloration often provide valuable indications of workmanship quality, structural performance, and material deterioration. Crack mapping and observation of the surface texture and colour support the identification of damage mechanisms. **All observations must be clearly documented on drawings or inspection records**, with defects classified according to their type and severity. Common concrete defects are shown in Fig. 8.1.

Fig. 8.1. Common defects in concrete

8.3. SCHMIDT REBOUND HAMMER TEST

The Schmidt rebound hammer is a non-destructive testing method primarily **used to assess the surface hardness of concrete**. The test is based on the rebound of a spring-driven mass after impact with the concrete surface, where **higher rebound numbers indicate harder surfaces**. Although no direct theoretical relationship

exists between rebound number and concrete compressive strength, empirical correlations have been established within certain limits, allowing the method to be used as **an indirect indicator of concrete strength and uniformity**.

8.3.1. EQUIPMENT FOR SCHMIDT REBOUND HAMMER TEST

The Schmidt rebound hammer is **a compact and portable device designed for both laboratory and in-situ testing of concrete**. The instrument has a mass of approximately 1.8 kg and consists of several key components, including the outer casing, a spring-loaded hammer mass, a plunger that makes contact with the concrete surface, and a main compression spring (Fig. 8.2).

During testing, **the hammer mass is released and impacts the plunger, after which it rebounds.** The rebound distance is captured by a sliding indicator, commonly referred to as a rider, which moves along a graduated scale. This scale is typically marked with arbitrary units ranging from 10 to 100. **The position of the rider after impact defines the rebound number, which represents the measured response of the concrete surface and serves as the basic output of the test**.

Fig. 8.2. Schmidt rebound hammer [12]

8.3.2. TESTING PROCEDURE AND PRACTICAL APPLICATION OF THE SCHMIDT REBOUND HAMMER

The Schmidt rebound hammer **test is performed by pressing the plunger firmly and perpendicularly against the concrete surface and** gradually compressing the internal spring until the hammer mass is released and impacts the surface. After rebound, a sliding indicator records the maximum rebound distance, which is read as the rebound number. **The test may be conducted in horizontal, vertical, or inclined positions**; however, the orientation of the instrument influences the results due to gravitational effects and must be considered during the interpretation stage. **Rebound numbers are commonly used as indirect indicators of concrete strength, but their reliability depends on proper calibration. Meaningful strength estimation requires the development of site-specific correlation curves based on specimens**

made with the same materials and tested under comparable curing conditions. For this purpose, laboratory specimens are tested using both rebound measurements and compression tests, and the resulting data are statistically correlated. Manufacturer-supplied calibration curves should be used with caution, as they may not accurately represent the properties of concrete used in a specific structure.

The Schmidt rebound hammer is a fast and inexpensive tool for assessing concrete uniformity and surface hardness; however, **its results are affected by several limiting factors**. Reliable measurements require smooth and well-prepared surfaces, as rough or porous concrete may lead to inaccurate readings.

The rigidity and size of the tested element influence the rebound values. Small or poorly supported members may absorb impact energy, resulting in lower rebound numbers. Concrete age also affects results, with younger concrete often producing higher values than mature concrete of similar strength. Testing of very young or low-strength concrete is not recommended due to the risk of surface damage.

Moisture condition plays an important role, as saturated surfaces usually yield higher rebound numbers than dry ones. When moisture content is uncertain, surface pre-wetting and appropriate calibration should be applied. In addition, **material composition significantly influences test results**. Variations in aggregate type, aggregate source, and cement type may alter the relationship between rebound number and compressive strength.

In older structures, surface **carbonation may considerably increase rebound values**, leading to an overestimation of concrete strength. For this reason, carbonation depth should be considered during results interpretation. Overall, **the rebound hammer test is best suited for comparative and preliminary assessments** and should be supported by calibration and complementary testing methods for reliable strength evaluation.

8.4. ULTRASONIC PULSE VELOCITY (UPV)

In the ultrasonic pulse velocity test, **a short pulse of mechanical vibrations is generated by an electro-acoustic transducer placed in contact with the concrete surface**. To ensure effective transmission of ultrasonic energy, a coupling medium such as grease or cellulose **paste is applied between the transducer and the concrete**. After entering the material, the **pulse propagates through the concrete** in the form of stress waves, undergoing reflections and refractions at interfaces between different phases of the composite material.

During wave propagation, both longitudinal and shear waves are generated; however, the longitudinal waves travel at the highest velocity and reach the receiving transducer first. **These waves are converted into electrical signals** by the receiving transducer. The travel time of the pulse is measured using electronic timing circuits,

enabling the calculation of wave velocity based on the known distance between the transducers.

Longitudinal pulse velocity (in km/s or m/s) is given by:

$$v = \frac{L}{T}$$

where:
v – longitudinal pulse velocity,
L – path length,
T – time taken by the pulse to traverse that length.

8.4.1. EQUIPMENT FOR ULTRASONIC PULSE VELOCITY TESTING

The **equipment** used for the ultrasonic pulse velocity testing consists of several basic components, **including an electrical pulse generator, a pair of transmitting and receiving transducers, an amplifier, and an electronic timing system for measuring wave travel time**. The pulse generator produces short electrical signals that are converted into mechanical vibrations by the transmitting transducer. After passing through the concrete, the received signal is amplified and processed to determine the transit time between the two transducers.

The selection of the transducer's frequency is an important factor in UPV testing. Frequencies commonly range from 20 to 150 kHz, although the lower frequencies may be used for long transmission paths and the higher frequencies for short paths or fine-grained materials such as mortars and grouts. The high-frequency signals provide better resolution but are more rapidly attenuated, while the low-frequency signals penetrate deeper but offer lower sensitivity. **For most practical applications in concrete structures, transducers operating in the range of 50 to 60 kHz are considered optimal.** The device for recording the UPV measurements is shown in Fig. 8.3.

Fig. 8.3. UPV test instrument [13]

8.4.2. APPLICATIONS OF THE UPV METHOD

The Ultrasonic pulse velocity testing **is commonly used to assess the uniformity and internal condition of concrete structures**. Variations in measured velocity indicate changes in the material quality and may reveal defects such as voids, poorly compacted zones, or damaged areas.

The method is also **applied to monitor changes in the concrete properties over time**, as velocity generally increases with material maturation and decreases during deterioration. In quality control, the UPV provides information directly related to in-situ concrete, which may be more representative than laboratory test specimens.

When appropriate correlations are established, pulse velocity measurements can be used to estimate compressive strength and elastic properties. However, such interpretations are influenced by material composition, curing conditions, and concrete age and should be applied with caution, particularly for high-strength concrete. For reliable assessment, UPV testing is best used together with other testing methods.

8.4.3. MEASUREMENT CONFIGURATIONS AND INTERPRETATION OF THE UPV RESULTS

The Ultrasonic pulse velocity measurements can be performed using three main transducer arrangements: direct transmission (opposite faces), semi-direct transmission (adjacent faces), and indirect or surface transmission (same face). **Direct transmission provides the highest accuracy and sensitivity** and should be used whenever access to both sides of the element is possible. Indirect transmission is applied when only one surface is accessible but produces lower signal strength and results that mainly reflect surface properties. Reliable measurements require proper acoustic coupling between the transducers and the concrete surface using a thin layer of coupling material.

The UPV results are influenced by several factors, including moisture content, temperature, path length, specimen dimensions, and the presence of reinforcing bars. These factors must be considered during data interpretation to avoid inaccurate assessment. Variations in pulse velocity are used to estimate concrete uniformity and to identify zones of inferior quality or internal defects, particularly large voids. Repeated measurements arranged in grids support spatial analysis of the material's homogeneity.

Table 8.2. Concrete Quality Classification Based on Ultrasonic Pulse Velocity

Longitudinal pulse velocity (km/s·10^3)	**Quality of concrete**
> 4.5	excellent
3.5–4.5	good
3.0–3.5	doubtful
2.0–3.0	poor
< 2.0	very poor

The Ultrasonic pulse velocity measurements can be used to estimate the dynamic elastic modulus of concrete, assuming the material behaves as an isotropic elastic medium. **The relationship between the pulse velocity and elastic properties is expressed by the following equation**:

$$E_d = \rho v^2 \frac{(1+\upsilon)(1-2\upsilon)}{(1-\upsilon)}$$

where:
E_d – dynamic elastic modulus (in MN/m^2),
υ – dynamic Poisson's ratio,
ρ – density (in kg/m^3),
v – pulse velocity (in km/s).

If the density and Poisson's ratio are known, the dynamic elastic modulus can be determined directly from the UPV measurements. This relationship is valid for concrete elements of various shapes and sizes, provided that their lateral dimensions are not small in relation to the wavelength of the ultrasonic pulse. Similarly, the Poisson's ratio may be estimated when the density and elastic modulus are known. This approach enables the non-destructive evaluation of the elastic properties of concrete and supports the assessment of structural condition.

8.5. IMPACT ECHO TESTING

The impact echo method is a non-destructive testing technique that **enables the detection of internal features in concrete structures using access from only one surface.** The method is based on generating a mechanical or ultrasonic impulse on the concrete surface and measuring the time required for the reflected wave to return from internal interfaces, such as voids, cracks, or the opposite surface.

If the velocity of longitudinal waves in concrete is known, the distance to an internal reflector can be determined from the measured transit time using a simple time–distance relationship. Due to strong scattering and attenuation of the ultrasonic waves by aggregates and air pores, relatively low frequencies**, typically around 50 kHz, are required for effective signal penetration in concrete**. Even at these frequencies, signal attenuation often limits direct echo detection.

$$d = \frac{v_L}{2T}$$

where:
T – transit time,
v_L – velocity of the longitudinal wave,
d – distance.

8.5.1. PRINCIPLE OF THE IMPACT ECHO METHOD

The technique is based on generating mechanical stress waves by surface impact and analysing their reflections from internal interfaces and external boundaries. The distance to reflecting surfaces, such as the back face of a slab or internal voids, is determined from dominant frequencies in the recorded signal and the known velocity of compression waves in concrete.

The method relies on stress waves with frequencies typically ranging from 1 to 60 kHz, generated by controlled mechanical impacts. The frequency content of the pulse depends on the contact time between the impactor and the surface, which is influenced by the diameter and material of the impactor. Smaller impactors generate higher frequencies suitable for thin elements, while larger impactors are used for thicker members. **Proper selection of the impactor size is therefore essential for obtaining clear and interpretable signals.**

Fig. 8.4. Impact Echo instruments [14]

The equipment needed for impact echo testing (Fig. 8.4) typically consists of a data acquisition unit, one or more hand-held transducers, interchangeable spherical impactors of different diameters, connecting cables, and a dedicated signal- processing software. Some systems are equipped with multiple transducers and spacer bars, enabling simultaneous measurements and improved spatial resolution. **During testing, the impactor size is adjusted until a clear dominant frequency peak appears in the frequency spectrum, indicating suitable signal penetration and reflection**.

8.5.2. APPLICATIONS AND LIMITATIONS OF THE IMPACT ECHO METHOD

The impact echo method has been successfully **applied in the investigation of various structural problems in concrete engineering**. Typical applications include the detection of internal cracking caused by material degradation processes, measurement of pavement and slab thickness, identification of voids in post-tensioning ducts, and location of delamination in bridge decks and car park structures. The method has also been used to assess cracking in beams, columns, and composite structural elements, with results often verified by core testing.

In pavement and slab thickness measurements, accuracy depends on sub-base conditions and material properties. The method is particularly effective for detecting large defects and discontinuities parallel to the surface, especially in plate-like structures. However, its resolution is limited by the wavelength of the generated stress waves, and shallow defects can only be detected if their depth exceeds approximately half of the wavelength.

The detection capability of impact echo testing is fundamentally limited by the wavelength of the generated stress waves, which is related to wave velocity and excitation frequency according to:

$$\lambda = \frac{V}{f}$$

where λ is the wavelength, V is the wave velocity, and f is the frequency.

Experimental studies indicate that the minimum detectable depth of a defect is approximately equal to half of the wavelength ($\lambda/2$). Assuming a typical wave velocity of about 4000 m/s in sound concrete, a 10 kHz excitation frequency results in a minimum detection depth of approximately 0.20 m. For lower-quality or younger concrete, where velocity may be closer to 3500 m/s, detection resolution is further reduced.

The excitation frequency depends on the contact time between the impactor and the surface and is controlled by the size of the spherical hammer. **The**

smaller impactors generate higher frequencies and improve near-surface resolution, while the larger impactors are required for thicker elements. Surface deterioration or crumbling increases contact time, reduces excitation frequency, and leads to longer wavelengths and poorer defect resolution.

Geometrical effects related to the size and shape of structural elements may produce misleading reflections, particularly in small or irregular components. For this reason, measurements should be performed at multiple locations to distinguish between structural geometry and true defects. In addition, near-field effects may prevent reliable detection of shallow anomalies, which may instead appear as apparent increases in slab thickness.

Good testing practice requires multiple measurements at each location, with the first two readings commonly discarded to ensure stable signal conditions. Interpretation should not rely on single measurements, and the absence of detected anomalies does not necessarily indicate the absence of defects. Reliable diagnosis therefore requires careful frequency selection, repeated testing, and, where possible, confirmation using complementary non-destructive or destructive methods.

8.6. TORRENT PERMEABILITY TEST

The Torrent permeability test is a non-destructive, **in-situ method used to evaluate the resistance of near-surface concrete to gas penetration**. The method is based on measuring the rate of air flow into the concrete cover under a controlled pressure difference. This flow is governed primarily by the pore structure, connectivity, and microcracking of the cementitious matrix. Since the ingress of aggressive agents such as carbon dioxide, oxygen, and chlorides is closely related to gas and liquid transport properties, air permeability is widely regarded as a practical indicator of concrete durability.

8.6.1. EQUIPMENT AND MEASUREMENT PROCEDURE

The Torrent permeability testing system consists of a double-chamber vacuum cell, a pressure control unit, pressure sensors, and a data acquisition and processing module (Fig. 8.5). The outer chamber, known as the guard ring, surrounds the inner measuring chamber and is maintained at a similar pressure level. This configuration restricts lateral air flow and forces air to penetrate mainly in the direction normal to the concrete surface.

Prior to testing, **the concrete surface must be carefully prepared**. Loose particles, dust, laitance, and surface contaminants are removed, and the surface is

inspected for visible defects. The test area should be free from standing water and excessive moisture. An airtight seal between the vacuum cell and the concrete surface is essential and is usually achieved by means of a soft sealing ring.

Fig. 8.5. Torrent air permeability test setup [15]

The standard measurement procedure includes the following steps:

First, **the vacuum cell is positioned** on the prepared surface and pressed firmly to ensure proper sealing. Next, **a controlled pressure reduction is applied** to both chambers, creating a pressure gradient between the concrete pores and the measuring chamber. After stabilisation of the pressure conditions, **air begins to flow** from the concrete into the inner chamber.

During this phase, the instrument continuously records the pressure change as a function of time. Based on the measured pressure decay, the system calculates the **kT coefficient**, taking into account the chamber geometry and air properties. A typical measurement lasts several minutes, depending on the permeability of the concrete and environmental conditions.

For reliable assessment, multiple measurements are usually performed at different locations. **Environmental parameters such as surface temperature, ambient humidity, and concrete moisture condition should be recorded, as they significantly influence the results**.

8.6.2. APPLICATIONS AND CLASSIFICATION

The Torrent permeability test is **widely used for durability-oriented evaluation of concrete structures, particularly in aggressive exposure environments** such as marine zones, regions subjected to de-icing salts, and industrial environments. Typical applications include the quality control of cover concrete in new structures,

comparative surveys of existing elements, assessment of curing efficiency, and support of service life predictions. The method is also valuable in maintenance planning, where areas with elevated permeability can be prioritised for detailed investigation or preventive treatment.

When interpreted correctly, **the kT coefficient provides a practical basis for classifying concrete quality**. A commonly used technical classification is presented in Table 8.3.

Table 8.3. Concrete Quality Classification Based on the kT Coefficient

kT Coefficient (E^{-16} m^2)	Quality Class	Concrete Quality	Durability Assessment
< 0.01	Class 1	Very Good	Excellent resistance to ingress
0.01–0.1	Class 2	Good	High durability
0.1–1.0	Class 3	Normal	Acceptable, monitoring recommended
1.0–10.0	Class 4	Poor	Increased risk of deterioration
> 10.0	Class 5	Very Poor	Low durability, remedial action required

8.6.3. INFLUENCE OF MOISTURE AND ADDITIONAL LIMITATIONS

One of the most critical limitations of the Torrent method is its **strong sensitivity to concrete moisture content**. The physical mechanism underlying this effect is related to the presence of water within the pore system. When pores are partially or fully filled with water, the continuity of air-filled pathways is reduced. Since water has a much lower permeability to gas than air, it acts as an effective barrier to gas flow.

As a result, **wet or partially saturated concrete may exhibit artificially low kT values**, even if its pore structure is highly porous or poorly connected. In such cases, concrete of inferior quality may appear "impermeable" when assessed by air permeability testing. This phenomenon can lead to significant misinterpretation of the durability performance, particularly after rainfall, washing, or in young concrete with high internal moisture.

For this reason, the moisture condition must always be evaluated prior to testing. Where possible, **measurements should be performed under standardised dry conditions or after controlled preconditioning**. If this is not feasible, the results must be interpreted cautiously and preferably combined with complementary methods, such as electrical resistivity, sorptivity, or core-based laboratory tests.

Besides moisture effects, several other factors influence Torrent test results. Surface carbonation, finishing techniques, curing regime, and local

microcracking may affect near-surface permeability. The method primarily reflects the properties of the cover zone and does not directly characterise deeper concrete layers. Furthermore, absolute kT values may vary depending on equipment calibration and testing procedure, which limits direct comparison between different projects.

Consequently, the Torrent permeability test should not be used as a standalone diagnostic tool. Its greatest value lies in the comparative analysis, trend monitoring, and integration with other non-destructive and destructive testing methods within a comprehensive durability assessment programme.

8.7. WATER PERMEABILITY TEST (GWT)

The Germann Water Permeability Test (GWT) **is an in-situ, non-destructive method used to evaluate the resistance of concrete to water penetration under controlled hydraulic pressure.** The method is based on forcing water into the near-surface zone of concrete and measuring the resulting flow. This process reflects the connectivity, size, and continuity of capillary pores and microcracks within the cementitious matrix.

The principal **outcome of the GWT is the permeability coefficient**, which expresses the ability of concrete to transmit water under pressure. Low permeability values indicate high resistance to fluid ingress and enhanced durability, whereas high values suggest increased susceptibility to chemical attack, corrosion processes, and freeze–thaw damage. For this reason, the permeability coefficient is widely used as an indirect indicator of concrete quality and service life potential.

8.7.1. EQUIPMENT AND MEASUREMENT PROCEDURE

The GWT system is designed for in-situ testing of concrete under service conditions and consists of a rigid pressure chamber mechanically fixed to the concrete surface and connected to a water supply and pressure control unit. The main components include the pressure chamber, sealing rings ensuring watertight contact with the surface, a transparent capillary tube or reservoir for monitoring water level, a hand-operated pressure pump equipped with a pressure gauge, and valves and connectors for system control (Fig. 8.6).

Prior to testing, **the selected area is cleaned to remove dust, laitance, and loose particles, and a location free from major cracks and surface defects** is chosen. The pressure chamber is then mounted on the concrete using anchor bolts and sealing rings, and the chamber and capillary system are filled with clean water, with all trapped air carefully removed. Hydraulic pressure is applied using the hand pump and stabilised

at the required level, after which the water level in the capillary tube is monitored over time. **The decrease in water level is recorded at regular intervals and used to calculate the flow rate based on the measured volume change and elapsed time.** To ensure representative assessment of structural conditions, several measurements are typically performed at different locations on the tested element.

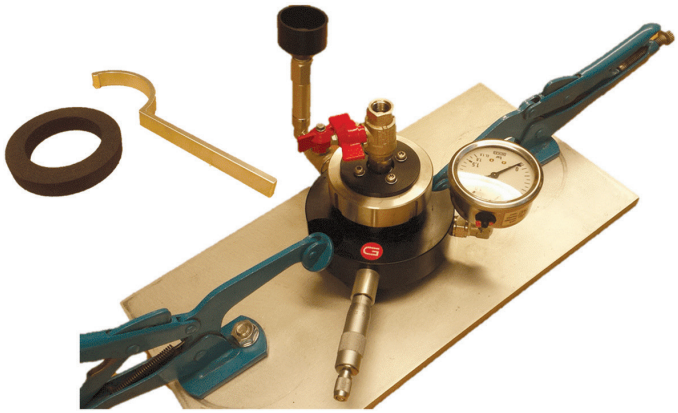

Fig. 8.6. Germann Water Permeability Test Instruments [16]

The primary **result of the GWT is the permeability flux *q***, which represents the rate of water flow through the concrete surface under applied pressure. It is commonly expressed in:

$$\mathrm{ml}/(\mathrm{m}^2 \cdot \mathrm{s}) \text{ or } \mathrm{mm}/\mathrm{s}$$

The permeability flux is calculated from the observed decrease in water level in the capillary tube:

$$q = \frac{\Delta V}{A \cdot \Delta t}$$

where:

q – permeability flux,
ΔV – volume of water penetrating the concrete (ml),
A – effective test area (m^2),
Δt – measurement time (s).

The volume change ΔV is determined from the drop in water level and the internal diameter of the capillary tube. **A higher value of *q* indicates greater water penetration and lower resistance to fluid transport.**

Because permeability measurements are strongly influenced by material composition, curing history, and environmental conditions, interpretation is typically

based on indicative ranges rather than strict quality classes. An example classification is presented in Table 8.4. These ranges should be treated as indicative engineering guidance. They are not universal acceptance criteria and must be interpreted in relation to exposure conditions, structural function, and complementary diagnostic data.

Table 8.4. Concrete Quality Classification Based on the Permeability Flux q

Permeability Flux q (mm/s)	**Indicative Interpretation**	**Durability Implication**
$< 1.0 \times 10^{-6}$	Very low water penetrability	Dense microstructure; high resistance to fluid ingress
1.0×10^{-6}–5.0×10^{-6}	Low to moderate penetrability	Generally adequate durability under normal exposure
5.0×10^{-6}–1.0×10^{-5}	Noticeable permeability	Increased susceptibility to environmental attack
$> 1.0 \times 10^{-5}$	High water penetrability	Significant transport potential; durability concerns

8.7.2. APPLICATIONS AND LIMITATIONS

The Germann Water Permeability Test **is primarily applied for in-situ evaluation of concrete structures exposed to moisture and aggressive environmental conditions**. It is commonly used for assessing the quality of cover concrete in bridge decks and viaducts, evaluating water-tightness in tanks, reservoirs, and tunnels, investigating deterioration in car park structures and industrial floors, verifying the effectiveness of rehabilitation measures and surface treatments, and supporting maintenance planning and service life assessment. Because the method directly measures water penetration under controlled pressure, it is **particularly suitable for structures in which hydraulic performance and resistance to fluid ingress are critical**.

Despite these advantages, **several limitations** must be considered during interpretation. The **initial moisture condition** of concrete strongly influences test results, and saturated or recently wetted surfaces may exhibit artificially low permeability values. Measurement reliability is also affected by **surface preparation**, as inadequate cleaning or sealing may lead to leakage and erroneous readings. In addition, the test **is locally invasive** due to the need for mechanical anchoring of the pressure chamber, and the results represent only a small surface area, which may not reflect the overall structural condition. **Local cracks, microcracks,** and surface defects may further dominate water flow and distort measurements. For these reasons, GWT results should be interpreted in conjunction with visual inspection, complementary non-destructive testing methods, and, where necessary, laboratory investigations to ensure reliable durability assessment.

REFERENCES

[1] Adámek J., Juránková V., Evaluation of durability of concrete by measurement of permeability for air and water, Brno University of Technology, Faculty of Civil Engineering, Brno 2009, pp. 1–5.
[2] ASTM Article, Methods of Test for Concrete Permeability: A Critical Review, ASTM ACEM Journal Article – includes GWT and other permeability test methods.
[3] International Atomic Energy Agency, *Guidebook on Non-Destructive Testing of Concrete Structures*, IAEA, Vienna 2002.
[4] Jain A., Combined Use of Non-Destructive Tests for Assessment of Concrete, Struct. Concrete 14 (2013) – includes overview of rebound hammer and UPV & their dependency on concrete condition.
[5] Lorenzi A., Campagnolo R., Silva Filho L.C.P., Concrete Structures Monitoring using Ultrasonic Tests, SciELO, 2020 – illustrating applications of UPV and tomography for deterioration monitoring.
[6] Malhotra V.M., Testing Hardened Concrete: *Non-destructive Methods, ACI Monograph No. 9*, Detroit 1976.
[7] Moczko A., Moczko M., GWT – New Testing System for "in-situ" Measurements of Concrete Water Permeability, Procedia Engineering 153 (2016), pp. 483–489.
[8] Popovics S., *Strength and Related Properties of Concrete: A Quantitative Approach*, John Wiley & Sons Inc., New York 1998.
[9] Saleem M.A., Siddiqi Z.A., Aziz M., Abbas S., Ultrasonic Pulse Velocity and Rebound Hammer Testing for Non-destructive Evaluation of Existing Concrete Structure, Pak. J. Engg. & Appl. Sci., 18 (2016), pp. 89–97.
[10] Schabowicz K. (Ed.), *Non-destructive Testing of Materials in Civil Engineering*, MDPI Books, Basel 2019.
[11] Xu X., Study of Water Permeability of Lightweight Concrete, Proc. Int. Conf. Durability of Concrete Structures, Purdue Univ., 2016.
[12] https://www.screeningeagle.com/en/products/original-schmidt [Accessed: 29.05.2026].
[13] https://www.screeningeagle.com/en/products/pundit-lab [Accessed: 29.05.2026].
[14] https://www.ndtjames.com/Vu_Con_System_p/v-v-100.htm [Accessed: 29.05.2026].
[15] https://www.screeningeagle.com/en/products/torrent [Accessed: 29.05.2026].
[16] https://www.germanninstruments.com/water-permeability-test-gwt/ [Accessed: 29.05.2026].

9

USE OF VR AND AR IN CONSTRUCTION

Julia Silezin-Tałach

9.1. INTRODUCTION TO VIRTUAL AND AUGMENTED REALITY

The development of digital technologies in recent years has significantly changed the way engineering processes are designed, manufactured, and personnel are trained. One of the tools supporting these activities is virtual reality (VR) and augmented reality (AR). These technologies enable the user to interact with a digital environment in a way similar to interacting with real objects.

9.1.1. VIRTUAL REALITY (VR)

Virtual reality is a fully computer-generated three-dimensional environment in which the user can move and perform tasks using dedicated devices such as VR headsets and motion controllers. The system tracks the movements of the user's head and hands, so the image changes accordingly, creating the impression of being present in a real space.

Unlike conventional simulations viewed on a monitor, VR engages the user directly – the user's body becomes part of the control interface. This makes it possible to reproduce manual operations that require motor coordination, including assembly tasks, machine operation, or welding processes.

In materials and manufacturing engineering, VR is primarily used as a training tool, enabling the learning of technological operations without material consumption, without the risk of equipment damage, and without hazards to the operator's health.

9.1.2. AUGMENTED REALITY (AR)

Augmented reality involves overlaying digital elements into the view of the real world. The user sees the real environment while simultaneously receiving additional information in the form of models, labels, or instructions.

AR is mainly used in assembly, service, and inspection tasks, where the operator receives guidance regarding the order of actions or identification of structural components. The technology is used, among others, to support installation work, execution control, and the operation and maintenance of engineering facilities.

9.1.3. DIFFERENCES BETWEEN VR AND AR

The key difference between these technologies lies in the degree of contact with the real environment:

– VR completely replaces reality with a digital environment,
– AR enhances reality with digital elements.

Therefore, virtual reality is particularly useful in training that requires repeated practice of technological tasks, while augmented reality supports work performed on real objects.

9.2. WELDING IN MATERIALS ENGINEERING AND CONSTRUCTION

9.2.1. IMPORTANCE OF MATERIAL JOINING PROCESSES IN STRUCTURES

Joining processes are one of the fundamental stages in manufacturing structural components. In many cases, the safety of the entire structure depends on the quality of the joint. This is particularly relevant for steel structures, tanks, industrial installations, and elements of construction infrastructure. Unlike many other technological operations, welding is not only about setting machine parameters. The quality of the joint largely depends on the operator's skills – motion stability, maintaining arc distance, torch/gun angle, and travel speed. Even with correctly selected technological parameters, improper technique may lead to welding imperfections (weld discontinuities).

For this reason, welding is classified as a so-called special process, where quality cannot be fully verified solely by final inspection of the product. Proper technological preparation and supervision of the competence of personnel performing the joints are required.

9.2.2. EXAMPLES OF APPLICATIONS IN CONSTRUCTION

Welding processes are widely used in construction and in manufacturing structural elements used in engineering facilities. Typical applications include:
– fabrication of steel structures for halls and industrial facilities,
– joining bridge components and load-bearing structures,
– welding of reinforcing bars (rebar),
– stud welding,
– prefabrication of structural components.

In many cases, these are critical joints, where failure may lead to loss of load-bearing capacity. Technical requirements for the execution of steel structures are specified in EN 1090 [2], which places strong emphasis on weld quality and personnel qualifications.

9.2.3. QUALITY REQUIREMENTS AND CRITICALITY OF WELDED JOINTS

Welded joints are subject to defined quality levels depending on the intended use of the structure. Welding imperfections such as lack of penetration, undercuts, or gas pores may reduce joint strength and service life. Acceptable levels of imperfections are defined in EN ISO 5817 [3].

Due to the nature of welding, it is impossible to eliminate the risk of errors solely through final product inspection. Quality control must also cover the joint execution stage and personnel preparation. The welding quality system described in EN ISO 3834 [4] indicates that the competence of the person performing the weld directly affects the quality of the final product.

9.2.4. THE ROLE OF OPERATOR SKILLS IN JOINT QUALITY

A welder must simultaneously control several factors affecting joint quality:
– arc length,
– electrode or torch/gun angle,
– welding speed (travel speed),
– body position and motion stability,
– observation of the weld pool.

Acquiring these skills requires repeated practice and hands-on experience. In traditional training, this involves significant consumption of materials and energy and results in production waste.

Therefore, training methods that enable learning motor coordination and understanding the relationship between process parameters and the final effect –

without performing real welding – are becoming increasingly important. One such tool is the use of virtual reality.

9.3. TECHNOLOGICAL TRAINING IN VIRTUAL REALITY

9.3.1. SPECIFIC CHARACTERISTICS OF LEARNING WELDING

Learning to make welded joints is among the most demanding forms of technological training. Unlike many production operations, it does not only involve memorising steps, but also simultaneous control of process parameters and motor coordination.

During welding, the operator must observe the molten weld pool and at the same time maintain proper torch/gun position. A slight change in distance from the material, torch angle, or travel speed immediately changes the weld bead shape. This means the process requires the development of muscle memory, which cannot be achieved through theory alone.

An additional difficulty is limited visibility of the welding process due to the need for eye protection and the presence of intense arc radiation. Beginner operators often focus mainly on maintaining the arc, which makes it difficult to simultaneously control weld bead geometry.

9.3.2. LIMITATIONS OF TRADITIONAL TRAINING

Traditional welder training takes place at a real welding station. It allows contact with the real process but involves many limitations:

- consumption of base and filler materials,
- consumption of shielding gases,
- electrical energy consumption,
- welding fume emissions,
- risk of burns and injuries,
- the need for constant supervision by an instructor.

At the initial stage of learning, most welds contain numerous imperfections and cannot be used in production. This means that a significant portion of material is consumed solely for training purposes. In addition, while torch handling can be corrected during welding, an objective assessment of weld quality is only possible after the process is completed, which makes it harder to immediately link movement errors to the final result.

9.3.3. VIRTUAL REALITY AS AN ENVIRONMENT FOR LEARNING MANUAL OPERATIONS

Virtual reality makes it possible to reproduce a technological workstation in a digital form while preserving real operator movements. The user performs the same actions as during welding, but the process takes place in a simulated environment.

The system tracks the position of the torch/gun and the user's head and reproduces the welding process in real time. This allows repeated practice without material consumption and without hazards related to the electric arc.

A key advantage of VR is immediate feedback. The user receives guidance on parameters such as arc length and torch/gun angle during task execution, which significantly accelerates the learning process.

9.3.4. TRAINING MOTOR COORDINATION AND PROCESS PARAMETERS

At the initial stage, the most important aspect of training is mastering correct hand movements and a stable body position. At this point, real technological parameters are less important than the ability to guide the torch/gun in a repeatable manner. A VR simulator allows the user to practise:

- maintaining a constant arc length,
- maintaining a stable travel speed of the torch/gun,
- maintaining the correct torch/gun angle,
- controlling the weld pool,
- coordinating movements.

After the basic movements are mastered, the influence of process parameters on weld bead shape can be introduced gradually. The user observes how changing settings leads to effects such as penetration, excessive fusion, or lack of penetration, which in real conditions would require many trial welds.

9.4. VIRTUAL REALITY IN THE CONTEXT OF SUSTAINABLE DEVELOPMENT

9.4.1. REDUCING MATERIAL CONSUMPTION IN THE TRAINING PROCESS

Virtual and augmented reality technologies (VR and AR) are increasingly used in technical training as tools to reduce material consumption and lower the risk of errors during the execution of work. This is especially evident in

technological training that requires repeated practice of manual tasks, such as welding processes.

Traditional welding training requires producing a large number of trial joints. Beginner operators create many welds containing imperfections that cannot be used in production. This results in significant consumption of base and filler materials solely for training purposes.

To perform a single exercise, components must be prepared; consumables must be used and then removed. Across the full training process, this leads to a considerable amount of metal waste.

Using a VR simulator enables the learning of torch/gun handling and arc control without the use of materials. Real material is used only after mastering basic movements in the virtual environment, which reduces the number of unsuccessful attempts performed on real components.

9.4.2. WASTE AND EMISSIONS

Welding involves the emission of welding fumes and gases generated during the melting of metal and filler materials. During training, these emissions are not associated with manufacturing a product, but only with learning.

In addition, part of the produced samples must be grounded off or scrapped. This leads to further energy consumption during mechanical processing and the remelting of waste.

In training supported by virtual reality, this stage is significantly reduced. Most errors made by beginner operators are eliminated before they start working at a real station.

9.4.3. ENERGY SAVINGS

A welding station requires power for the welding power source, local ventilation, and workplace lighting. During many hours of training, this energy is consumed regardless of the quality of the produced welds.

A VR simulator uses only the energy required to operate a computer and electronic devices. Compared to a real station, energy demand is significantly lower, especially during the stage of learning basic movements.

9.4.4. SAFETY AND HEALTH PROTECTION

During traditional training, the operator is exposed to electric arc radiation, high temperatures, and metal spatter. Personal protective equipment is required, as well as constant supervision by an instructor.

Training in a virtual environment makes it possible to master basic operations and understand the process without exposure to harmful factors. Participants can repeat exercises, analyse mistakes, and observe their impact on weld bead shape in safe conditions, which supports conscious learning of correct process execution.

9.4.5. REDUCING THE NUMBER OF PRODUCTION ERRORS

An operator who starts work without prior preparation produces a higher number of defective joints. In production conditions, this leads to repairs or scrapping of components, generating additional material and energy consumption.

VR training allows preliminary mastery of the process technique; therefore, the number of errors after starting work at a real station is reduced. This limits the need for repairs and the manufacture of replacement parts.

9.5. LABORATORY – TRAINING USING A WELDING SIMULATOR

9.5.1. PURPOSE OF THE EXERCISE

The purpose of the exercise is to introduce the participant to basic principles of welding and to the influence of technological parameters on joint quality.

The participant performs the task in a virtual environment, learning correct torch/gun positioning, maintaining arc length, and maintaining stable travel speed.

9.5.2. SIMULATOR DESIGN AND OPERATION

The VRTEX 360 simulator consists of a VR headset, a welding torch/gun equipped with motion tracking, and a computer workstation generating the process image.

The user's movements are recorded and reproduced in real time in a virtual environment. The user observes the weld pool and the shape of the produced weld bead in a way similar to the real process.

The system analyses the torch/gun position relative to the material and changes in travel parameters and then records the welding run.

9.5.3. PROCESS PARAMETERS

During the exercise, the user can configure the basic technological conditions of the welding process. The simulator allows selection of the material and process type, as well as changes in parameters affecting melting behaviour and weld bead shape.

It is possible to set to following:

- base material type,
- welding process/mode,
- shielding gas type and flow rate,
- current polarity,
- welding current,
- arc voltage.

This allows the observation of the influence of both electrical and technological parameters on the process course and the resulting joint quality without performing real welding.

9.5.4. EFFECT OF PARAMETERS ON WELD QUALITY

Changing parameters produces a visible change in weld bead shape and quality:

- too low current may lead to a lack of penetration,
- too high current may cause excessive fusion,
- too high travel speed may produce a narrow and irregular weld bead,
- too low travel speed may lead to weld reinforcement (excessive build-up),
- improper shielding gas flow may result in porosity in the weld.

The user can repeat the trial multiple times and observe the impact of changes in settings on the final result.

9.5.5. WELD QUALITY ASSESSMENT IN THE SIMULATION SYSTEM

After completing the task, the simulator generates a model of the performed weld and provides its assessment. The analysis includes the following:

- weld porosity,
- face shape (concave or convex surface),
- undercuts,
- excessive spatter,
- welding position,
- torch/gun angle,
- travel speed,

– arc length,
– CTWD (Contact Tip to Work Distance).

As a result, the participant receives immediate feedback and can improve their technique in subsequent attempts.

9.5.6. COURSE OF THE EXERCISE

1) Introduction to the workstation and safety rules
2) Putting on the VR headset and adopting a working position
3) Setting the initial parameters
4) Performing a trial weld
5) Result analysis and identification of errors
6) Correction of parameters or torch handling technique
7) Repeating the task

9.5.7. COMPETENCES ACQUIRED BY THE PARTICIPANT

After completing the exercise, the participant:
– understands the impact of welding parameters on joint quality,
– can maintain a constant arc length,
– controls the torch/gun travel speed,
– maintains the correct torch/gun angle,
– interprets weld quality assessment results.

9.6. ADVANTAGES AND LIMITATIONS OF TRAINING IN VIRTUAL REALITY

9.6.1. EDUCATIONAL BENEFITS

Using virtual reality in technological training makes it possible to introduce participants to the process without using a real workstation. The user can observe phenomena and relationships between parameters and joint quality in a safe and repeatable way.

The most important advantage of VR training is immediate feedback. In traditional training, weld quality can be assessed only after the process is completed, whereas in a virtual environment the participant receives the assessment and error indication immediately after completing the task.

Additionally, the participant can become familiar with the process without exposure to high temperatures, arc radiation, and metal spatter. This facilitates the first contact with the technology for people without prior experience.

Key advantages of VR-based training include:
- no consumption of training materials,
- no welding fume emissions,
- user safety,
- the ability to observe the influence of parameters on the process,
- quick feedback on mistakes,
- repeatability of exercises.

The technology also enables multiple participants to be trained without the need to prepare multiple real welding stations.

9.6.2. TECHNOLOGY LIMITATIONS

Despite its many advantages, virtual reality does not reproduce all phenomena occurring during real welding. The user does not observe the real behaviour of the weld pool and does not experience real temperature or intense light radiation characteristic of the electric arc; process perception is largely limited to visual stimuli.

The simulation also does not replace experience related to joint preparation, clamping, and workstation organization. In real conditions, joint quality is affected by additional factors such as material distortion, surface cleanliness, or ambient conditions.

For this reason, VR training should be treated as an educational tool for understanding the process and learning basic movements, not as a full representation of technological work.

9.6.3. VR AS A PREPARATION STAGE FOR REAL WELDING

Virtual reality can serve as a preparatory stage in welding training because it supports the understanding of the relationship between process settings and the resulting weld and allows the practice of basic movement habits in controlled conditions. The participant learns which errors lead to undesired effects (e.g. a lack of penetration, excessive fusion, irregular weld geometry, porosity) and can then transfer this knowledge to real conditions.

At the same time, it should be emphasised that VR does not fully replace practical training at a real station. Real welding involves factors not reproduced in full by the simulation, including joint preparation, clamping and fit-up tolerances, distortion, thermal effects, ambient conditions, and full workstation ergonomics.

Within this course, VR is used as an educational tool to become familiar with welding, to interpret the influence of parameters on weld quality, and to understand the principles of assessing welded joints.

9.7. BASIC TERMS

Virtual reality (VR) – a digital three-dimensional environment that enables the user to perform tasks in a way similar to working in real conditions.
Augmented reality (AR) – a technology that overlays digital information onto the view of the real environment.
Technological simulation – the reproduction of a manufacturing process in a digital environment for analysis or learning.
Training simulator – a device that enables the learning of technical tasks without using real material.
Feedback – a system message assessing task execution and indicating user errors.
Process parameters – technological settings influencing operation behaviour and the final result.
Operator motor coordination – the ability to perform repeatable movements required for correct process execution.
Weld pool – molten metal formed during welding; its observation allows the evaluation of correct process execution.
Welding imperfection (discontinuity) – an undesirable feature of a welded joint, representing a deviation from quality requirements, formed during welding.
Joint quality assessment – the evaluation of the correctness of a joint based on its shape and continuity.

REFERENCES

[1] Szóstak M., Napiórkowski M., Schabowicz K., *Zastosowanie wirtualnej rzeczywistości w budownictwie w aspekcie szkoleń w zakresie bezpieczeństwa i higieny pracy – stan wiedzy*. Przegląd Budowlany 2024, 4.
[2] EN 1090 – Execution of steel structures and aluminium structures.
[3] EN ISO 5817 – Welding – Fusion-welded joints in steel, nickel, titanium and their alloys (beam welding excluded) – Quality levels for imperfections.
[4] EN ISO 3834 – Quality requirements for fusion welding of metallic materials.
[5] Pilarczyk J., *Poradnik inżyniera. Spawalnictwo*, Vol. 1; WNT: Warszawa.

Cracow 2026